University of Kerbala

College of Science

Department of Chemistry

Extraction and Evaluation of Silicon Compounds from Local Soil, Extraction of Iron (III) Ions from Aqueous Solution and Their Analytical Application

A Thesis

Submitted to the College of Science, Kerbala University In partial Fulfillment of the Requirements for the Degree of Master of Science in Chemistry

By

Zahraa Abdulsahib Qasm Al- Saady

B.Sc.in Chemistry / College of Science /University of Kerbala (2021)

Supervised by

Prof. Dr. Ahmed Fadhil Khudhair

Assit. Prof. Dr. Atheer Hasan Yas Al Khudhair

2025 AD **1446 AH**

بِسْمِ ٱللَّهِ ٱلرَّحْمَٰنِ ٱلرَّحِيمِ

يَرْفَعِ اللَّهُ الَّذِينَ آمَنُوا مِنكُمْ وَالَّذِينَ أُوتُوا الْعِلْمَ دَرَجَاتٍ (١١)

صدق الله العلي العظيم

سورة المجادلة الآية (١١)

Supervisor Certification

I certify that this thesis was prepared by **Zahraa Abdulsahib Qasm** our supervision at the Chemistry Department, College of Science, University of Kerbala, as a partial requirement for the degree of Master of Science in Chemistry.

Signature:

Name: Prof. Dr. Ahmed Fadhil Khudhair

Title: Prof.

Address: University of Kerbala, College of Sciences, Department of Chemistry

Date: / / 2025

Signature:

Name: Assist. Prof. Dr. Atheer Hasan Yas

Title: Assist. Prof.

Address: University of Kerbala, College of Sciences, Department of Chemistry.

Date: 8/7/ 2025

Report of the Head of Chemistry Department Chairman of Postgraduate Studies Committee

According to the recommendation presented by the Chairman of the Postgraduate Studies Committee, I forward this thesis **"Extraction and Evaluation of Silicon Compounds from Local Soil, Extraction of Iron (III) Ions from Aqueous Solution and Their Analytical Application ."** for examination.

Signature:

Name: Prof. Dr. Sajid Hassan Guzar

Address: University of Kerbala, College of Science, Department of Chemistry

Date: / / 2025

Examination Committee Certification

We, the examining committee, certify that we have read this thesis (**Extraction and Evaluation of Silicon Compounds from Local Soil, Extraction of Iron (III) Ions from Aqueous Solution and Their Analytical Application**) and examined the student (**Zahraa Abdulsahib Qasm**) in its contents and that in our opinion, it is adequate as a thesis for the degree of Master of Science in chemistry.

(Chairman)
Signature: Name: Prof. Dr. Alaa Frak Hussain
Title: Professor
Address: University of Kerbala - College of Science, Department of Chemistry
Date: / /2025

(Member)
Signature:
Name: Prof. Dr. Hayder Hamid Mihsen
Title: Professor
Address: University of Kerbala-College of Science, Department of Chemistry
Date: / / 2025

(Member)
Signature:
Name: Prof. Dr. Mustafa AbdulKadhim Hussien
Title: Professor
Address: University of Kufa -College of Science, Department of Chemistry
Date: / / 2025

(Member & Supervisor)
Signature:
Name: Prof. Dr. Ahmed Fadhil Khudhair
Title: Professor
Address: University of Kerbala-College of Science, Department of Chemistry.
Date: / / 2025

Signature:
Name: Assist. Prof. Dr. Atheer Hasan Yas
Title: Assist Professor
Address: University of Kerbala- College of Science, Department of Chemistry.
Date: 3/7/ 2025

Approved by the council of the College of Science
Signature:
Name: Prof. Dr. Hassan Jameel Jawad
Title: Professor
Address: University of Kerbala - Dean of College of Science
Date: / / 2025

Dedication

I dedicate this thesis to my beloved parents, whose unwavering support, encouragement, and sacrifices have been the foundation of all my achievements.

To my family and friends, thank you for your constant love and belief in me.

To my professors and mentors Prof. Dr. Ahmed Fadel Khadir and Asst. Prof. Dr. Atheer Hassan Yas, your guidance and knowledge have shaped my journey in countless ways.

This work is also dedicated to everyone who dreams of learning and growing — may this be a small step forward on a long road of discovery.

Acknowledgents

I thank God Almighty for his continued blessings and grace that enabled me to successfully complete my studies.

I would like to take this valuable opportunity to express my deepest gratitude to the Department of Chemistry and all my professors for their continuous support and valuable assistance throughout my academic career. Their teaching experience has been instrumental in refining my understanding of these topics and instilling them in my scientific research.

I would like to extend my sincere thanks and gratitude to Professor Dr. Ahmed Fadhel Khudhair and Assistant Professor Dr. Atheer Hassan Yas, who have been instrumental in their continuous support and valuable information. Their advice, guidance, and encouragement have been instrumental in my success, from the time I first proposed my research title to the completion of my dissertation

Abstract

Silica was successfully extracted from selected local soil samples from different areas of Karbala city using Sol-Gel method. The extraction method was simple and environmentally friendly. Organosilica (1-nitroso-2-naphthal silica) was then synthesized by reacting the extracted silica from the sand sample with an organic chelating reagent (1-nitroso-2-naphthal). The silica and organosilica compounds were then characterized using different techniques such as EDX, SEM, BET, AFM, XRD, FTIR, and TEM. EDX measurement revealed that the sandy soil contains a high percentage of silica. SEM technique was used to study the morphology of silica and organosilica. XRD technique showed that the silica and organosilica had broad peaks indicating their non-crystalline nature, while the presence of some sharp peaks in the organosilica indicated the presence of the organic reagent. FTIR analysis revealed the functional groups in silica, organosilica, siloxane, and silanol in silica. The surface area and pore volume of silica and organosilica using BET confirmed that both are characterized by mesoporous structures. Furthermore, transmission electron microscopy (TEM) and atomic force microscopy (AFM) images provided insights into the internal structure and surface roughness of silica and organosilica. Silica and organosilica were successfully used as the solid phase for the dispersed solid-phase extraction method and were successfully applied to extract iron complexes from aqueous solutions. The physicochemical conditions of the extraction were studied. Iron complexes were separated using silica and organosilica under the optimum conditions (neutral medium, reagent concentration 0.04 mol/L, temperature 35 and 40°C respectively, and stirring time 15 min). The iron complex extraction rate at 99.5% of silica was higher than used 87% with organosilica due to the surface properties of silica and organosilica. The method was also successfully applied to pharmaceutical samples containing iron ions, and the value of this confirms that it is an accurate, selective, sensitive, easy and fast method.

List of contains

List of contains

List of contains

List of contains

List of Tables

List of Tables

List of Figures

List of Figures

List of Figures

List of Schemes

List of Abbreviations

Abbreviations	Term
SPE	Solid-phase extraction
LLE	liquid–liquid extraction
LSE	liquid–solid extraction
MSPE	Magnetic solid phase extraction
DSPE	Dispersive solid-phase extraction
B.D.H	British Drug House
D	Distribution ratio
FTIR	Fourier Transform Infrared
UV-Vis	Ultraviolet-visible
XRD	X-Ray Diffraction
EDX	Energy dispersive X-ray spectroscopy
SEM - EDX	Scanning electron microscope - Energy dispersive X-ray spectroscopy
AFM	Atomic Force Microscopy
TEM	Transmission Electron Microscopy
BET	Bruner Emmett Teller
Wt. %	Weight percentage
Conc.	Concentration
Abs	Absorbance
Ads	Adsorption
E%	Extraction percentage
Kex	Stability Constant
SD	Standard deviation
ΔG	Free energy
ΔH	Enthalpy
ΔS	Entropy
RSD	Relative standard deviation
Temp.	Temperature

Chapter One

Introduction

1.1. Solid-Phase Extraction (SPE)

is technique pattern to utilize in analytical chemistry to purify, isolate and detect analytes from complicated mixtures. It includes passing a liquid pattern through a stable adsorbent material (sorbent) to selectively compounds of interest preserve [1].

Solid-phase extraction (SPE) in chemistry is an effective method to prepare samples analysis and sample collection can be using SPE as one of the methods. It is used without further preparation steps, such as pH adjustment or dilution [2]. SPE is based on similar principles to liquid–liquid extraction (LLE). The distribution between two phases of analytes or solutes is similar in both procedures. SPE involves dispersion of the analyte between two liquid phases (sample medium and adsorbent) does not require mixing of two liquid phases, as in LLE [3]. The liquid sample is passed through adsorbent material to which have a greater affinity of analytes than the liquid phase. Subsequently, the analytes are extracted by extraction method simplifies the analysis removing by sample matrix[4].Its ease in terms of time and solvents economy. SPE is becoming preconcentration of analyte and removal matrix more prevalent than LLE. In addition, LLE is inefficient to extract polar compounds, labor-intensive and time-consuming [5], [6].

1.2. Historical of Solid-Phase Extraction (SPE)

liquid–solid extractions (LSE) method was depended liquid sample extraction was placed in contact with solid phase were commonly equilibrium between the two phases was allowed to occur of the liquid and solid phases which followed by physical separation (by filtering or decanting)[6] . In 1951 was reported of first application of sorbent SPE by Braus significant efforts to improve specificity or selectivity towards target analytes have been made with regard to development and characterization of new formats and advanced sorbent materials of SPE to enhance

physicochemical and higher sportive capacity or mechanical stability. Poole classified SPE sorbents into three classes [7], [8]:

(1) Normal phase (such as Florisil, alumina, silica, diol NH_2, and CN bonded phases)

(2) Ion exchange (such as ammonium (strong anion exchanger) bonded phases and sulfonic (strong cation exchanger).

(3) Reversed phase (such as C8 and C18 bonded phases), Moreover, on the basis of the identity of materials, sorbents can be classified into three types: carbon based, polymer based and inorganic based.

1.3. Advantages of Solid Phase Extraction (SPE)

Solid-phase extraction (SPE) is a technique that can be tailored to selectively extract specific analytes while removing interfering compounds.By concentrating analytes from large volumes, SPE enhances detection limits. Removes impurities, reducing matrix effects in subsequent analysis . Typically requires less solvent than traditional liquid–liquid extraction (LLE) [9].

1.4. Mechanism of Solid Phase Extraction Method

The selection of extraction sorbent of SPE depends on the mechanism understanding of interaction between the sorbent and analyte of interest. Which depends on of the polar, hydrophobic and inorganic properties of both the sorbent and solute. SPE are based on van der Waals forces (“non-polar interactions”), dipole-dipole forces (“polar” interactions), hydrogen bonding and cation-anion interactions (“ionic” interactions) of the most common mechanisms [10] such as magnetic solid phase extraction. The sorbents are added and dispersed in the sample, the analytes are adsorbed onto their surface and the material is separated easily with a magnetic field. The analytes while using magnetic separation the liquid phase is collected for further analysis. The main benefits of this method are the direct addition of the sorbent in the sample high dispersion, rapid and simple

separation of sorbent materials[11].

1.5. Types of Solid Phase Extraction

1. Normal and Reversed Solid Phase Extraction

Normal-phase SPE involves a polar phase stationary such as silica or alumina that retention from interaction between polar groups on the sorbent surface and polar functional groups of the analyte , while Reversed phase involves a nonpolar phase stationary (C18, C8) with a moderately polar or polar and mostly used for aqueous samples[12].

2. Magenatic Solid Phase Extraction (MSPE)

MSPE is consists of a magnetic material dispersed into a sample solution and easily and swiftly recovered by application of a magnetic field. Magnetic nanoparticles are incubated with a liquid sample (unprocessed sample, extract or diluted liquid sample) on the material analytes and equilibrium adsorption experiments[13]as shown in Figure 1-1.

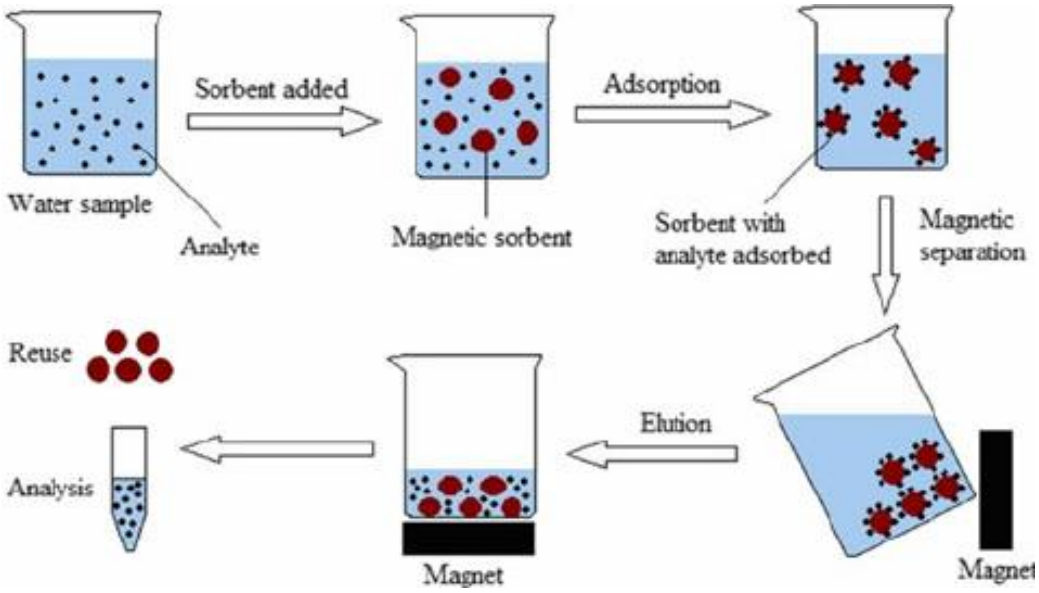

Figure 1.1. Solid phase extraction process [14].

3. Ion Exchange Solid Phase Extraction

It is contain Charge polar solutes (acid or base) can be extracted from polar ,

including less polar solvents and water. The mechanism isolation is depended on the high-energy electrostatic interaction between the charged functional groups of sorbent and analytes , the sorbent selection depends on the analyte charge [15]. The cation exchange extracts basic analytes (primary, secondary, tertiary, and quaternary amines). The anion exchange was used to isolate the acidic analytes (carboxylic acid, sulphonic acid, and phosphates) , according to the ionic group bonded to the surface[16].

4. Dispersive Solid-Phase Extraction

It is a variant of solid-phase extraction to extract efficiency of specific compounds from complex mixtures. A substance powder was added to a liquid sample and stirred, the amount of analyte deposited on the surface of the sorbent particles dispersed in the maximum value of solution reaches[17]. The liquid sorption is then separated from the sorbent. that DSPE has several advantages are used of solvents significantly reduced, and not require constant supervision[18].

1.6. Types of sorbents compounds

Solid Phase Extraction (SPE) is extensively method was used for the purification and separation of analytes from liquid solution. The preference of sorbent performs an important position with inside the performance of the extraction process[19]. Various sorts of sorbents are utilized in SPE every imparting precise houses and programs. Below are a number of the principle sorts of sorbents utilized in SPE[20].

1) Polymer Sorbents

Polymeric sorbents are primarily based totally Polymer sorbents may be designed to goal hydrophobic or hydrophilic compounds of the analysis bendy than silica substances[21]. As they may be tailor-made to have interaction with a broader variety of compounds, which include each polar and non-polar substances. These

sorbents are regularly utilized and require selective interactions with particular analytes[22].

2) Activated Carbon Sorbents

Activated carbon is one of mainly type, which are hydrophobic or have an excessive affinity for carbon-primarily based totally substances. carbon activated is noticeably powerful at adsorbing an extensive variety of natural contaminants.It is normally utilized in environmental , water pattern analysis and extensively for the extraction of natural compounds, due to its porous structure and huge floor place[23].

3) Acrylic Acid-primarily based totally Sorbents

Acrylic acid-primarily based totally sorbents are extracting polar or primary compounds powerful.These sorbents are regularly changed to improve their selectivity for positive sorts of molecules, which include particular natural useful groups or ions. Acrylic-primarily based totally substances are normally used whilst excessive specificity and potential for polar analytes are required [24]

4) Hydrogel Sorbents

Hydrogel as an adsorbent for contaminant removal in water. The most promising hydrogels for water purification are polymeric networks with high water absorption and contaminant immobilization capabilities[25].The interest for environmental remediation with hydrogels is also increasing, since hydrogels have excellent ability to trap and store different contaminants found in water into their structure. These polymeric hydrogels may present different characteristics regarding the gel volume, swelling, hydrophilic and hydrophobic surface properties [26] .

5) Alumina Sorbents

Alumina is another commonly sorbent used in SPE, mainly for the extraction of fairly polar to non-polar compounds. It has an excessive adsorption potential for huge natural molecules and is regularly utilized in commercial and environmental ,which

is green extraction of rapid and necessary[27] .

6) Membrane Sorbents

Membrane-primarily based totally sorbents constitute a more modern fashion in SPE. These sorbents integrate the blessings of selective separation and filtration with the power of sorption substances. Membrane sorbents are usually utilized in superior programs requiring specific manipulate over the separation process[28].

7) Silica Sorbents

Silica surface has been performed to obtain solid sorbents with greater selectivity and has good can undergo heat treatment and mechanical strength, it can be used as a very successful adsorbing[29]. In addition, silica with high stability, or be bound chemically to support easily loaded on chelating agents. In particular, silica presents high sorption capacity for metal ions, such as Cu, Ni, Co, Zn or Fe[30].Where silica surface groups and some the organic compound (functionalized sorbent) are chelating molecules on silica surface provides immobility, mechanical stability and water insolubility chemical modification of silica surface by organic chelating group acts which provides greater selectivity for the analyte[31] .The most convenient way to develop a chemically modified surface is by simple immobilization (or fixing) of the group on the surface by adsorption or electrostatic interaction or hydrogen bond formation of other type of interaction[32].

1.7. Definition of Silica

Silicon is a non-metallic element Second only to oxygen in the abundance on earth crust. Silicon is undergo reaction with oxygen to form silica, silica is the most abundant elements in the earth's crust and the approximately 59 weight % of the Earth's crust and can be found in nature as quartz, sand, or flint[33].

1.7.1. Silica Compounds Structure

Each silicon atom (Si) is covalently bonded to four oxygen atoms (O) to form tetrahedral structure. Silica is classified in two forms, also known as crystalline forms and amorphous forms (non crystalline) , these tetrahedral are regularly arranged and share corners to form a 3D network and structure arranged randomly[34].The silica structure is represented in Figure 1.2.

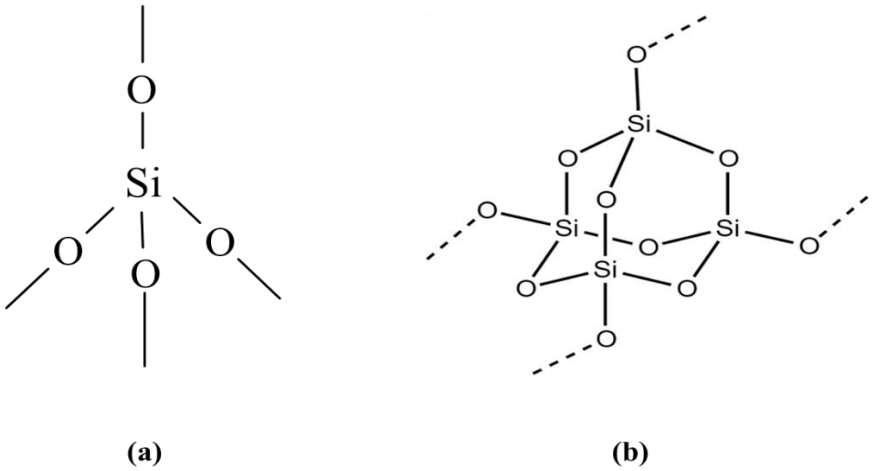

Figure 1.2.Silica structure: (a) Tetrahedral structure, (b) 3D network and structure [35]

1.7.2. Silica properties

Silica have many properties such as controllable pore size, modifiable surface, strong mechanical properties, and a comparatively inert chemical composition, which it is safe and non-toxic nature [36]Additionally, the silica is insoluble in water.The silicon atoms surface tend to be a complete tetrahedral configuration and in an aqueous medium of free valence electron become saturated with hydroxyl groups (surface OH groups: isolated, and H-bonded), siloxane groups (Si-O-Si or bridges with oxygen atoms on the surface), the surface of SiO_2 based materials is usually achieved by adsorption, due to surface active sites[37].

1-7-3. Extraction of silica methods

Silica is extracted in different methods as shown in the Table 1-1 to obtain: silica particles with uniform size and high purity.

Table 1-1. Review of extraction silica methods

Names of Extraction methods	Condition used	Product	Refrencess
Sol-Gel	ΔpH	Mesoporous silica	[38]
Stöber	Concentration of gold or silver metal	Silica Nanoparticles	[39]
Precipitation	ΔpH	Silica gel	[40]
Aggregation	(ΔpH and different additions of PVP)	Silica colloids	[41]
Plasma	Three different for electrolyte	Si particles	[42]
Emulsion	A fixed oil–water ratio	Nano-silica particles	[43]
Combustion	Δ Temperatures	Mesoporous silica nanoparticles	[44]
Alkali extraction	Δ Ph	Silica	[45]
Ballmilling	Δ Temperature	Silica Nanoparticles	[46]
Thermal Decomposition	Δ Temperature	Silica	[47]
Wet chemical	Δmolar ratio	Silica Nanoparticles	[48]
Mmicroemulsion	Δ Temperature	Silica Nanoparticles	[49]
Spray pyrolysis	Ultrasonic and Δ pH	Silica Nanoparticles	[50]
Vapor phase hydrolysis	(ΔTemperature , ΔNitrogen gas)	Silica Nanoparticles	[51]
Hydrothermal	ΔpH	Silica Spheres	[28]

1.7.4. Sol – gel method

The sol-gel method is used to extract silica.Sol-gel is flexible and common away for the prepare of inorganic, organic networks such as glasses, films ,ceramics or powders[52]. For long time, sol-gel techniques have been used for manufacturing glasses and ceramics. The formation of sol-gel of mineral phases involves starting from soluble molecular precursors, following an polymerization inorganic reaction[53]. The reaction is at room temperature, a wide range of pH/ionic strength conditions and in water or organic solvents. In 1950, make the sol-gel silicate powders quite popular , and transition from a liquid (solution or colloidal solution) into a solid (gel) [54]. Furthermore , sol-gel process is widely used to produce pure silica particles due to its ability to control the particle size, size distribution and morphology. The method for sol-gel process includes four main steps [55]as shown in Figure 1-3.

- The first step is to form the solution by mixing the suitable solvent with the catalyst starting material.
- The precipitating agent will be added dropwise with vigorously stirring for a few hours.
- The aging process will be done at room temperature.
- The sol-gel will be left and after that will be dried to remove the excess water. This step is to eliminate the trace amount of the solvents in the gel.

That found three different forms of gel with virous temperature [56]

a) When using water as a solvent, the substances are known as an aqua sol or aqua gels, and when using alcohol, they are known as aquosol or alcogel.

b) The product that results from evaporating gels is known as xerogel.

c) Aerogels are the dried gels produced by supercritical drying of gels. High porosity and high pore volume are retained by the aerogel.

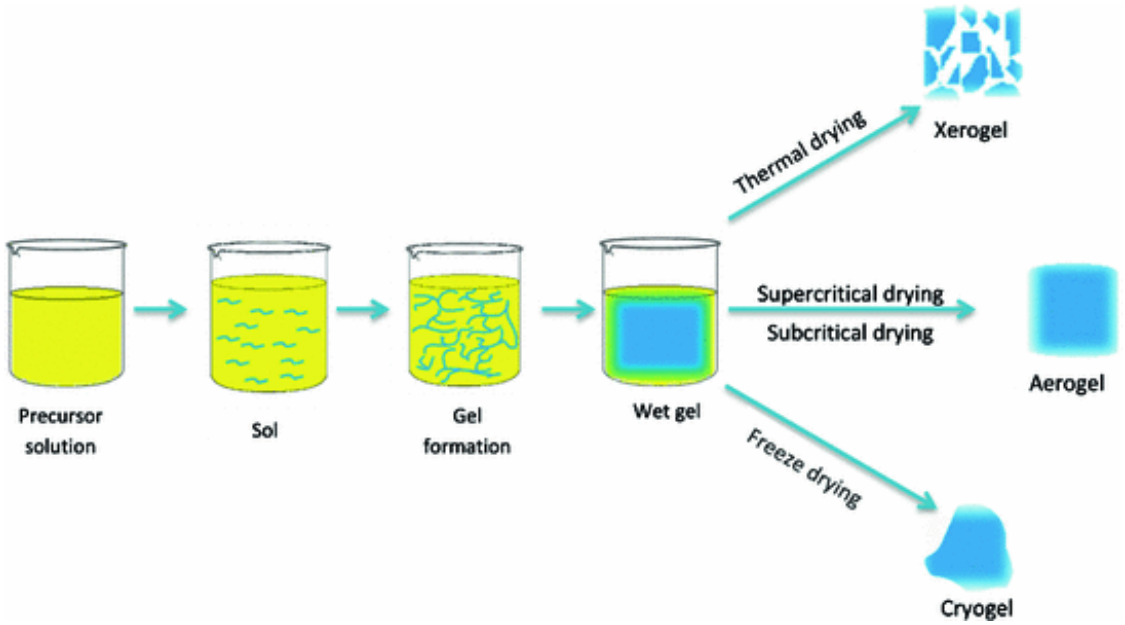

Figure 1.3. Different steps of sol gel process

The equation of sol gel process as shown in scheme 1-1 these reaction equationin reaction equations below[57]:

firstly , hydrolysis of the precursor produces a sol of soluble

hydroxylated monomer (equation 1).Secondly, the polymerization and phase separation to form a hydrated oxide hydrogel(equation 2). Finely,controlled removal of water from the wet gel by extraction or drying produces the dry, porous xerogel(equation 3).

$\equiv Si–OR + H_2O \longrightarrow \equiv Si–OH + ROH$ (equation 1)

$\equiv Si–OH + RO–Si\equiv \longrightarrow \equiv Si–O–Si\equiv + ROH$ (equation 2)

$\equiv Si–OH + HO–Si\equiv \longrightarrow \equiv Si–O–Si\equiv + H_2O$ (equation 3)

Scheme 1-1. The suggested reaction equation for the hydrolysis and condensation processin the sol gel process

1.7.5 Application of silica

Silica has been a key precursor in many different applications, including water treatment systems (adsorbents), catalyst supports, catalyst, drug delivery, agriculture, cosmetics, sensors materials, thin films and coatings for electronic

optical materials[58]. It is also used in modern industries, such cosmetics, biomaterial, and energy device industries. Some applications of silica are the main ingredients of ceramic industries, raw materials for solar cells [59] and cement mixture. Silica in nanocomposite bioactive materials was applied in medicine like bone tissue repair[60], pigents pharmaceuticals , photo catalyst support, filler material for polymer material modification,adsorbent of industrial waste and adsorbent of plant nutrients[61].

1.8. Sources of silicon compounds

Silicon in soil and plants; The most of silicate minerals are locked up in recalcitrant and only a much smaller fraction is available for plants which are recycled to the soil solution with the decay of dead plant material and may again be absorbed by plants[62]. Soil is commonly present in carbonaceous rocks such as limestone and carbonites, while rocks such as basalt and orthoquartzite contain high concentrations of Si (23%–47%). Si in plant the most included grain crops (wheat, rice and sugarcane). Rice husk is a agricultural practices and is the main concern silica (SiO_2) [63].

1.8.1. Silicon forms in soil

Silicon is the second most abundant element in the earth's crust with approximately 28% by weight. The Si availability in soils varies strongly with soil type and composition of a solid phase (primary and secondary minerals and amorphous form) and a liquid phase (monosilicic acid, polysilicic acid and complexed forms)[64]. Silicon occurs in many forms in the soil. The solid forms of soil Si include crystalline forms of primary (e.g. Feldspars, quar, micas) and secondary silicate minerals (e.g., the different clay minerals), as well as poorly crystalline minerals or microcrystalline (e.g., imogolite , allophane, opal-CT). Amorphous silica (ASi) includes both Si of mineralogical origins that is included in pyogenic oxides (e.g., iron oxides) and biogenic Si (e.g., photoliths) [65]as shown in scheme

1-2.

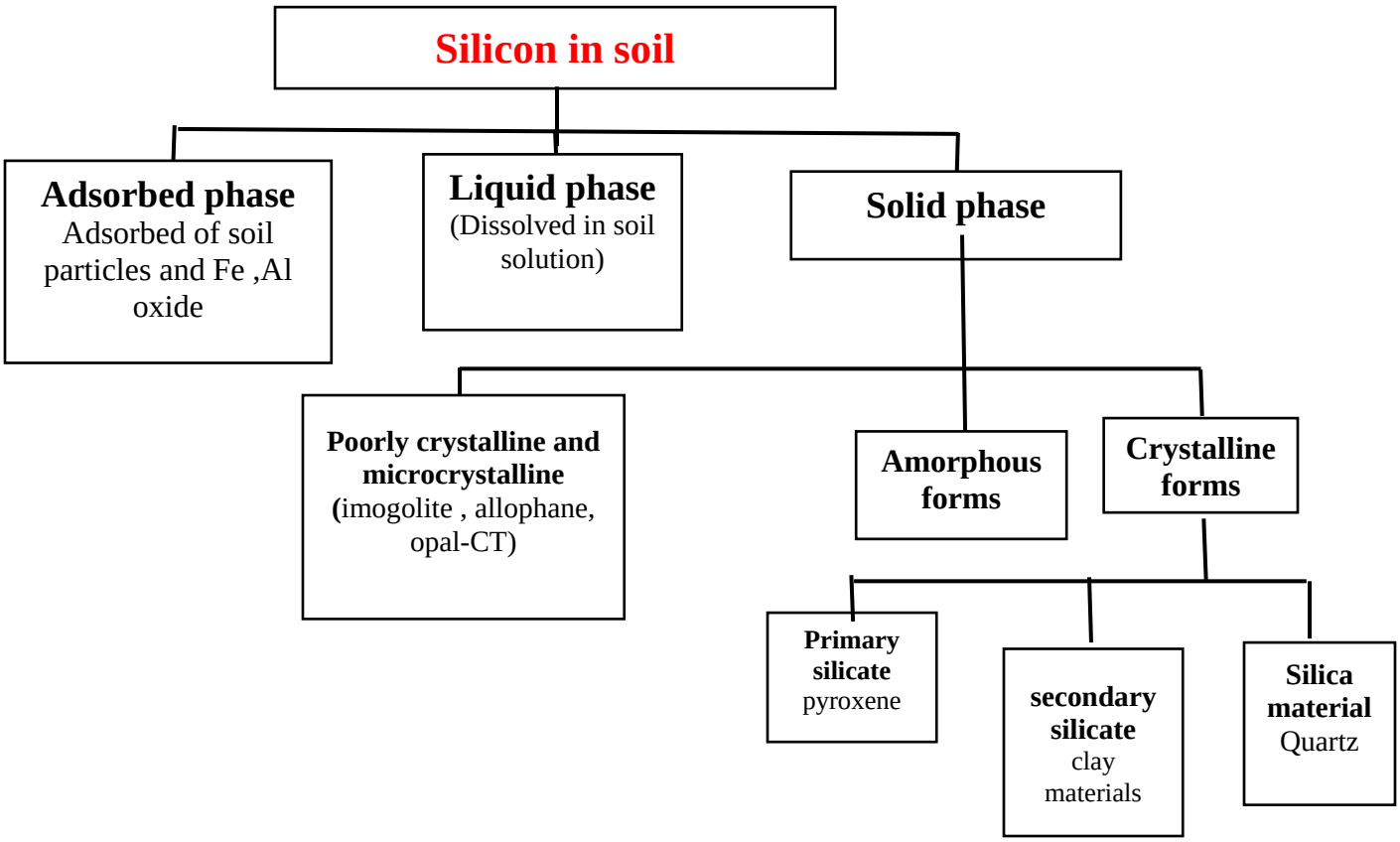

Scheme 1.2. Different forms of silicon in soil

1.8.2. Soil

Soil is define as a layer surface solid material that consists of the highest amount of inorganic mineral matter in form of rocks and earthly material i.e., 45%. and mostly in organic material of the dead remains of animals and plants is 5% by volume, liquids almost 25%, and gases are air is almost the same amount at 25%[66]. That provides the structural support to plants. It is varying greatly in their chemical and physical properties. Processes such as leaching, weathering and microbial activity combine to make a whole range of different soil types. That have most of elements make up approximately 99.6 % continental of the earth crust [67] as shown in Table 1-2.

Table 1.2. chemical composition in the earth crust[68]**.**

Elements	Percent%
Oxygen (O_2)	46.1 %
Silicon (Si)	28.2 %
Aluminum (Al)	08.2 %
Iron (Fe)	05.6 %
Calisum (Ca)	04.1 %
Magnesium (Mg)	02.3 %
Sodium (Na)	02.3 %
Potassium (K)	02.0 %
Others	0.50%

1-8-3. Types of Soil

Soil is divided into four categories, i.e., clay, sand, silt, and loam. Although different soils have a wide range of colors, textures, and other distinguishing features, there are only four types of soil particles that geologists consider distinct[69]. The quality of soil depends upon the amounts of sand, loam, silt, and clay that it contains, because varying the amounts of these particles results in very different soil characteristics[70]. Clay soil is fine-grained natural rock or soil materail that combines one or more clay minerals with of organic matter and metal oxides . Sandy soil has a light texture and loose structure, which causes rapid water drainage . Silt Soil is having a greater tendency to form a crust that is often very hard , it can become compact, which decreases its ability to infiltrate water in wet periods[71]. Loam soil is composed of most of the sand, silt, and a smaller amount of clay about a 20–40% concentration of sand, silt, and clay respectively [72]as shown in Figure 1-4.

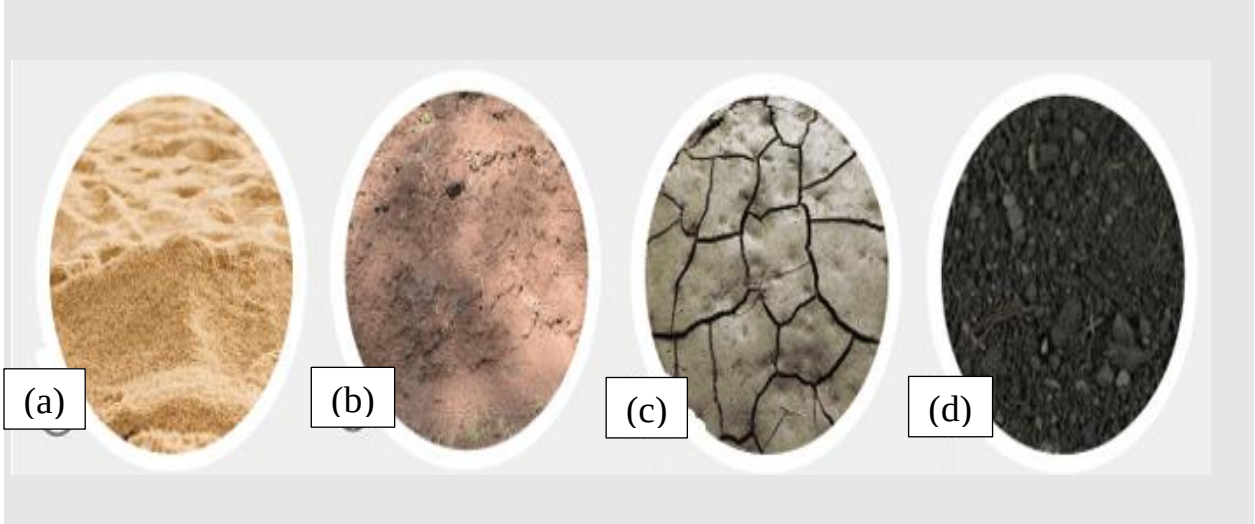

Figure 1.4. Different types of soil(a) Sandy soil, (b) Silt soil, (c) Clay soil and (d) Loamy soil[73]**.**

1.9. Modified Silica Compounds

Modified silica is prepared to improve its properties for specific applications. Key reasons include enhancing dispersibility in various media, introducing new functionalities, improving compatibility with other materials, and increasing surface area. These modifications allow for tailored performance in areas like catalysis, adsorption, and composite materials[74]. Modified silica compounds are materials depend on silica (SiO_2), whose surface, structure, or chemistry has been altered modified to improve specific properties. These modifications can enhance how silica interacts with other materials, such as organic reagent , resins, or even liquids. Silica particles are coated or chemically bonded with other molecules to improve compatibility with organic materials like rubber or plastics[75]. The Structural Modification have changes in the particle size, porosity, or morphology shape. Silica was incorporating functional groups (e.g., amines, thiols, epoxies) onto silica surfaces to enhance dispersion, increase surface area, or tailor mechanical properties [76]. Where , silica modified are often combined to create inorganic materials with diverse properties and applications. This combination can

result in materials with enhanced strength, thermal stability, and catalytic activity, depending on the specific ratios and preparation methods such as silica-alumina materials.

1-9-1 Inorganic silica

1. Alumina (Al_2O_3)

Silica modified with alumina is proved to be an active and selective catalyst. The high catalytic activity of these samples was due to the high content of surface acid sites, mainly of the Lewis type, and their optimal strength, as well as the mesoporous structure, which ensures rapid internal diffusion of the reactants [77]. Zeolites are microporous crystalline aluminosilicates are generally composed of silicon, aluminum and oxygen. They are effective esterification catalysts due to their high Brønsted acidity and ability to change physical and chemical properties [78] as shown in Figure 1-5.

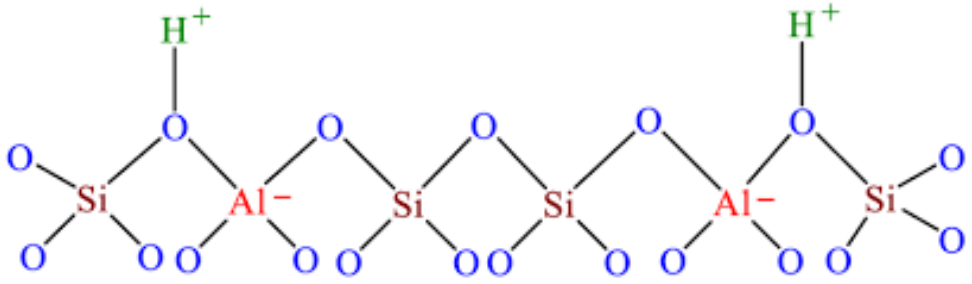

Figure 1-5. Linkage silica with alumina

2. Titania (TiO_2)

It is the simplest and friendly industrial for post-synthesis methodologies such as grafting and precipitation. However, the titania–silica mixed oxides involve the formation of the active TiO_2 species from titanium alkoxides deposited inside the pores of (ordered) silica's [79] as shown in Figure 1-6. It is structurally different Ti- and Si-containing provides better catalytic performance in these reactions than Ti-substituted molecular sieves (TiS and TiMCM-41) and silica-supported titania

(Shell-type catalyst) [80].

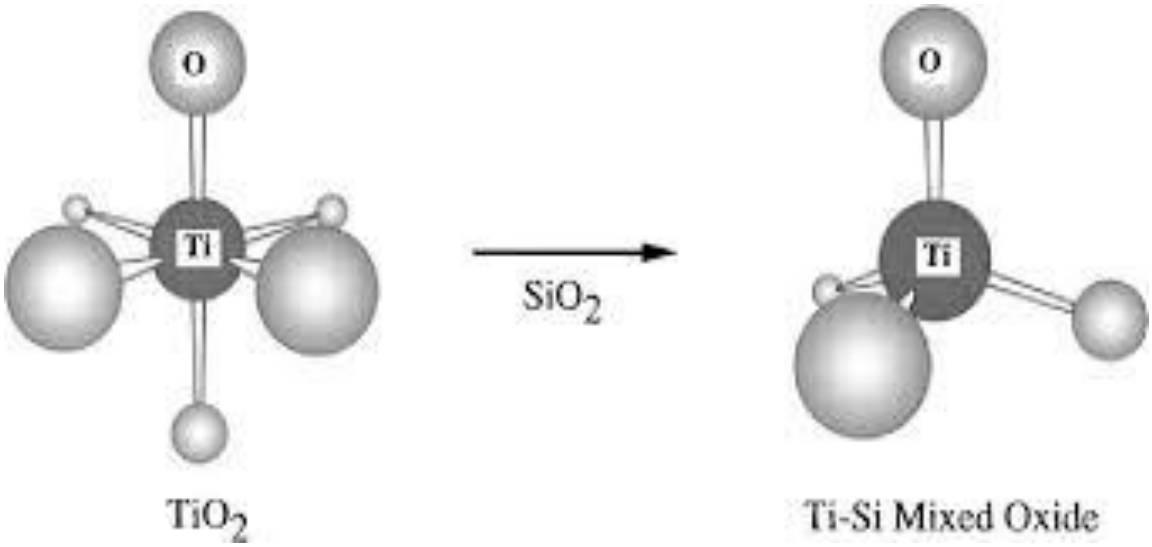

Figure 1-6. 3D shapes of Titania support with silica[81]**.**

1.9.2 . Organosilica

The introduction of organic groups into the silica molecule allows researchers to achieve customized properties of the molecules (hydrolytic stability, thermal stability)[82] .

In organic modification, organosilanes such as trimethyl(chloro)silane (TMCS), methyl(triethoxy)silane (MTES). And phenyl(triethoxy)silane (PTES] have been used to replace the -OH group with $-CH_3$ on the silica gel surface to ensure effective indicator fixation and to enhance the flexibility, hydrophobicity, hydrolysis resistance, and thermal stability of the film [83]

Silica functionalized with various reagents have been recently reported as efficient collectors for a wide range of metal ions, for example: Gallic acid , sulfasalazine , 2,3-dihyroxy benzaldehyde , 4-amino-2-mercaptopyrimidine ,Salicylaldehyde, 2,6-diamino4-phenil-1,3,5-triazine, 8-hydroxyquinoline, 4-acetyl-3-hydroxyaniline, and Benzyl-L-Cysteine . Most of these reagents are immobilized using silane

coupling agents as linkage to silica surfaces. Selectivity is difficult to achieve, although structuring ligands with affinities toward certain metals is possible. One of the reagents that a good selectivity is 1-nitroso-2-naphthol structure, silica has linkage with organic ligands [84] as shown in figure 1-7 .

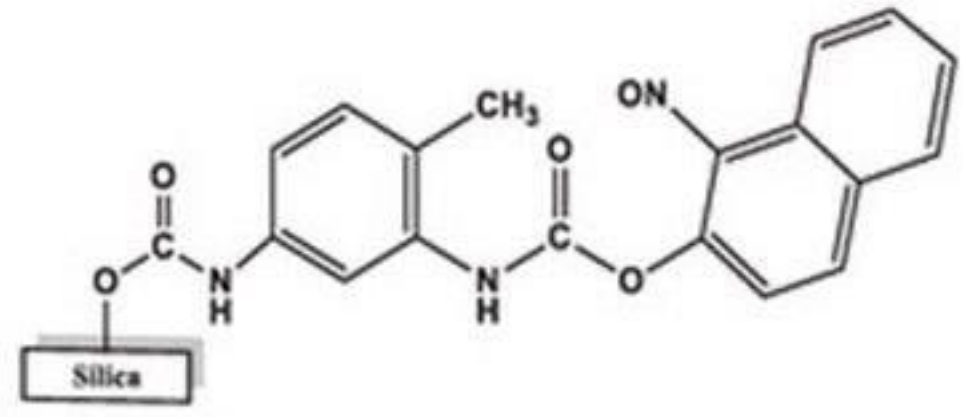

Figure 1-7. Silica linked with 1-nitroso-2-naphthol.

1.10. Aim of the study

The study aim to evaluate of viral local soil samples contents especially silica and the essential elements, and extraction of silica martial by sol-gel method from sandy soil sample and using the extracted silica to prepare new organosilica compounds. The extracted silica and organosilica compounds are used as a sorbents in solid phase extraction method to extract the elements from aqueous solutions.

Chapter Two

Experimental Part

2. Equipment and Chemical

2.1 Apparatus

The instruments used in this study can be seen in Table (2.1).

Table (2.1) Instruments uses in study

No	Instrument name	Mark	Place
1	Senstive balance	ABS 220 -4 electronic balance KERN / [Germany]	College of Science, University of Kerbala
2	FTIR Spectrophotometer	8400, Shimadzu [Japan]	College of Science, University of Kerbala
3	UV-Visible Spectrophotometer	Double Beam UV visible spectrophotometer - 1800, Shimadzu, [Japan]	College of Science, University of Karbala
4	Visible Spectrophotometer	Single Beam - Visible spectrophotometer Model 721, Faithful [China]	College of Science, University of Kerbala
5	XRD	Shimadzu X-ray Diffractometer	Beam Goster Taban Lab/ Iran
6	SEM - EDX	Axia Chemi SEM , Thermo Scientific Company [Holinda]	AlKhora Company/Baghdad
7	Oven	Model im 110 plus	College of Science, University of Kerbala
8	Hot plate Magnetic stirrer	LMS 1003, Labtech , Techco , LTD	College of Science, University of Kerbala

9	Muffle Furnace	ELF 11 / 14 B Carbolite, Ltd (United Kingdom)	College of Science, University of Kerbala
10	AFM	CSPM – AA3000	Beam Goster Taban Lab/ Iran
11	TEM	Philips CM12	Beam Goster Taban Lab/ Iran
12	BET	BEL BESORB MINI II	Beam Goster Taban Lab/ Iran
13	Shaker	Germany Orbit VRN -480 (England)	College of Science, University of Kerbala
14	pH – Meter	pH–meter, model H1271, at HANNA/ Romania	College of Science, University of Kerbala
15	Centrifuge	Model EBA -20, Germany	College of Science, University of Kerbala

2.2. Chemical Materials and Reagents

The chemical materials and reagents can be used as shown in Table (2.2).

Table (2.2) Chemicals materials and reagents used

No	Name of Compound	Chemical Formula	Supplier	Purity %	Molecular Weight ($g.mol^{-1}$)
1	Hydrochloric acid	HCl	THOMS	36.0 %	36.460
2	Sodium hydroxide	NaOH	(Merck)	96.0 %	40.00
3	Acetone	C_3H_6O	(Merck)	98.0 %	58.08
4	Ammonia	NH_3	(B.D.H)	99.0 %	17.031
5	1-Nitroso-2-naphthol	$C_{10}H_7NO_2$	(B.D.H)	98.0 %	173.16
6	Salicylaldehyde oxime	$C_7H_7NO_2$	(B.D.H)	98.0 %	137.135
7	Iron (III) chloride	$FeCl_3$	(B.D.H)	99.0 %	162.195
8	Absulute Ethanol	C_2H_5OH	THOMS	99.0 %	46.08
9	Methanol	CH_3OH	THOMS	99.0 %	32.04
10	Nickel (II) nitrite -6- hydrate	$Ni(NO3)_2.6H_2O$	(B.D.H)	96.0 %	290.693
11	Copper (II) nitrite -3- hydrate	$Cu(NO_3)_2.3H_2O$	(B.D.H)	96.0 %	241.602
12	Lead (II) nitrite	$Pb(NO_3)_2$	(B.D.H)	99.0 %	331.209
13	Chromium (III) nitrite -9- hydrate	$Cr(NO_3)_3.9H_2O$	(B.D.H)	99.0 %	400.148
14	Cobalt (II) nitrite -6- hydrate	$Co(NO_3)_2.6H_2O$	(B.D.H)	99.0 %	290.933

15	Cadmium (II) nitrite -4- hydrate	$Cd(NO_3)_2.4H_2O$	(B.D.H)	99.0 %	308.41
16	Potassium iodide	KI	MERCK	99.0 %	166.0028
17	Dimethylglyoxime (DMG)	$C_4H_8O_2N_2$	MERCK	99.0 %	116.120
18	Bismuth (III) nitrite	$Bi(NO3)_3$	(B.D.H)	99.0%	485.07
19	Pyrogallol	$C_6H_6O_3$	MERCK	97.0%	126.11

2.3. Preparation of reagent

2.3.1. 0.1% of 1-Nitroso-2-naphthol solution

The reagent (1-Nitroso-2-naphthol) solution with concentration 0.1% were dissolved 0.1 g of reagent in 100 g of distilled water.

2.3.2. Salicylaldehyde oxime (0.05 mol/L)

Prepared stock solution of Salicylaldehyde oxime reagent took amount 0.6713 g of reagent dissolved in 100 mL of distilled water and can prepare 0.01 to 0.04 mol/L by diluting stock solution with distilled water.

2.4. Preparation of standard solution

2.4.1. Iron (III) ion standard solution preparation (100mg/L)

The preparing of the standard iron (III) solution involved the dissolved of 0.3477g from iron (III) chloride in 100 mL os distilled water . The produced of solution has been utilized through dilution process by distilled water.

2.4.2. Preparation of hydrochloric acid (3mol /L)

The dilution of concentrated hydrochloric acid (36 % and sp.gr. 1.18 %) by dissolved 25.7 mL of the acid in 100 mL of distilled water . Hydrochloric acid can be used as a standard solution to prepare concentrations of 2 and 0.1 mol /L using

dilution with distilled water.

2.4.3. Preparation of sodium hydroxide solution (0.1mol /L)

Prepare sodium hydroxide with concentration 0.1mol /L by diluting 0.4116 g in 100 mL of distilled water

2.5. Sampling of Soil Samples

Soil samples were collected from three locations in Karbala city as shown in Table 2.3. Two samples were taken from Al-Hussainiya village northeast of Karbala city , while one sample was taken from the desert area near Al-Razzaza Lake to the west of Karbala city. The soil samples were collected in December 2023. After collecting, samples were washed severail times with distilled water to remove impurities. After washing samples were filtered using filter paper and well dried in oven . The samples were then stored in coverd plastic container for later analysis using (EDX) analysis to determine their main components and the elements present in the soil samples before purifying them using HCl (3 mol/L). Figure 2.1 shows the sample, name and map of the study area, respectively.

Table 2.3. Type samples and location

Samples	Type of soil	Location of samples
ZA_1	Sandy	Desert area near AL-Razzaza Lake
ZA_2	Clay	Near the Al Husseiniya River
ZA_3	Loamy	Orchards in the Al Husseiniya district,

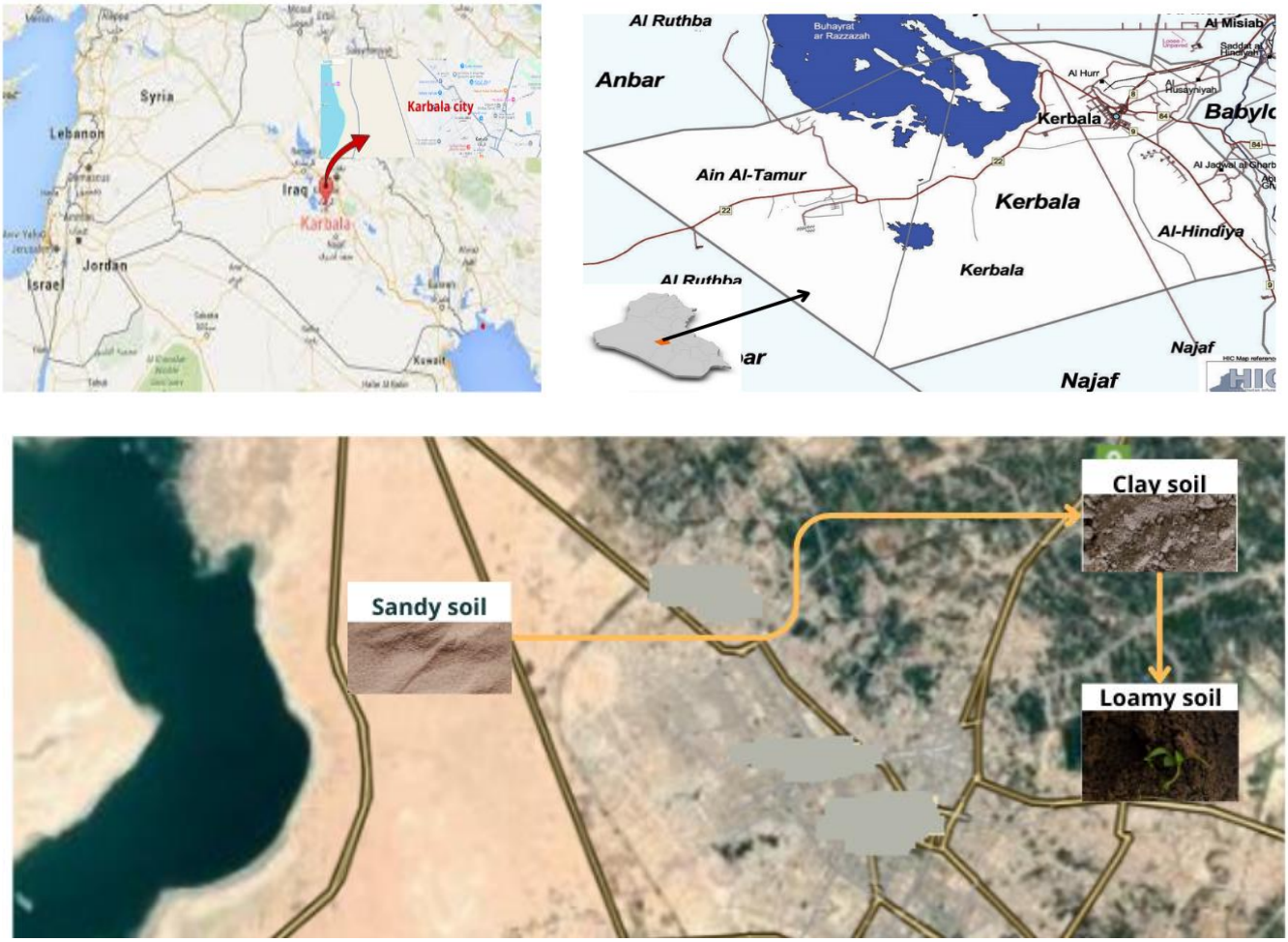

Figure 2.1 The soil sampling location and map of the study area in Karbala city

2.6. Extraction of silica from soil samples

Silica was extracted from local soil sample by using sol-gel method[85] as shown in scheme 2-1,2-2 .They were washed seven times with distilled water to remove adhering materials. They were then dried in an oven at 100°C for 24 h and sieved using a 100-mesh sieve. 6 g of samples were dissolved in 12 mL of 3M HCl, and the solution were transferred into a reflux system with continuous stirring at 90°C over night to separate other elements from the samples. Afterward, it was filtered, washed with distilled water to remove any remaining HCl and other salts, and then dried in an oven at 100°C for 24 h. The sodium silicate was prepared from sodium hydroxide to purify silica in titration 1:7 weight ratio from pure silicate residue with sodium hydroxide in a and heated in a muffle furnace at 600°C for 2 h using the alkali fusion method to get rid of organic impurities. After heating, the obtained dry sodium silicate (Na_2SiO_3) as shown in Figure 2.3 was diluted with distilled water and stirred on a hot plate at 250 rpm at 106°C. followed by titration of the solution with 2M HCl until the pH reached around 1–2 as tested with litmus paper and formation of a clean white gel of ($Si(OH)_4$). The silica gel was filtered using filter paper and washed multiple times with distilled water to remove NaCl from the solution. It was dried in an oven at 80°C for 24 h. The product of silica was ground to obtain 3.4 g and stored in covered plastic container and labeled ZA_1 is sandy soil, ZA_2 is clay soil and ZA_3 is loamy soil[86].

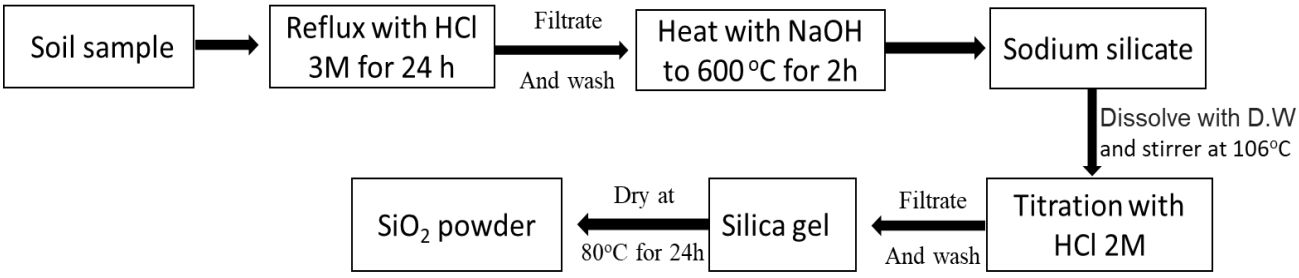

Scheme 2.1. The extraction silica from local samples

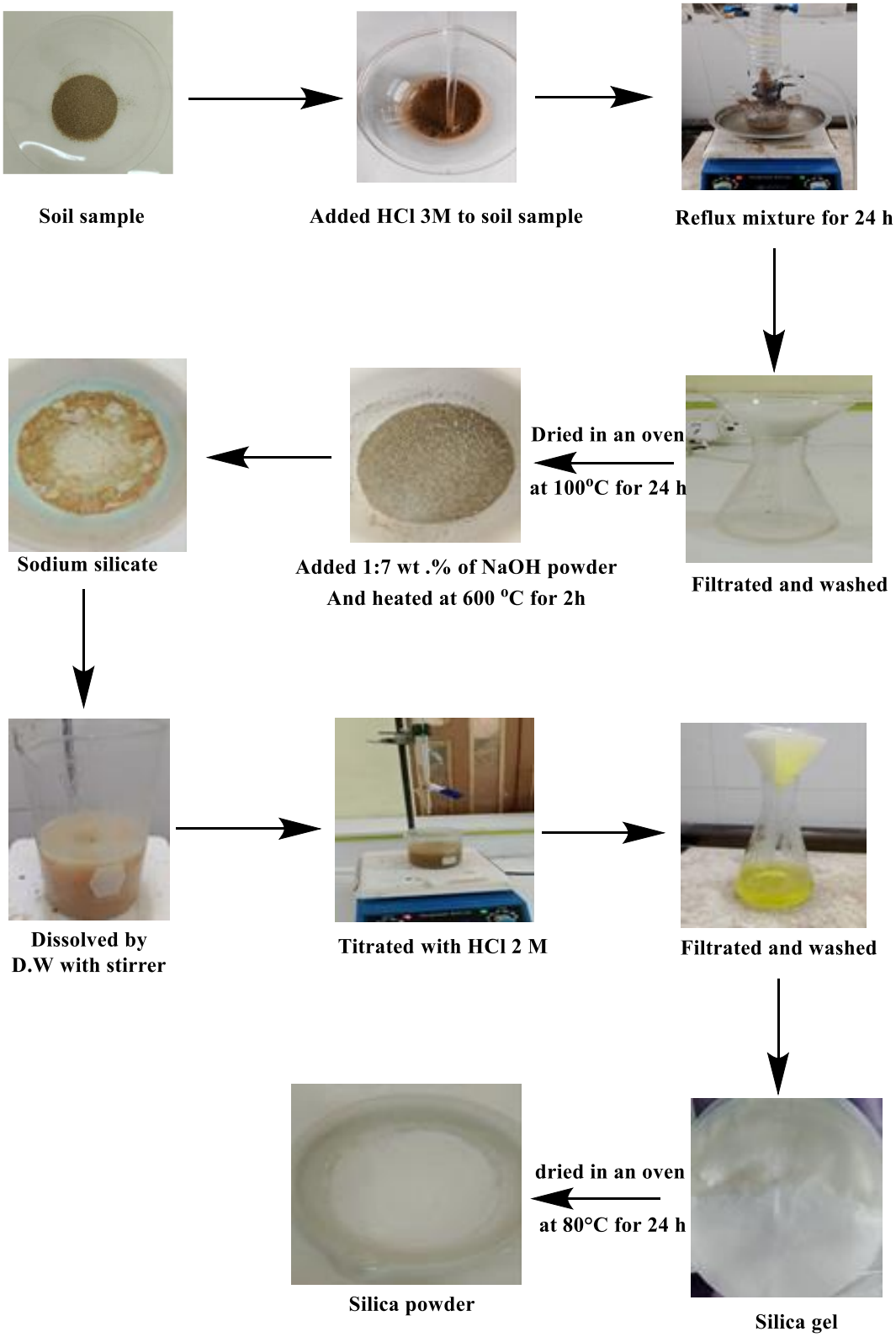

Scheme 2.2 . preparation of silica by sol – gel method

2.7. Pre elementery testing

Pre elementery study of set of metals with different reagents were testing with silica to determine surface ability of silica for the removal metal complex from aqueous solutions and apperanse result in Table 2.4.

Table 2.4 . pre elementery testing metals with silica

Metals + Reagents	Result	Apperance
Cu^{2+}+ KI+ SiO_2	+ve	Red brown ppt
Cu^{2+}+ KI+ SiO_2+ pH(acid)	+ve	Yellowish brown ppt
Cu^{2+}+ KI+ SiO_2+ pH(bace)	+ve	Red brown ppt
Pb^{2+}+ KI+ SiO_2	+ve	Yellow ppt
Pb^{2+}+ KI+ SiO_2+ pH(acid)	-ve	Clear
Pb^{2+}+ KI+ SiO_2+ pH(bace)	-ve	Clear
Bi^{2+}+ Pyrogallol+ SiO_2	+ve	Green yellow ppt
Bi^{2+}+ Pyrogallol+ SiO_2+ pH(acid)	+ve	Darck brown ppt
Bi^{2+}+ Pyrogallol+ SiO_2+ pH(bace)	+ve	Darck brown ppt
Ni^{2+}+ Dmg + SiO_2	+ve	Dark pink ppt
Ni^{2+}+ Dmg + SiO_2 + pH(acid)	+ve	White ppt
Ni^{2+}+ Dmg + SiO_2 + pH(bace)	+ve	Dark pink ppt
Co^{2+}+ Dmg + SiO_2	+ve	Yellow brown ppt
Co^{2+}+ Dmg + SiO_2 + pH(acid)	+ve	White ppt

Co^{2+}+ Dmg + SiO_2 + pH(bace)	+ve	Yellow brownish ppt
Cr^{3+}+ Dmg + SiO_2	+ve	White ppt
Cr^{3+}+ Dmg + SiO_2 + pH(acid)	+ve	Grownish ppt
Cr^{3+}+ Dmg + SiO_2+ pH(bace)	-ve	Clear ppt
Fe^{3+}+ Salicylaldehyde oxime + SiO_2	+ve	Red brown ppt
Fe^{3+}+ Salicylaldehyde oxime + SiO_2+ pH(acid)	+ve	Red ppt
Fe^{3+}+ Salicylaldehyde oxime + SiO_2+ pH(bace)	+ve	Red ppt

2.8. Iron (III) with salicylaldehyde oxime extract by solid phase (silica) method.

The complex is better able to bind to silica surfaces, the adsorption is more selective for iron and increases the adsorption efficiency to the silica surface. Using to procedures of solid phase extraction method, (2mg/2ml) of Fe (III) solution (1000 mg/L) were added to 2mL of (0.01 mol/L) salicylaldehyde oxime to yield dark violet colored solution. The pH was adjusted of complex solution to 7 using 0.1 mol $.L^{-1}$ HCl or NaOH solution .It was resulting as red ppt complex with maximum absorption wavelength 520 nm. After that , silica was added to the solution . Silica extracted from ZA_1 was used to sorbent materail to extract iron (III) complex with 0.1 g of solid phase (silica) and it was shaken for five minutes the covalent binding between iron (III) complex and silica as shown in Scheme 2.3 . The mixture was filtered through conical flask to separate the silica particles, then

residual of metal complex was measured absorbance at maximum wavelength of 520 nm.

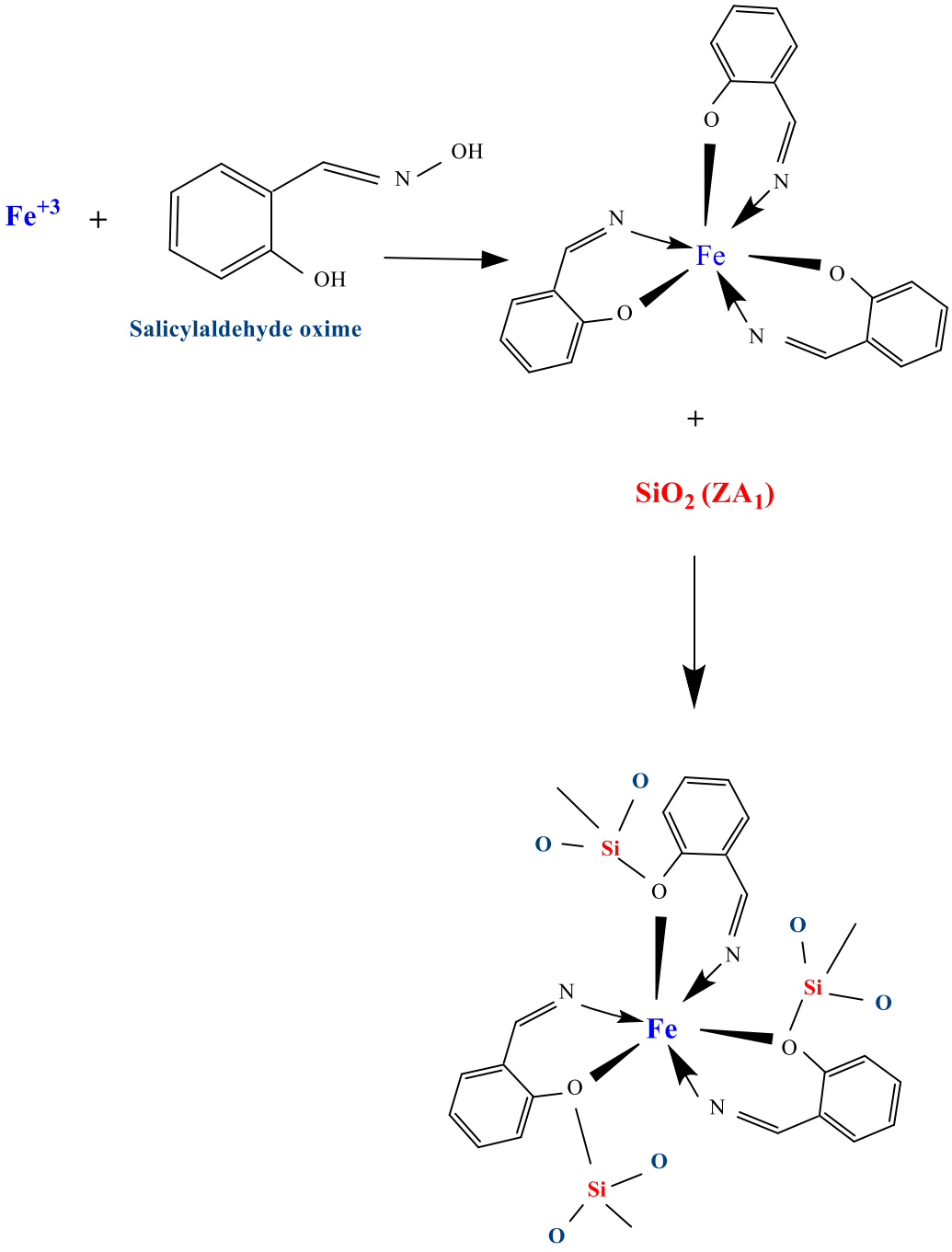

Scheme 2.3.Proposed reaction equation of Fe(III) – Salicylaldehyde oxime complex extraction by silica.

2.9. Preparation of modified silica (organosilica)

Modified silica was prepared from extracted silica from sandy soil sample and organic reagent solution (1-nitroso -2- napthal solution) as shown in Figure 2.3

2.9.1.Preparation of 1-nitroso -2- napthal solution

The 1-nitroso -2- napthal reagent solution was synthesized from a 0.1% of 1-nitroso-2-naphthol solution. A 0.1 g of the reagent was dissolved in 10 mL of acetone and 8 mL of concentrated ammonia. The mixture was diluted to 100 mL with distilled water.

2.9.2. Preparation of organosilica (1-nitroso -2- napthal silica)

The organosilica was prepared from 4 g of extracted silica from $ZA_1$and dissolved in 100 mL with distilled water as shown in scheme 2.4,2.5 and 2.6 . Then it was added to the organic reagent solution (0.1% 1-nitroso-2-naphthol solution). It was mixed on a magnetic stirrer for 24 h. The product was filtered, washed with distilled water, and dried in an oven at 100^{o}C for 24 h . After dried, organosilica weight is 3.8 g and kept in cover plastic container for later use charecterazation and applications.

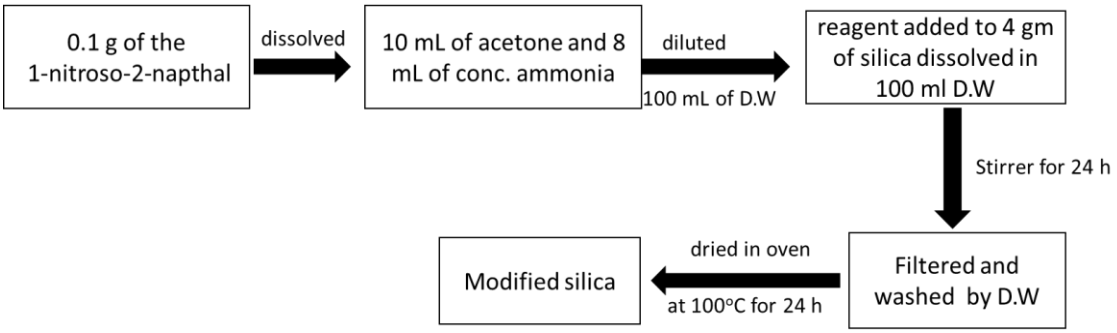

Scheme 2.4. Preparation steps of 1-nitroso -2- napthal silica

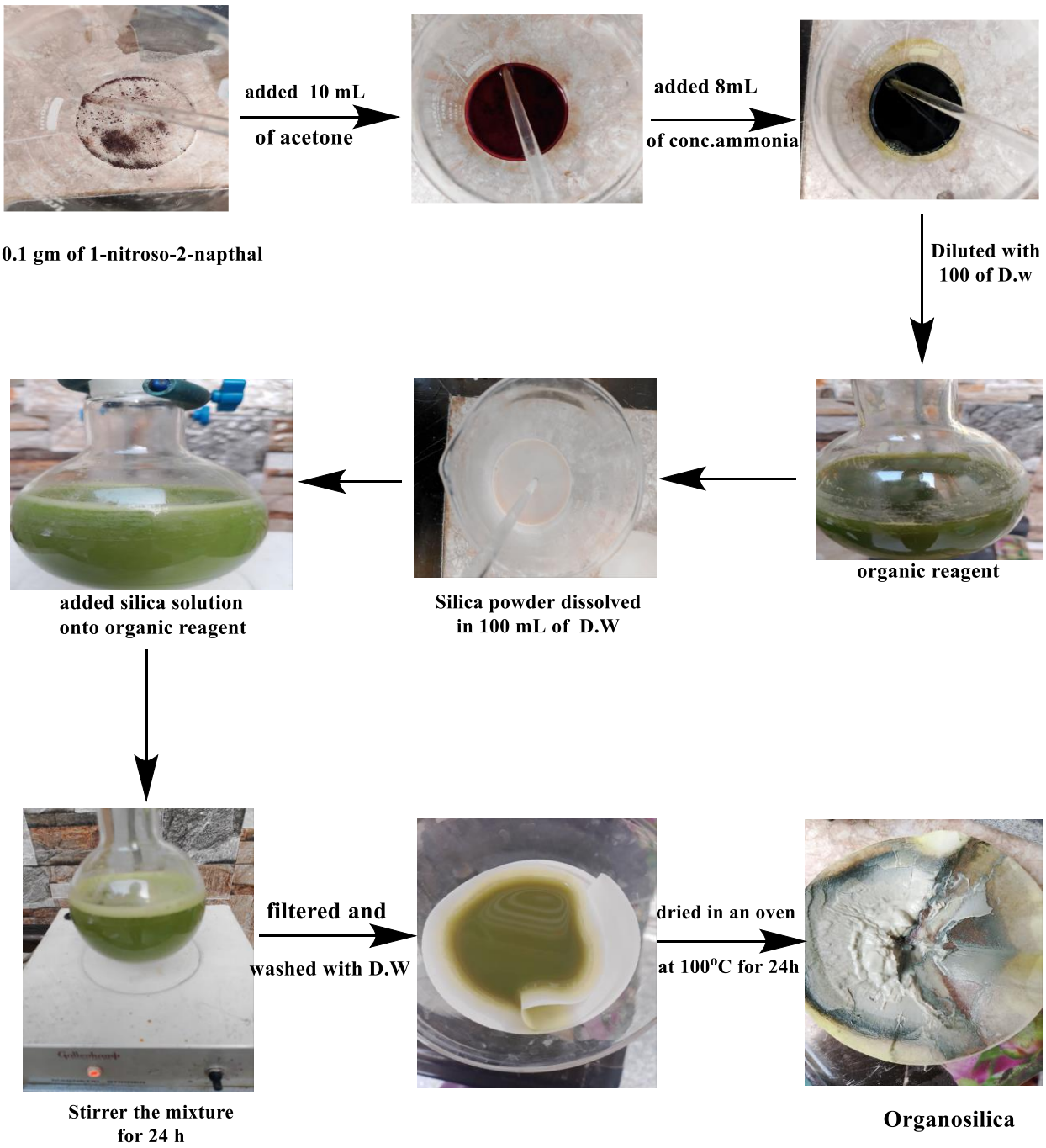

Scheme 2.5. preparation of 1-nitroso -2- napthal silica.

SiO_2 (Soil) + 2NaOH ⟶ Na_2SiO_3 + H_2O

Na_2SiO_3 + 2HCl + H_2O ⟶ $Si(OH)_4$ + NaCl + H_2O

$Si(OH)_4$ ⟶ SiO_2 + H_2O

Step 2 : Prepare of 1-nitroso-2-napthal solution

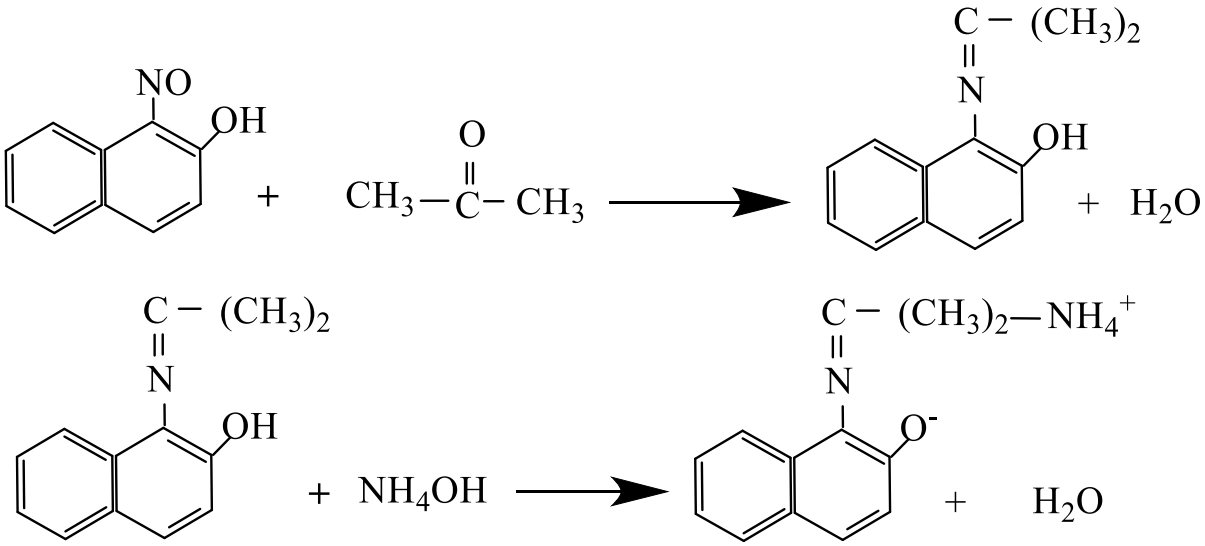

Add silica extracted from $ZA_1$to 1-nitroso-2-napthol solution

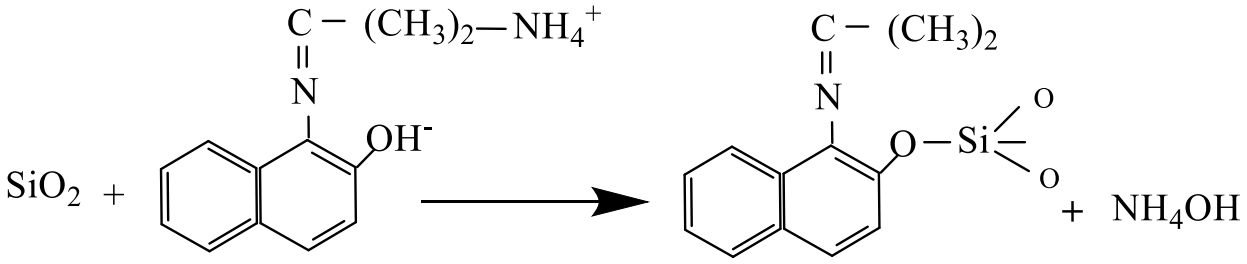

propsed stracture of 1-nitroso-2-napthal silica

Scheme 2.6 Mechanism synthesis steps of silica and organosilica

2.10. Organosilica as sorbent surface with Iron (III) Salicylaldehyde oxime complex

It was prepared Fe (III) solution with (50 mg/1000 mL) , where it was added 2mL of Fe (III) solution to (2mL) of 0.01 mol/L of salicylaldehyde oxime reagent to yield dark violet colored solution . The pH was adjusted to 7 using 0.1 mol $.L^{-1}$ HCl and NaOH solution .It was resulting as red ppt complex with maximum absorption wavelength 520 nm.0.1 g of organosilica was transferred to 4 mL of the Fe (III)-Salicylaldehyde oxime complex solution. The mixture is then shaken at an agitation speed of 200 rpm for 10 min to ensure effective interaction between the sorbent (organosilica) and iron (III) complex as summarized in Scheme 2.7.Finelly, the mixture was filtered to elemente surface sorbent (organosilica), and it is measured the absorbance of residue (Iron (III) complex) with amiximum wavelength of 520 nm.

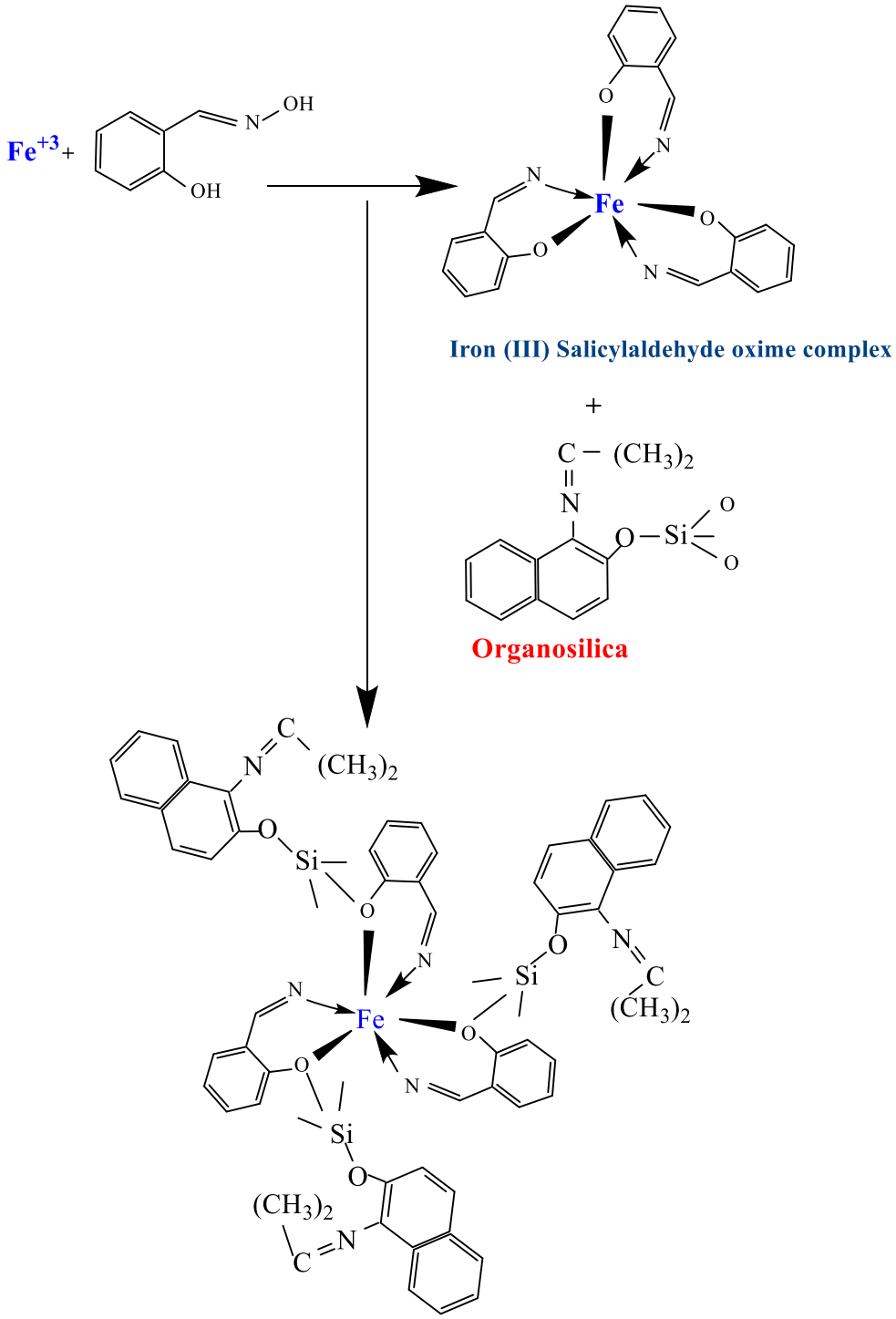

Scheme 2.7. Proposed mechanisim reaction of Fe(III) – Salicylaldehyde oxime complex with sorbent surface organosilica method.

2.11. Calibration curve of Fe (III) - Salicyaldehyde oxime complex

The calibration curve of Fe (III) - Salicyaldehyde oxime complex was constructed under optimum conditions at pH 7 and temperature 40^{o}C . The absorbance was measured at 520 nm against Fe (III) - Salicyaldehyde oxime complex prepared in similar conditions. Fe (III) complex was indicated increasing the absorbance with increased concentration of Fe (III) complex in different ranges of concentration from 6 to 70 mg.L^{-1} at the linerty line as shown in Figure 2.5, the calibration curve plotted between concentration of Fe (III) complex and. Absorbance [87].

Table 2.5 Calibration curve of the concentration iron (III) - Salicyaldehyde oxime complex

Concentration of Iron (III) (mg.L^{-1})	**Mean of Absorbance ±SD**
05	0.008 ± 0.00100
10	0.016 ± 0.00124
20	0.029 ± 0.00047
30	0.045 ± 0.00124
40	0.058 ± 0.00081
50	0.073 ± 0.00124
60	0.085 ± 0.00081
70	0.101± 0.00169

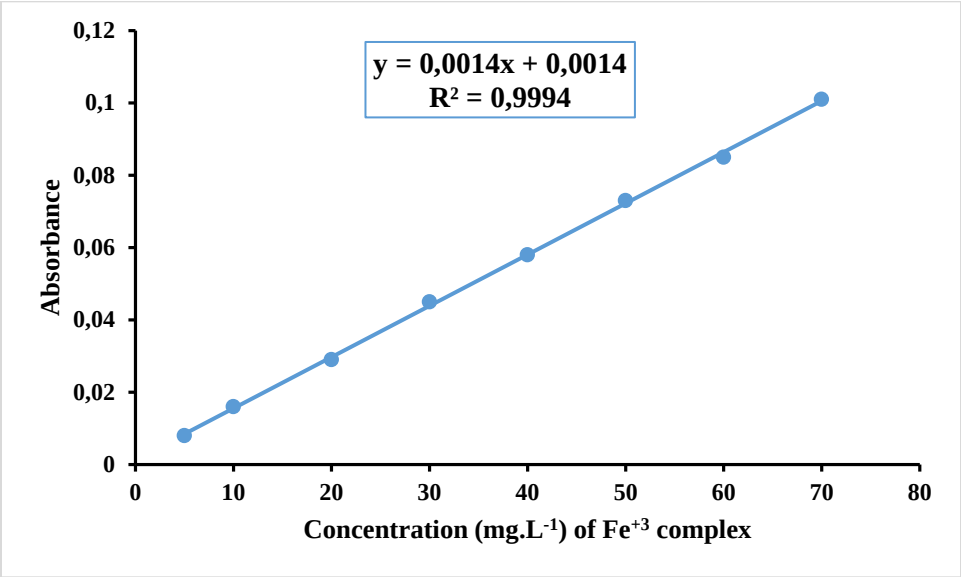

Figure 2.2 . Calibration curve of Iron (III)- Salicyaldehyde oxime complex.

2.12. Pharmaceutical samples containes Iron (III) ions.

A set of pharmaceutical samples including (Hemafer, Ferblex, Ferimax, Akourose ampules and Sorbifer Duroles tablet) containing iron ions were used most important application for extraction iron ions by using a solid phase (silica or organosilica). The samples were prepared at concentration (25 mg/L) with optimum condition at (pH 7 , concentration of reagent 0.04 mol/L and temperature 35 ^{o}C), and it was added reagent to the test tube. the absorbance of yielding was measured at a maximum wavelength of 520 nm before adding the solid phase. 0.1 g of silica or organosilica was used to extract iron ions from the pharmaceutical samples and shaken using shaker for 10-15 minutes. The mixture was filtered, and the absorbance of the residue was measured at a maximum wavelength of 520 nm.

2.13. Elution of Iron (III) complex from (Silica and Organosilica) by liquid solid extraction (LSE)

After adsorption Iron (III) complex solution by solid phase silica or organosilica . It is difficult to elute the iron complex from silica or organosilica because the iron is bound to the reagent, so it is not completely eluted, but is eluted partially. It was used set of solvent (methanol, ethanol and distilled water) to deadsorbent Iron (III) complex from solid phase. 0.05 g of solid phase were added to 2mL of solvent and transferred this mixture solution in cover plastic tube to seprate by centrifuge at 10 min . After sepration the absorbance of iron (III) complex solution was measured using visible spectrophotometer at 520 nm.

Chapter Three

Results and Discussion

3. 1. Introduction of Silica extracted

Soil samples were collected from different areas from Karbala city, silica was extracted using sol-gel method [88] The extraction method involved washing, drying, and treating soil samples with hydrochloric acid (3 mol/L). Pure silica was titrated to sodium hydroxide (1:7) and burned at 600°C to produce sodium silicate. It was then dissolved and titrated with hydrochloric acid (2 mol/L) until the pH reached 1-2 to produce silica gel. The silica was then dried in an oven to produce silica powder. The silica content was high in Sample ZA_1 (sandy soil), and this res\ult is close to the results obtained researches Basra [89] . Silica from sandy soil was used as an adsorbent to extract iron (III) complex from aqueous solutions using the solid-phase extraction method under optimum condition including pH (2-11), concentration of salicylaldehyde oxime: (0.01-0.05) mol/L, amount of sorbent 0.025-0.125) g, different temperature (25- 50 °C) and shacking time (5 -30) min. After that , the silica was then applied to pharmaceutical samples contains iron (III) ions to be extracted at same method and conditions.

This part includes characterization of silica and experimental optimization of Iron (III) salicylaldehyde oxime complex. Several techniques used in this part to charecterize silica including:

- Scanning electron microscopy (SEM) determine the surface morphology, size and crystalline nature of silica sample produces
- EDX determine the percent's of elements in the three samples before and after extraction.
- X-ray diffraction is technique that it is used to determine the structure of the samples and understand the crystalline or amorphous nature of materials.
- Fourier Transform Infrared Spectroscopy (FTIR) to determine functional groups of the samples

- Surface area analysis measures the total surface area of particles in a samples, providing insights into properties such as reactivity and dissolution rate.
- Atomic force microscopy (AFM) is studying the structure and properties of solid surfaces with subnanometer spatial resolution.

Silica can also be used for adsorption of specific heavy metals from wastewater [90], and used efficient adsorbing material for separation of metals from solid-phase extraction (SPE) . Silica was stable and insoluble porous matrix having suitable active groups typically organic groups that interact with metal ions. Silica is an ideal support for organic groups because it is a stable under acidic conditions and non-swelling inorganic material and has high mass exchange characteristics and very high thermal resistance. It was used to adsorbent Fe (III)- salicylaldehyde oxime complex from aqueous solutions [51].

3.1.1. Characterization of Silica extracted

3.1.1.1. Fourier Transform Infrared Spectroscopy (FTIR)

Infrared spectroscopy (IR spectroscopy) is used to determine functional groups of the samples as shown in (Figure 3.1). The bands at spectral regions between 3500-3300 cm^{-1} are characteristic for hydroxyl groups (O-H; stretching vibration) [91] .The adsorption wave number at 1620 cm^{-1} to the O-H bending vibration and peak found at wavenumber 1100 to asymetery Si-O-Si, while the wave number at 961 cm^{-1} assigned to Si-O groups of the stretching vibration [92]Moreover,the peak presence at wave 798 cm^{-1} indicates the vibrational strain of the Si-OH bond (silanol) in the amorphous SiO_2 structure. Finelly, the peak at wave number 475 cm^{-1} refer to the O-Si-O (siloxy) bending vibrations [93] .

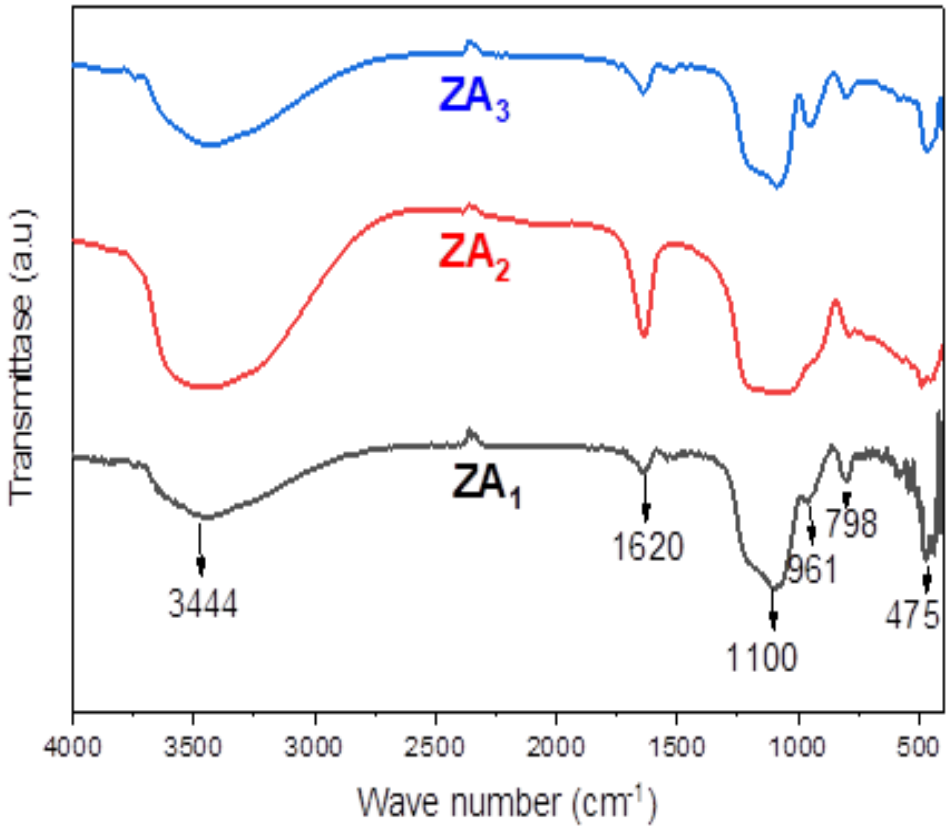

Figure 3.1. FTIR spectrum of SiO_2 samples ZA_1, ZA_2 and ZA_3

3.1.1.2. Specific surface area (BET) analysis of silica

The physical adsorption isotherm is the dependence of the amount of adsorbed substance on the equilibrium pressure or equilibrium concentration at a constant temperature. This method is used for calculate some morphological parameters: surface area, pore size and pore volume. The empirical classification of physical adsorption isotherms according to the IUPAC classification [94] are shown in Figure 3.2.

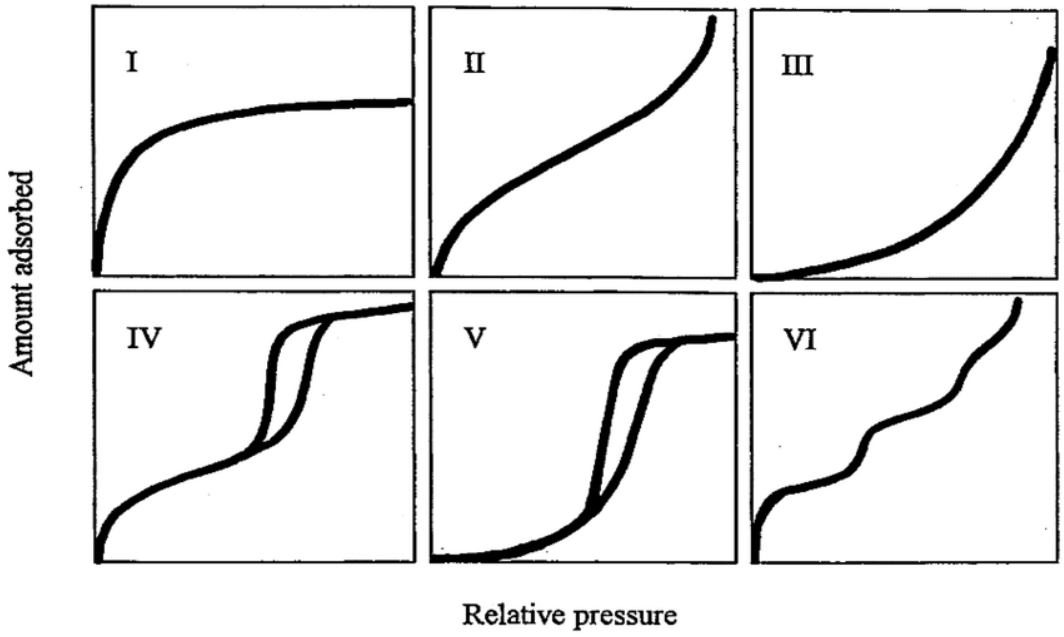

Figure 3.2. IUPAC classification physical adsorption isotherm [95]**.**

Type I characterizes adsorption on microporous materials. Isotherms of types II and III are typical for microporous materials with strong and weak adsorbate-adsorbent interaction, respectively. Types IV and V having a hysteresis loop, reflect the process of capillary condensation in mesoporous. The convex and concave nature of the initial section indicates respectively, strong and weak adsorbate-adsorbent interaction. The isotherm of a stepped type (type VI) reflects layer-by-layer filling of the surface with adsorbate molecules. This type of isotherm is extremely rare in practice and is observed during nitrogen adsorption on some types of activated carbon [96].

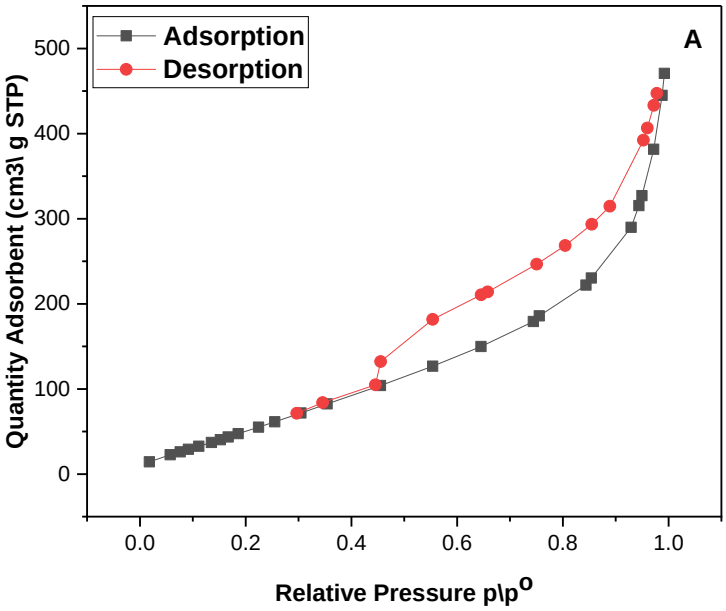
Adsorption
Desorption
A
Quantity Adsorbent (cm3\ g STP)
500
400
300
200
100
0
0.0
0.2
0.4
0.6
0.8
1.0
Relative Pressure p\p^o

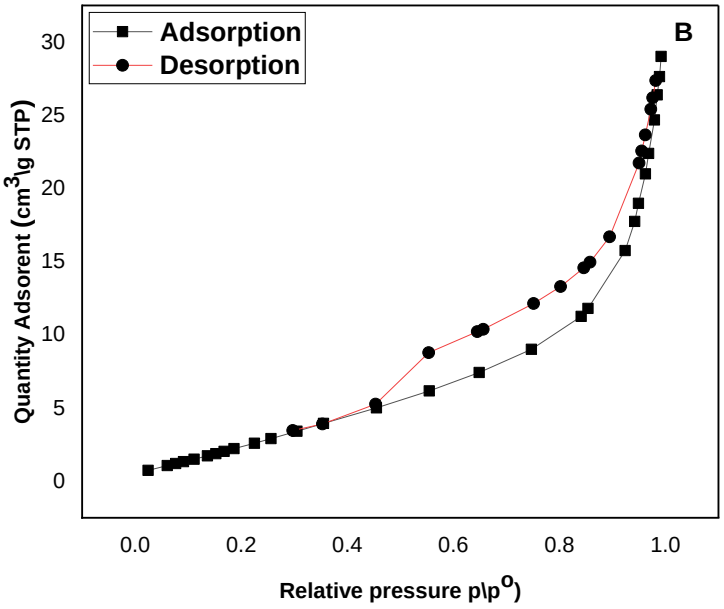
Adsorption
Desorption
B
Quantity Adsorent (cm3\g STP)
30
25
20
15
10
5
0
0.0
0.2
0.4
0.6
0.8
1.0
Relative pressure p\p^o)

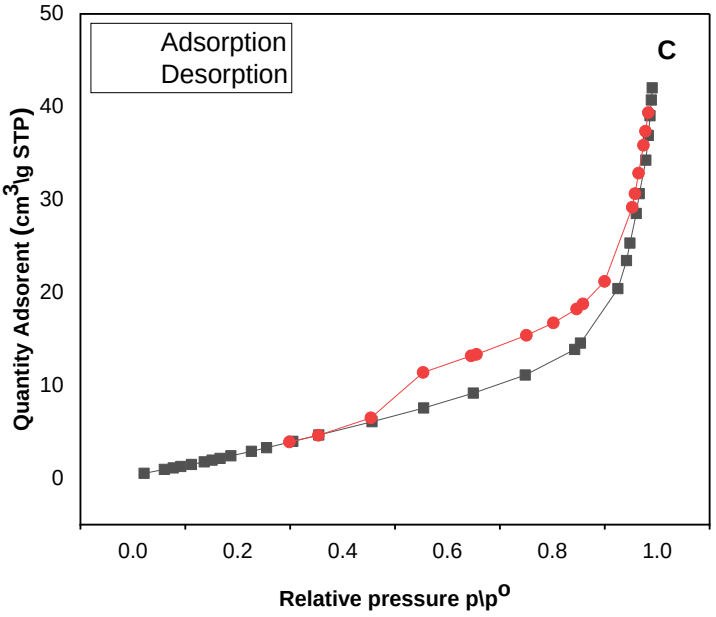

Figure 3.3. Nitrogen adsorption and desorption isotherms of amorphous silica of three samples (A-ZA_1, B-ZA_2 and C-ZA_3).

Table 3.1. Surface area analysis (BET) of ZA_1, ZA_2, ZA_3.

Samples	Specific surface area S_{BET} (m^2/g)	Average pore volume Vp (cm^3/g)	Mean pore diameter Dp (nm)
ZA_1	252.710	0.781500	11.207
ZA_2	12.767	0.047463	13.611
ZA_3	19.778	0.070416	13.023

The BET specific surface areas, calculated using the parameters obtained from the isotherms are summarized in Table 3.1 for each amorphous silica studied by sol-gel method from different type of samples. The pore dimeter was ranged from (11 nm to 13 nm), indicating to silica produced is mainly mesoporous According to the International Union of Pore and Applied Chemistry, a mesoporous material is a

material whose pores measure less than 50 nm in diameter (pores 2 nm −50 nm)[97] are shown in (Figure 3.3). The surface area are various from 12.7 to 252.7 m^2/g depending on the place of origin. The surface area is determined to be 252.7 m^2/g and the corresponding pore volume is 0.781500 cm^3/g of sand sample (ZA_1) which have high specific area that increase extraction percent when binding wih complex[98] .Compare with ZA_2 and ZA_3 that have low specific area and pore volume. while ZA_2 have largest pore dimeter at 13.6 from ZA_1 and ZA_3. Furthermore, the adsorption isotherms obtained for different amorphous silica samples. The characteristic shape and the maximum volume of nitrogen adsorbed obtained from the adsorption and desorption isotherms varied, depending on the type of nano- or micro-silica studied. In general, silica micro particles produced at temperature 77 K that the adsorption desorption isotherms indicated type IV and hysteresis loop H_3, this indicates the process of capillary condensation in mesoporous [99].

3.1.1.3. X-Ray Diffraction analysis

X-ray diffraction is a technique that it is used to determine the structure of the sample and understand the crystalline or amorphous nature of materials. The X-ray diffraction pattern of SiO_2 samples are shown in (Figure 3.4). The samples (ZA_1, ZA_2 and ZA_3) have exhibited high intensity peaks at around 20^oindicated the amorphous nature[100]. clay soil (ZA_2) has shown low intensity . Different sharp peaks appeared in ZA_2 sample at 32^o , 48^o ,58^o,78^o belong to (Al_2O_3), MgO, CaO and Fe_2O_3 respectively. Loamy soil (ZA_3) displayed small sharp peak at 48^o of Fe_2O_3.[101]

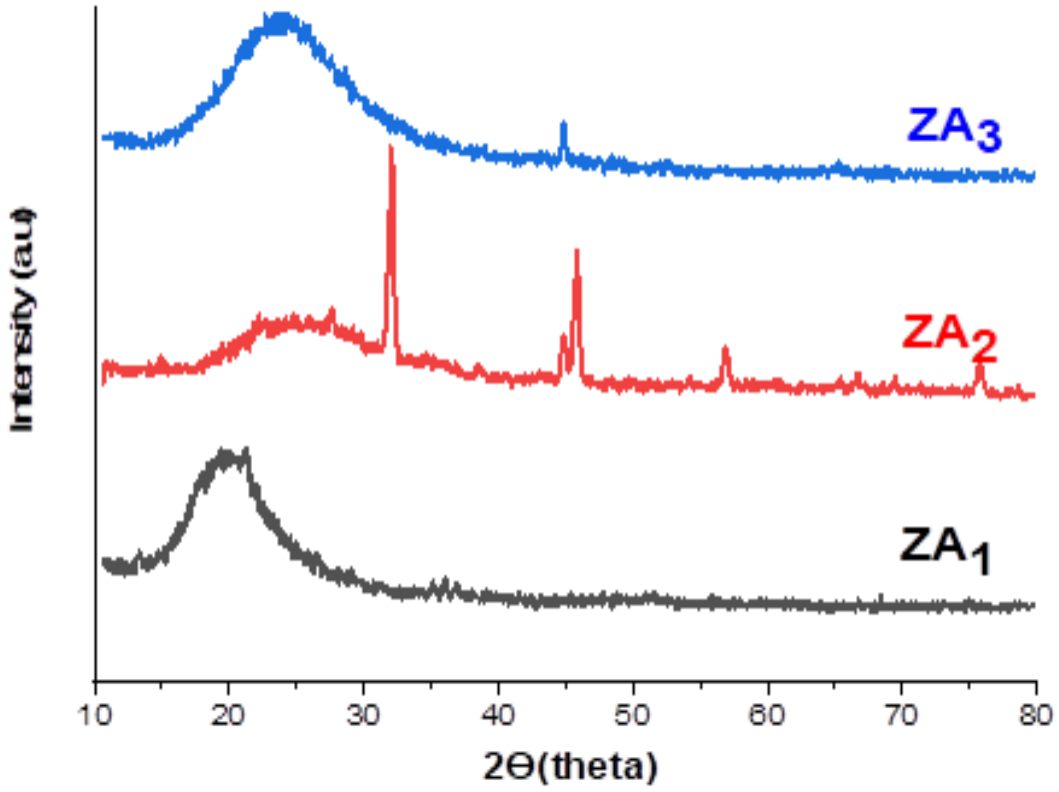

Figure 3.4. XRD patterns of SiO_2 samples ZA_1, ZA_2 and ZA_3.

3.1.1.4. Scanning Electron Microscopy (SEM).

This type of microscope gives information about the composition and topography of the sample from interaction of electrons with the atoms of the sample. This interaction gives signals that contain information about the surface. Scanning electron microscopy (SEM) has been used to observe the surface morphology, size and crystalline nature of silica sample produces by sol gel process. The morphology of silica particles was shown in Figure 3.5. (A,D), (B,E) and (C,F) images belong to ZA_1,ZA_2 and ZA_3 respectively. SEM images revealed that silica particles are highly agglomerated and spherical shaped and appear porous in nature. Where all images of different samples are similar.

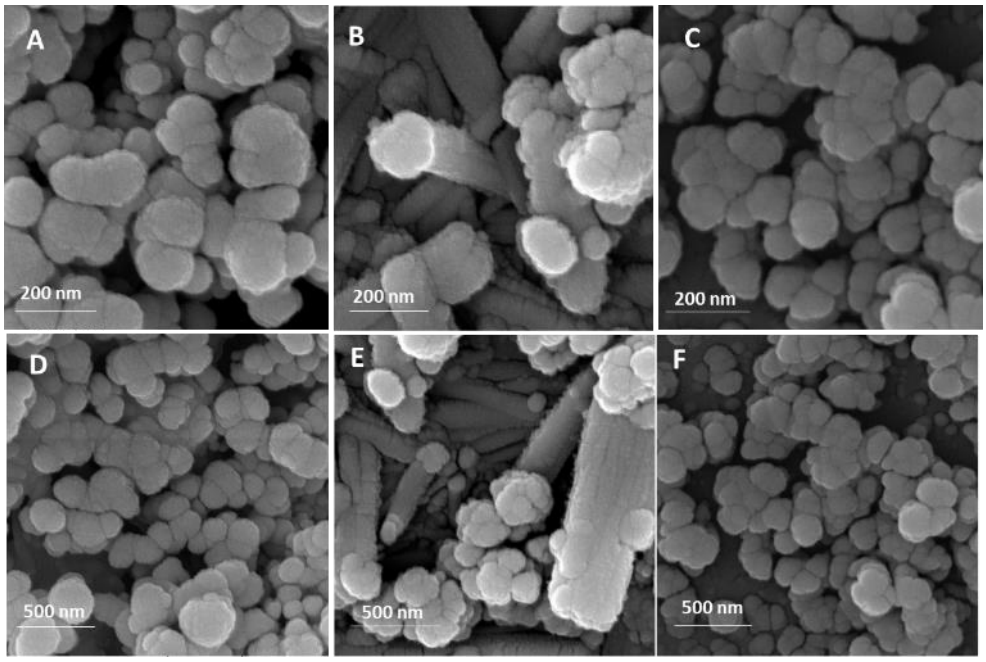

Figure 3.5. SEM images of samples with different extracted silica: ZA_1 (A, D), ZA_2 (B, E), ZA_3 (C, F) .

3.1.1.5. Energy dispersive X-ray spectroscopy.

EDX is an analytical method for the elemental analysis of a solid substance based on analysis of the emission energy of its X-ray spectrum.
In this study, the EDX technique was used to determine the percent's of elements in the three samples before and after extraction. As shown in Table 3.2 the weight values of the elements before and Figure 3.6 after extraction. As to silica percent, the results showed that sandy soil (ZA_1) contains the highest percentage of silica from clay and loamy samples (ZA_2, ZA_3)[102].

Table 3.2. EDX analysis result of elements percent's in samples

	ZA_1		ZA_2		ZA_3	
Element Wt.(%)	**Before Extraction**	**After Extraction**	**Before Extraction**	**After Extraction**	**Before Extraction**	**After Extraction**
Si	34.4	31.8	13.0	12.4	15.2	12.5
O	53.9	50.8	49.4	48.3	50.2	50.1
C	8.50	7.00	27.4	11.1	12.1	10.6
Mg	1.00	0.00	3.50	0.50	3.20	0.00
Al	1.80	1.70	3.70	2.30	4.90	0.20
Ca	1.00	0.00	12.8	0.00	8.00	0.00
Fe	0.90	0.80	5.00	1.30	4.30	0.20

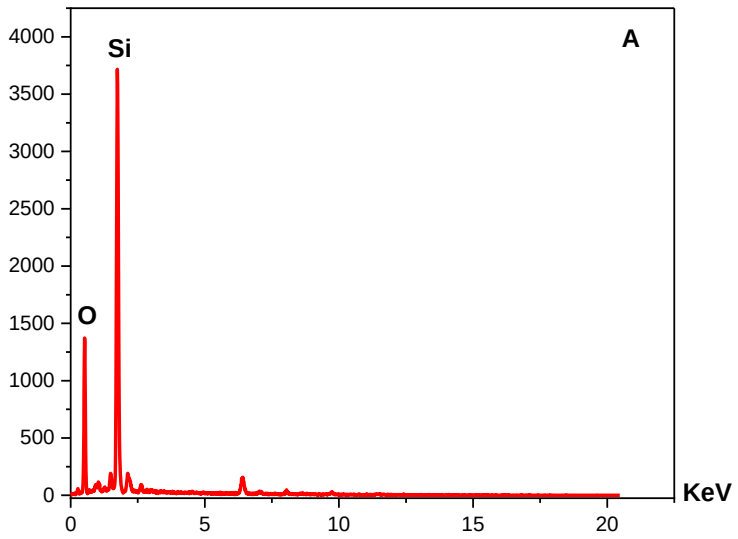

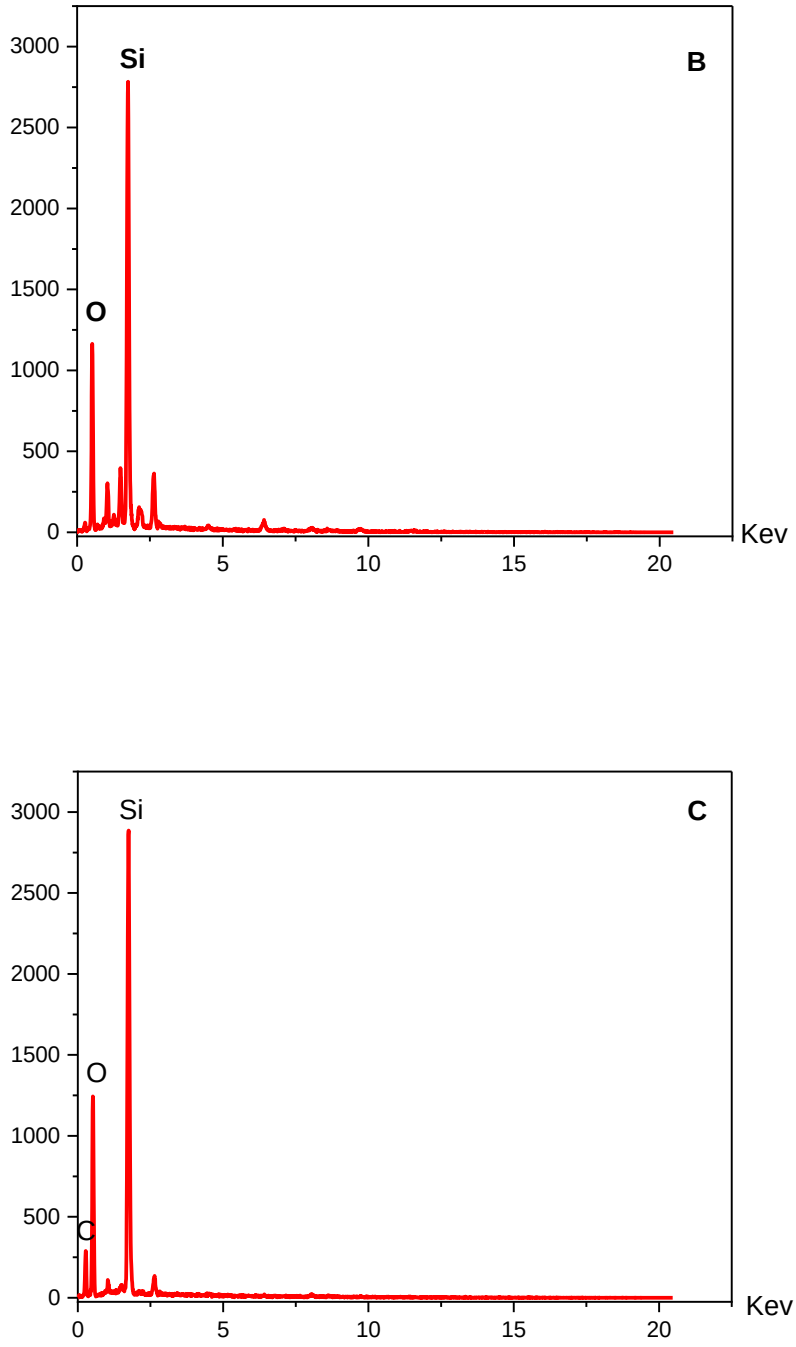

Figure 3.6. EDX chart of silica after extracted from different samples :ZA_1 (A), ZA_2 (B) and ZA_3 (C) .

3.1.1.6. Atomic Force Microscopy (AFM)

Atomic force microscopy (AFM) is a method for studying the structure and properties of solid surfaces with subnanometer spatial resolution. The principle of operation is based on recording the force interaction between the surface of the sample. In order to a change in the magnitude of the cantilever bending by recording the bending value an image of the surface relief can be obtained [103].

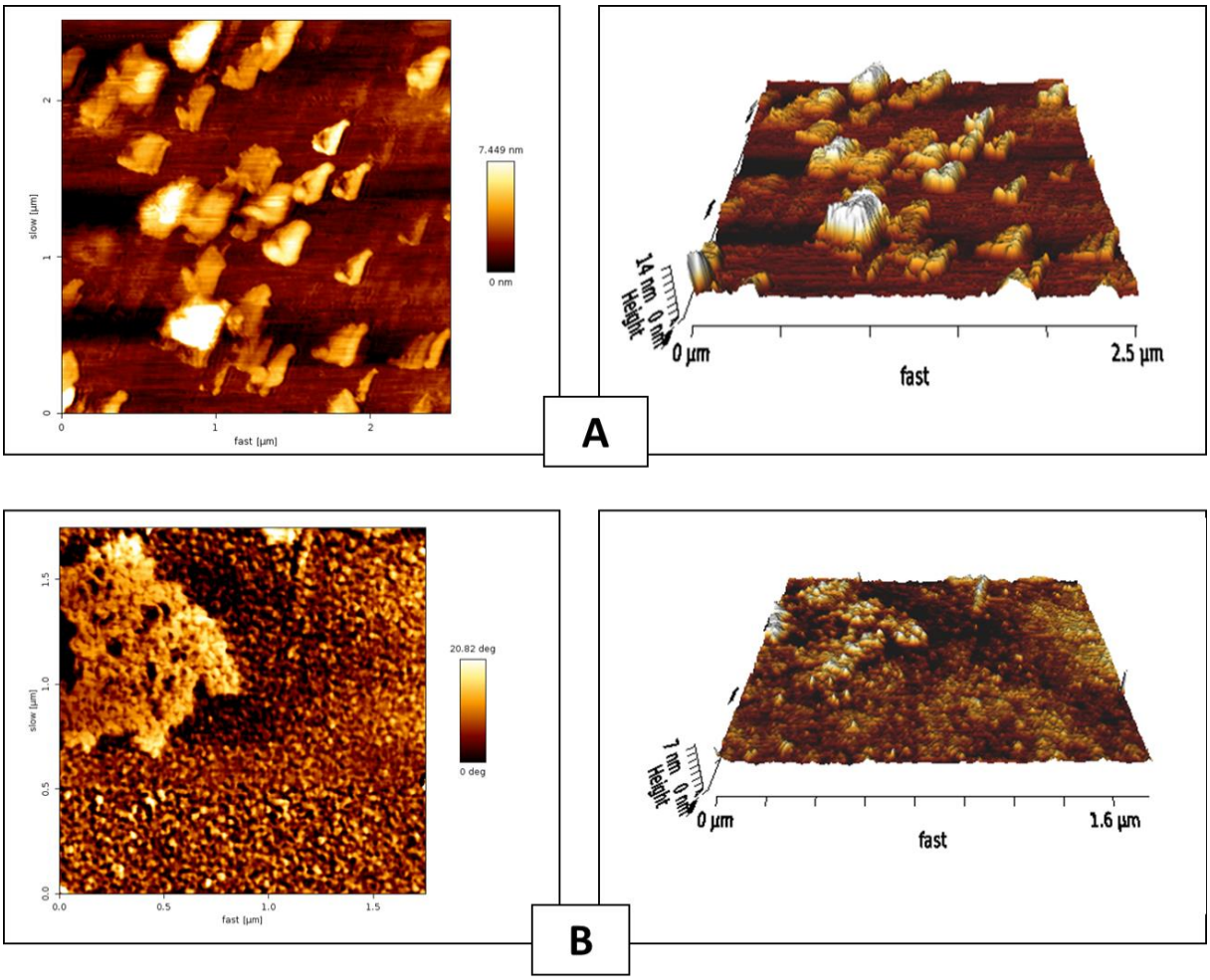

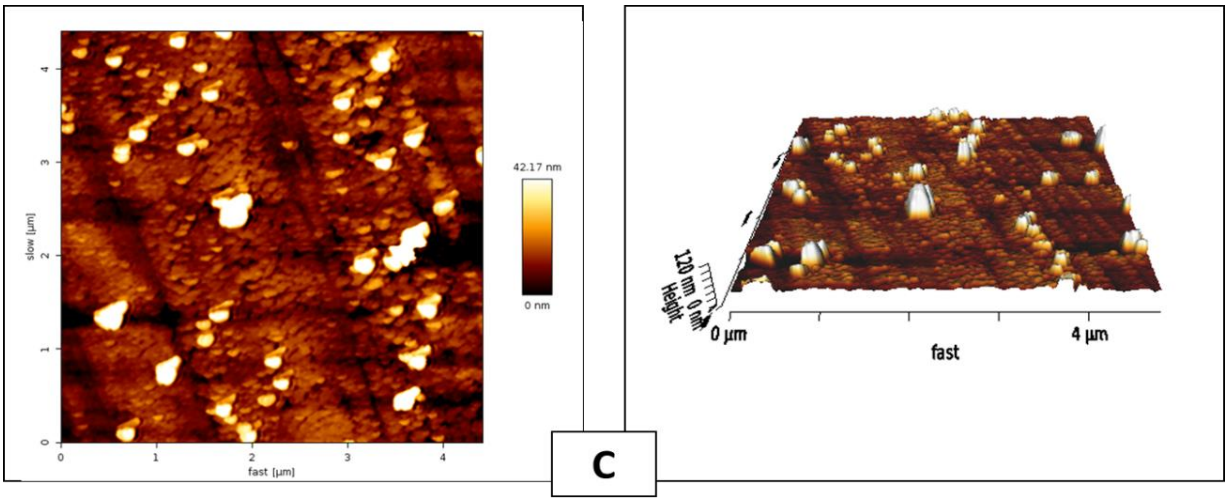

Figure 3.7: 2D and 3D images of A (ZA_1), B(ZA_2), C(ZA_3).

Table (3.3): the AFM analysis

Samples	Average roughness Ra (nm)	RMS roughness Rq (nm)	Peak – to – valley Roughness Rt (nm)
ZA_1	1.213	1.693	14.16
ZA_2	0.297	0.453	6.569
ZA_3	5.639	9.584	120.2

The results of atomic force microscopy of the studied samples are shown in (Figure 3.7) (A,B,C images). In sample ZA_1, the image showed the presence of blocks of various shapes and sizes with peak-to-valley roughness values of 14.16 mm and a root-mean-square roughness value of 1.693 mm[104]. The arrangement of the blocks is mostly agglomerated. In sample B, the image showed a significant decrease in the peak-to-valley roughness and a significant decrease in the root-mean-square roughness of 0.453 nm [105]. The arrangement of the blocks, compared to other samples (ZA_1, ZA_3), is more uniform, as is the height of the blocks themselves. On the other hand, in sample ZA_3, the image showed a significant increase in the peak-

to-valley roughness value of 120.2 nm and a significant increase in the root-mean-square roughness of 9.584 nm, compared with samples ZA_1 and ZA_2. The blocks are of different heights, diffusely located, not agglomerated (single) [106].

3.1.2. Silica using as sourbent to extract Iron (III) complex

3.1.2.1. Absorption spectra.

UV-Visible spectrum of the Iron (III), and salicylaldehyde oxime, and Fe (III) – Salicylaldehyde oxime were measured. It was shifted towards the visible area when compared to Iron and reagent alone. The wavelength Iron (III) Ion was 292nm, and the wavelength of the reagent at 304 nm. When the highest wavelength of the Fe (III) – Salicylaldehyde oxime at 520 nm was absorbed. Figure 3.8.a,b,c and d shows the spectrum absorption of the Iron (III) ions and salicylaldehyde oxime, and Fe (III) – Salicylaldehyde oxime complex.

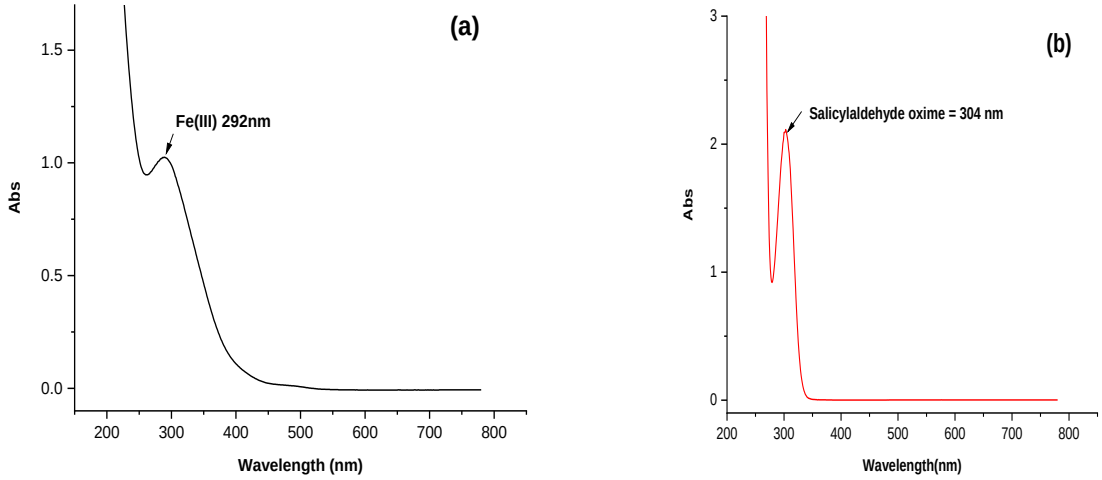

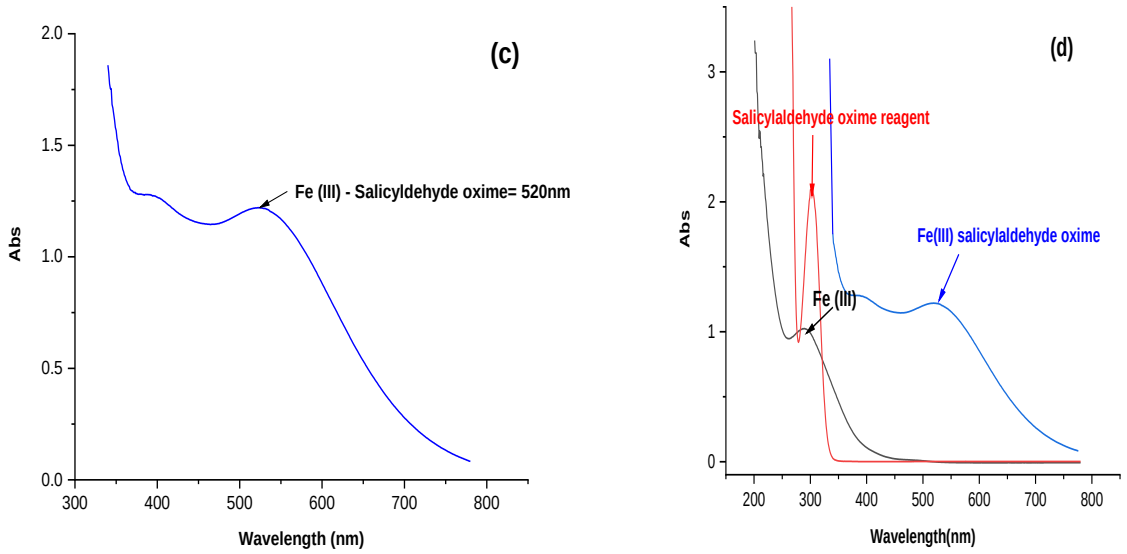

Figure 3.8. spectra of absorbtion for (a) Fe(III)ion solution ,(b) salicylaldehyde oxime reagent and (c) Fe (III) – Salicylaldehyde oxime solution . (d) overlapping for every spectrum a,b,c

3.1.2.2. Optimization of experimental condition

The experimental condition of a highest efficiency for extract iron reagent complex by solid phase (silica) included: pH, concentration of reagent (salicylaldehyde oxime), amount of sorbent (silica), temperature equilibrium and shaking time.

3.1.2.2.1. Influence of pH

The pH is most important variables to impact effectiveness of extraction solid phase silica. the pH effect factor was studied in the complex formation using 0.1 mol/L from NaOH and HCl, and examined pH between 2 to 11 on extraction Fe(III) – salicylaldehyde oxime complex by silica. The result were shown in (Figure 3.9) and tabulated in Table 3.4 that obtained increasing adsorption of extracted complex with increase hydrogen ion function. where best extraction percent at neutral medium pH 7, The extraction rate decreases in acidic medium due to the competition between iron and hydrogen ions ,while in basic medium was decreased for extraction percent

of salicylaldehyde oxime complex due to the formation of complexes between iron and hydroxide ions [107].

Table 3. 4. The effect of pH on Fe(III) – salicylaldehyde oxime complex before and after adsorption.

Ph	Mean of three Abs ±SD before adsorption	Mean of three Abs ±SD after adsorption	D.	E %
2	0.121 ± 0.00100	0.036 ± 0.00058	03.416	77.35
3	0.140 ± 0.00058	0.054 ± 0.00152	02.635	72.49
4	0.176 ± 0.00264	0.074 ± 0.00360	02.405	70.63
5	0.221 ± 0.00351	0.051 ± 0.00321	04.427	81.57
6	0.238 ± 0.00493	0.023 ± 0.00264	10.959	91.64
7	0.317 ± 0.00378	0.012 ± 0.00300	29.770	96.75
8	0.299 ± 0.00360	0.015 ± 0.00100	21.880	95.62
9	0.174 ± 0.00152	0.044 ± 0.00351	05.750	85.19
10	0.142 ± 0.00264	0.026 ± 0.00152	05.710	85.09
11	0.080 ± 0.00100	0.016 ± 0.00152	05.380	84.59

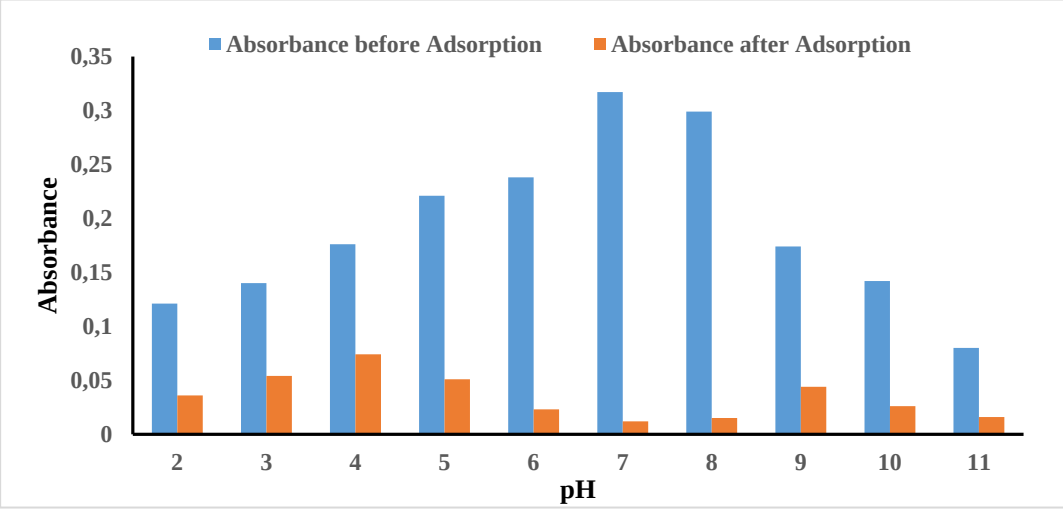

Figure 3.9. Effect of pH solution on Fe(III) – salicylaldehyde oxime complex adsorption on to Silica at 520 nm . Condition 2mL of 1000mg/L Fe(III) and 2mL of 0.01 mol/L Slicylaldehyde oxime.

3.1.2.2.2. Influence of Reagent Concentration:

The impact of the concentration reagent on value absorbance of salicylaldehyde oxime reagent solution using a range of concentration from 0.01 mol/L to 0.05 mol/L under pH 7. It was increased the absorbance of Fe(III) –salicylaldehyde oxime complex with increasing concentration of reagent, and the best extraction the on Fe(III) – salicylaldehyde complex at 0.04 mol/L,while at a concentration of 0.05 the reaction rate increases, and there is a maximum limit to this increase as it leads to side reactions, and these reactions reduce the extraction efficiency.as shown in Table 3.5 and Figure 3.10. The effect concentration of salicylaldehyde oxime reagent to Fe (III) before and after adsorption.

Table 3.5. The effect of concentration reagent on Fe(III) – salicylaldehyde oxime complex before and after adsorption at 520 nm.

Conc. of reagent (mol/L)	Mean ±SD before Adsorption	Mean ±SD after Adsorption	D	E%
0.01	0.317 ± 0.00378	0.012 ± 0.00300	29.775	96.75
0.02	0.812 ± 0.00416	0.036 ± 0.00152	23.428	95.90
0.03	0.832 ± 0.00264	0.063 ± 0.00152	13.480	93.09
0.04	0.882 ± 0.00585	0.012 ± 0.00300	83.080	98.81
0.05	0.684 ± 0.00351	0.031 ± 0.00208	23.061	95.84

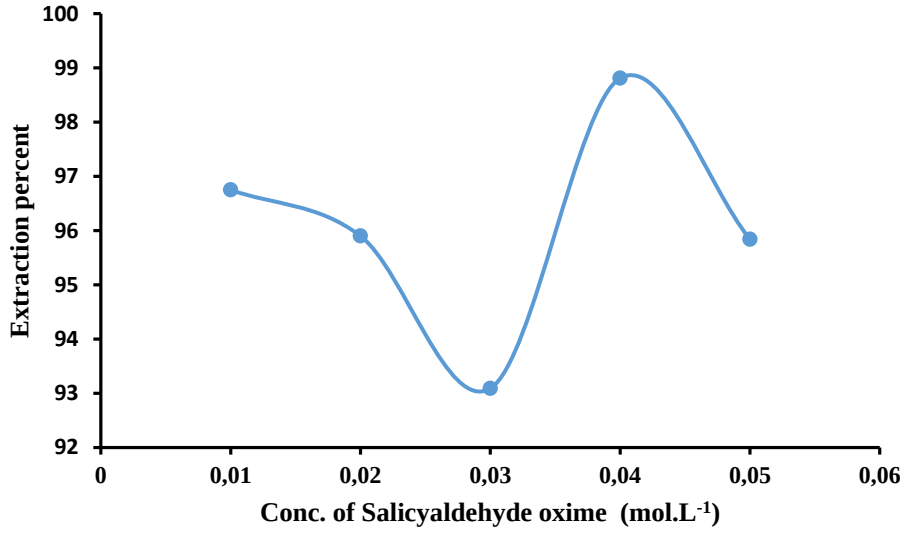

Figure 3.10. Effect of concentration reagent (salicyalaldehyde oxime) on Fe(III) – salicylaldehyde oxime complex adsorbent by silica at 520 nm . at: 2mL of 1000mg/L Fe(III), pH (7) .

3.1.2.2.3. Amount of Sorbent Influence

The effect of Amount Sorbent was used to adsorption Fe(III) – salicylaldehyde oxime complex under optimum condition at pH 7 and concentration salicylaldehyde oxime reagent 0.04 mol/L, with complex absorbance at 0.882. However, it was used different amounts sorbent of solid phase (silica) at (0.025 -0.125) g as shown in Table 3.6 and Figure 3.11 to extraction Fe(III) – salicylaldehyde oxime complex, with favorite amount sorbent to extraction iron (III) ligand complex at 0.1 g . It is observed that increasing the amount of silica from 0.100 g to 0.125 g did not lead to any further increase in adsorption efficiency (E%) or adsorption capacity (D). This suggests that the system reached a state of saturation, where all the available active sites on the silica surface were occupied. As a result, adding more sorbent beyond this point did not enhance adsorption performance, indicating an equilibrium condition in the adsorption process.

Table 3.6 . The effect of amount surface sorbent (Silica) on Fe(III) – salicylaldehyde oxime complex after adsorption at 520 nm

Amount of sorbent silica(g)	Mean ±SD after adsorption	D	E%
0.025	0.030 ± 0.00100	30.791	96.85
0.050	0.024 ± 0.00173	38.966	97.49
0.075	0.016 ± 0.00300	60.318	98.36
0.100	0.012 ± 0.00300	83.080	98.81
0.125	0.012 ± 0.00300	83.080	98.81

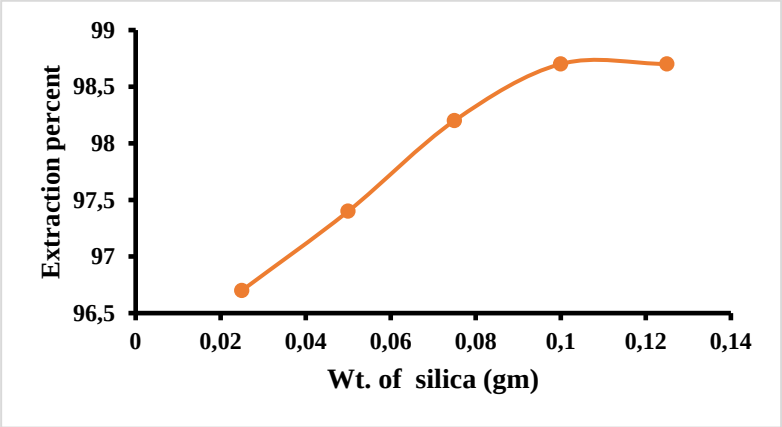

Figure 3.11 Effect of different amount of sorbent (Silica) on Fe(III) – salicylaldehyde oxime complex , at pH (7), 2mL of 1000mg/L Fe(III), 2mL of 0.04 mol/L Slicylaldehyde oxime .

3.1.2.2.4. Equilibrium Temperature effect

The influence of temperature changes on solid phase (silica) of Fe(III) – salicylaldehyde oxime complex x extraction, the temperature was raised in the water bath from (25 to 50) ^{o}C all results are investigated are shown in Table 3.7. The temperature is the most favorable at 35 ^{o}C to Fe(III) – salicylaldehyde oxime complex. Figure 3.12. (a) and (b) show the effect of the temperature equilibrium on extraction Fe(III) – salicylaldehyde oxime complex. Thermodynamic function (ΔHex) have been collected and determined (41.453 kJ/mol), entropy indicates positive values

Fe(III) – salicylaldehyde oxime complex stability. The thermodynamic function result of extraction process Fe(III) – salicylaldehyde oxime complex by using solid phase is an endothermic process due to value positive of ΔHex and great formation electrostatic bonding of extracted ionic complex with silica [108].

Table 3.7. The effect of temperature on Fe(III) – salicylaldehyde oxime complex before and after adsorption

Temp. (K)	Mean ±SD before ads	Mean ±SD after ads	$1/T \times 10^{-3}$ (K^{-1})	Log D	ΔG (kJ/mol)	ΔS (kJ/mol. K)
298	0.976 ±0.02577	0.081 ± 0.00650	3.35	1.087	-62030	20.676
303	0.918 ±0.01861	0.042 ± 0.00529	3.30	1.345	-78010	25.882
308	0.882 ± 0.00585	0.012 ± 0.00300	3.25	1.919	-11323	36.904
313	0.824 ±0.01276	0.012 ± 0.00300	3.19	1.889	-11327	36.320
318	0.684 ±0.01212	0.012 ± 0.00300	3.14	1.808	-11006	34.740
323	0.638 ±0.00404	0.012 ± 0.00300	3.10	1.778	-10990	34.180

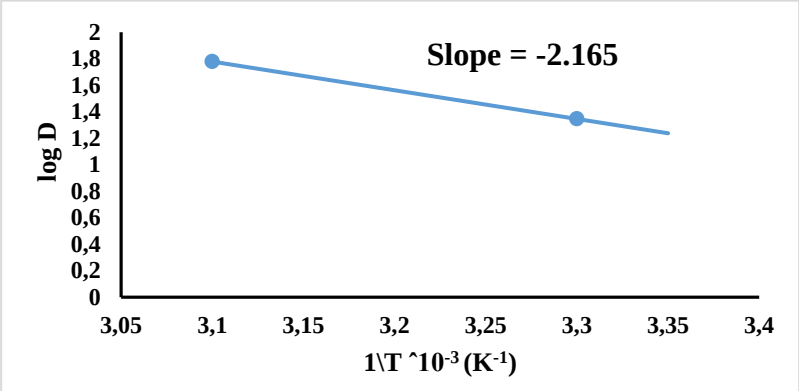

Figure 3.12. The effect of temperature on Fe (III) – salicylaldehyde oxime complex before and after adsorption at pH (7), 2mL of 1000 mg. L^{-1} Fe(III), 2mL of 0.04 mol/L Slicylaldehyde oxime , 0.1 g of silica.

3.1.2.2.5. Time effect

The solid phase (silica) was extraction the complex solution by shacker for five to thirty minutes in order to seprate Fe(III) – salicylaldehyde oxime complex . It was best time to separat iron(III) ligand complex from solid phase (silica) at 15 min that indicate silica surface have high selectivity to extract complex with reduce time [109] as shown in Table 3.8 and Figure 3.13 .(a) and (b) Time effect on Absorbance Fe(III) – salicylaldehyde oxime complex and Extraction percent at pH 7, 2mL of Fe(III) , 2mL of 0.04 mol/L Salicylaldehyde oxime , 0.1 g of silica and temperature 35 ^{o}C.

Table 3.8. The Time effect on Fe(III) – salicylaldehyde oxime complex before and after adsorption

Time (min)	Mean ±SD after adsorption	D	E%
5	0.012 ± 0.003	83.080	98.81
10	0.008 ± 0.002	133.432	99.25
15	0.004 ± 0.002	338.718	99.70
20	0.004 ± 0.002	338.718	99.70
25	0.004 ± 0.002	338.718	99.70
30	0.004 ± 0.002	338.718	99.70

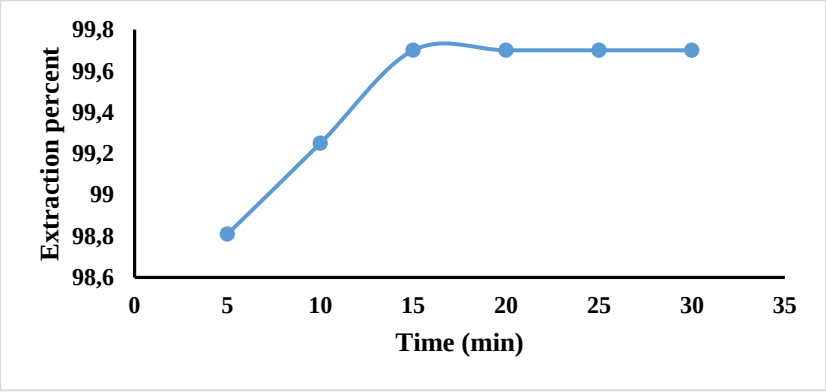

Figure 3.13. The effect of time on Fe(III) – salicylaldehyde oxime complex before

and after adsorption at pH (7), 2mL of 1000mg/L Fe(III), 2mL of 0.04 mol/L Slicylaldehyde oxime , 0.1 g of silica, Temp. 35 ^{o}C .

3.1.3. Elution of iron (III) complex from Silica

Iron (III) was desorbed from silica, with interaction between the adsorbed iron by different solvents such as distilled water, methanol, and ethanol, as shown in Table 3.9 Silica often contains silanol groups (Si–OH) that can bind to iron (Fe^{3+}) or its complexes through chemisorption bonds. These bonds are relatively strong. Methanol, ethanol and distilled water are polar solvents, but they do not break these coordination bonds very efficiently. These solvents may remove a small portion of the physically absorbed iron, but not the strongly chemically bound complex. Therefore, the removal efficiency (desorption) will typically be low. It was found that ethanol have high desorption for iron (III) complex from silica.

Table 3.9. Desorption of iron (III) from Silica

Solvents	Mean Conc.	Desorption % $\% D = \frac{Cads}{Cdes} \times 100$
Distilled water	3.14	5
Ethanol	9.78	15.5
Methanol	6.57	10.4

3.1.4. Application of extraction Iron (III) ions from pharametrical samples.

Mesoporous silica has been used as a surface adsorbent for a range of pharmaceutical samples containing iron(III) ions [110] such as (Hemafer, Ferblex, Ferimax, Akourose, and Sorbifer Duroles). Silica is one of the most widely used silica solutions for iron(III) ion extraction. Pharmaceutical samples were used at a concentration of 25 mg L^{-1} under experimental conditions (at 35°C, pH 7, 0.1 g solid phase, and 15 min adsorption time). Iron(III) ion adsorption from the pharmaceutical samples was determined, as shown in Table 3.10, which indicates the best extraction percent

Iron(III) ion of pharmaceutical samples for adsorbing iron compounds due to the surface properties and chemical properties of silica. the polarity of the silica surface improves the extraction percent where silica particles interaction between iron (III) ions to allow better separation in pharmaceuticals.

Table 3.10. Extraction iron (III) ions in pharametrical samples by silica

Name Of Drug	Dos of drug	Mean ±SD before ads	Mean ±SD after ads	D	E %
Hemafer	100mg/5mL	0.072 ± 0.00264	0.008 ± 0.00251	9.0	90.0
Ferblex	40mg/15mL	0.088 ± 0.00757	0.024 ± 0.00264	3.7	78.7
Ferimax	100mg/2mL	0.071 ± 0.00300	0.022 ± 0.00458	3.2	76.2
Akouros	100mg/5mL	0.078 ± 0.00251	0.012 ± 0.00153	6.5	86.7
Sorbifer Duroles	100mg/60mg	0.148 ± 0.00251	0.027 ± 0.00472	5.5	84.6

3.2. Introduction of Organosilica

Organosilica was prepared from silica was extracted from sandy soil and reacted with chelating reagent to produce organosilica. It is most making to excellent candidate for adsorption-based applications, especially in the removal of heavy metals from aqueous solutions [111] and another applications in several fields such as food, cosmetics, pharmaceutical materials, electronic materials. The organosilica materials have gained significant attention as solid sorbents for the removal of ionic metals from aqueous solutions . These selective binding properties of organic functional groups, making them highly effective for metal adsorption[112].Organosilica interact with metal ions through various mechanisms, including electrostatic attraction, surface complexion, chelation, and ion exchange, solid phase extraction, allowing for the efficient removal of contaminants such as Fe^{3+} from aqueous environments [113]

3.2.1. Characterization of Organosilica

3.2.1.1. Fourier Transform Infrared Spectroscopy (FTIR)

Fourier Transform Infrared Spectroscopy (FTIR) analysis was used to determine the functional groups of organosilica, as shown in Figure 3.14. The broad band between 3454 $cm^{-1}$and 3444 cm^{-1} is attributed to the O–H stretching vibration of Si-OH groups, as well as absorbed water on the surface of silica[114]. Meanwhile, the bending vibration of this group appears at 1645 cm^{-1} and 1639 cm^{-1}. Furthermore, the asymmetric stretching vibration of Si–O–Si absorbed about 1100cm^{-1}, while symmetric stretching vibration observed about 802 cm^{-1}, while the peaks at 441 cm^{-1}, 536 cm^{-1}, and 472 cm^{-1} belong to the bending vibrations of Si–O–Si groups [115]. Peaks of 1176 to C–O stretching present in functional organic groups of ligand. In addition, the organosilica spectrum exhibits additional peaks at 1176 cm^{-1} and 1408 cm^{-1}, which can be attributed to C–O stretching and bending, confirming the modification of functional groups [97].Moreover, the peaks at 613 cm^{-1} and 802 cm^{-1} indicate Si–C stretching and bending, further verifying the successful integration of the organic ligand into the silica matrix [116].

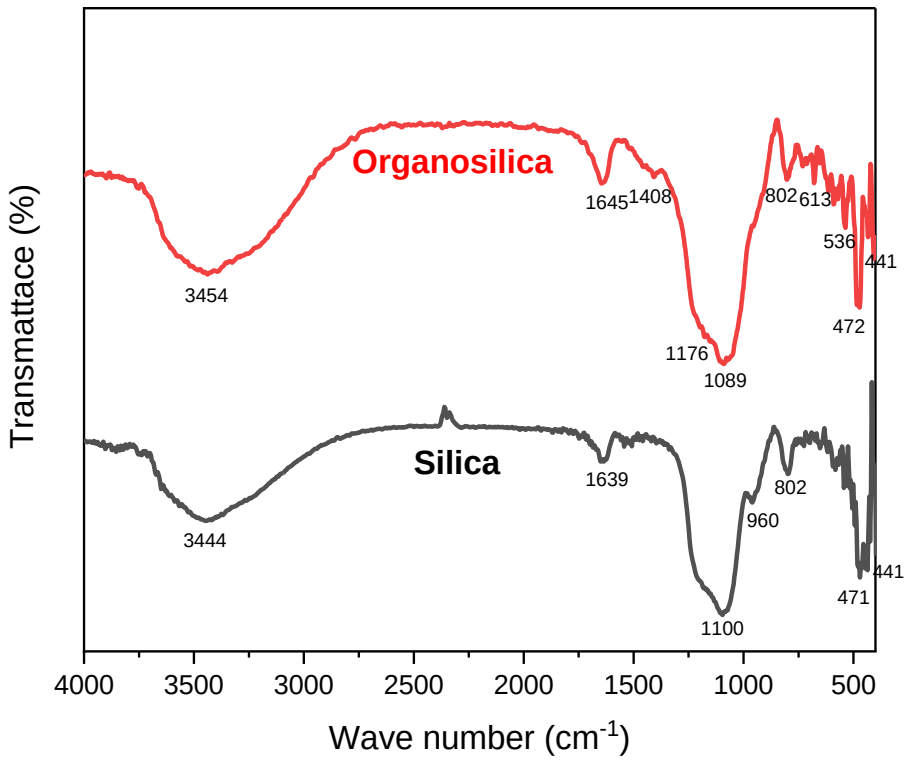

Figure 3.14. FTIR spectrum of silica and organosilica.

3.2.1.2. Specific Surface Area (BET) analysis

The specific surface areas, pores volume, and pores size distribution results calculated from adsorption isotherms were advertised in Table 3.11. Both silica and organosilica showed high specific surface area. Moreovere, the pore volume data of silica and organosilica are good evidence of mesoporous materials [117]

Table 3.11. The BET parameters of Silica and organosilica

Samples	Specific surface area S_{BET} (m^2/g)	Average pure volume Vp (cm^3/g)	Mean pore diameter Dp (nm)
Extracted silica	252.71	7.815	11.207
Organo silica	87.154	5.534	14.173

The adsorption-desorption isotherms of nitrogen for both silica and organosilica are shown in Figure 3.15, exhibit a type IV isotherm and functionlized organosilica gave a hysteresis loop observed in range 0.3 and 1, which is associated with capillary condensation , acharacteristic of mesoporous materails. All the silica and organosilica were categorized as mesoporous structures, which have an average pore size range between 2 and 50 nm [118].

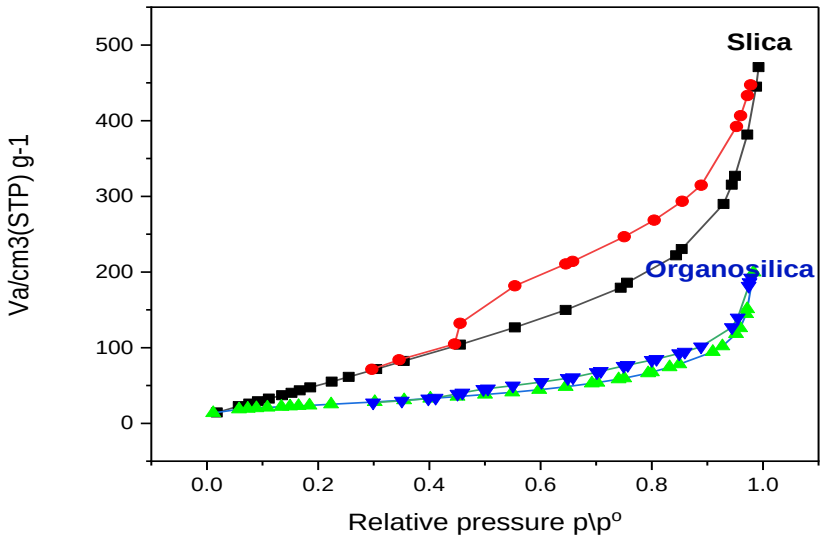

Figure 3.15. Nitrogen adsorption-desorption isotherms of silica and organosilica

3.2.1.3.X-Ray Diffraction analysis

The X-ray diffraction (XRD) patterns reflecting of silica and organosilica are showed in Figure 3.16. Both silica and organosilica exhibited broad peaks around 20° attributed to amorphous silica [119]. Organosilica loading leads to decreased intensity of this peak. Furthermore, the appearance of two sharp peaks at 25–30° indicate the presence of the organic group into the silica matrix [120].

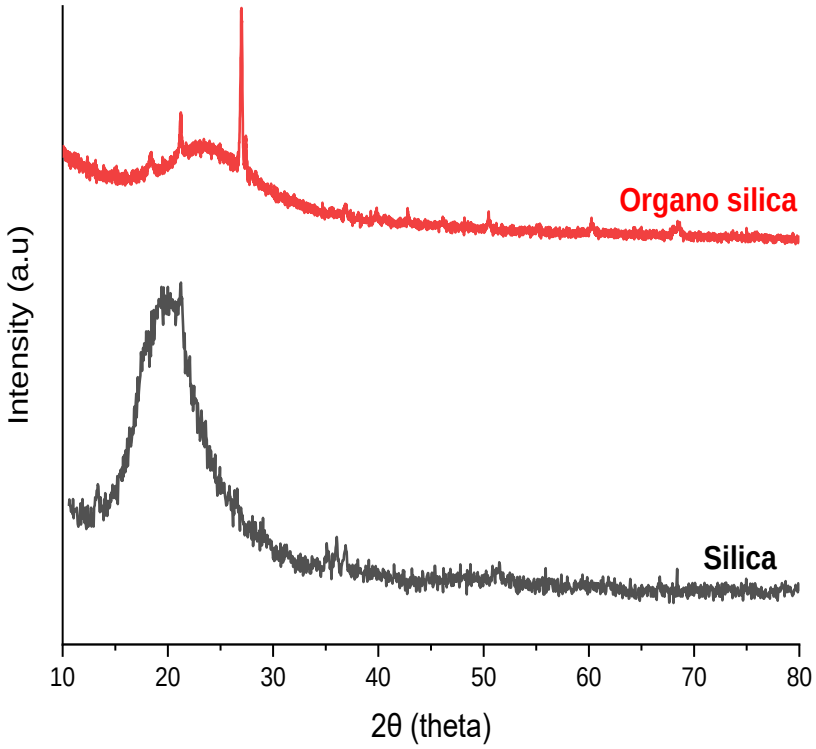

Figure 3.16. XRD pattern of silica and organosilica

3.2.1.4. Scanning Electron Microscopy (SEM).

Scanning electron microscopy (SEM) has been used to determine the compare morphology between silica and organosilica as shown in Figure 3.17. SEM images revealed that silica particles are highly agglomerated , spherical shaped and porous . while organosilica were highly agglomerated particles due to the strong interactions between silica particles and organic functional groups. The white particles in image (B,D) belonged to organic compounds which reacted with silica[121].

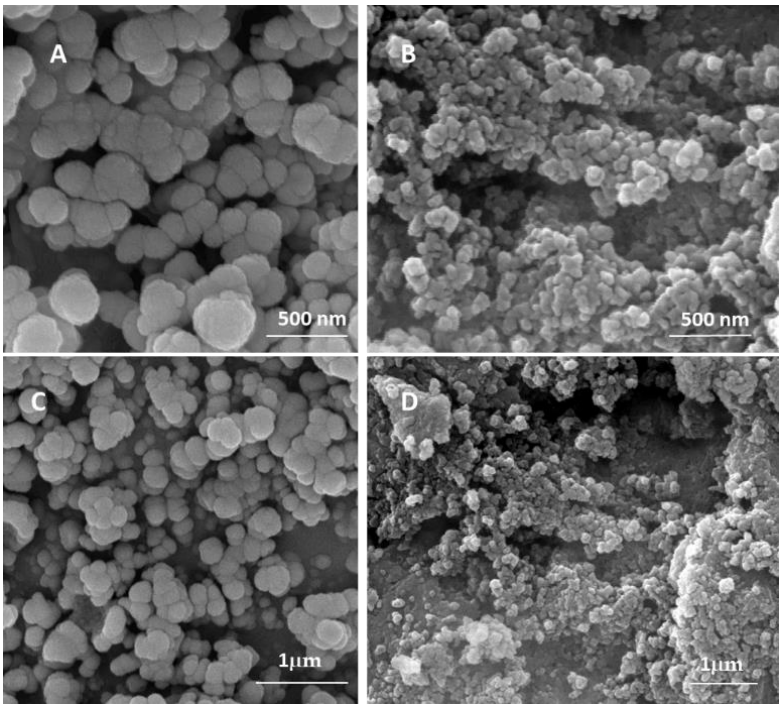

Figures 3.17. SEM images of silica and organosilica: (A, C) silica and (B, D) organosilica.

3.2.1.5. Transmission Electron Microscopy (TEM)

Transmission Electron Microscopy (TEM) images were used to observe the morphology and internal structure at the nanoscale of silica and organosilica materials. Through the images shown in Figure 3.18. The TEM images confirm that silica and organosilica nanoparticles exhibit a flattened spherical shape. The silica particles appear dark in color, while the organic groups appear lighter and are heterogeneously distributed between the layers of silica particles[122] .These results are in agreement with SEM results.

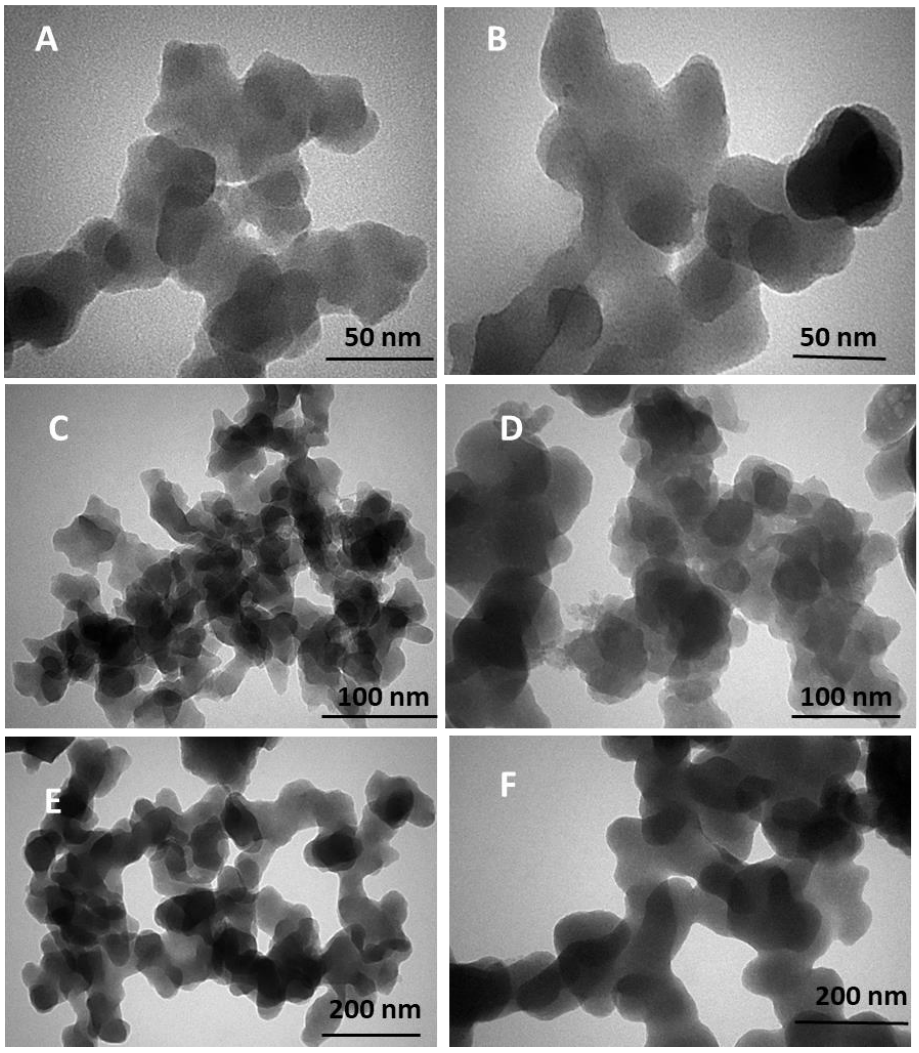

Figures 3.18. TEM images of silica and organosilica:(A, C,E) of silica and (B, D,F) of organosilica

3.2.1.6. Atomic Force Microscopy (AFM)

Atomic Force Microscopy (AFM), the surface roughness (Root–mean–square roughness–Rq and roughness average–Ra) was observed for silica and organosilica, in Table 3.12. It showed moderate roughness, with Ra = 39.35 nm and a relatively large Rt, indicating a large surface [123].

Table 3.12. The surface roughness parameters from the AFM images.

Samples	Average roughness Ra, (nm)	RMS roughness Rq, (nm)	Peak – to – valley Roughness Rt, (nm)
Extracted silica	35.73	64.78	789.6
Organosilica	39.35	62.98	545.3

The 3D surface exhibited and distributed the membrane, as shown in Figures 3.19. The silica and organosilica displayed a sub-micrometer-scale roughened surface in different physical sizes between (10 to 10µm), with a roughness due to the agglomerated structures of individual nanoparticles [124].

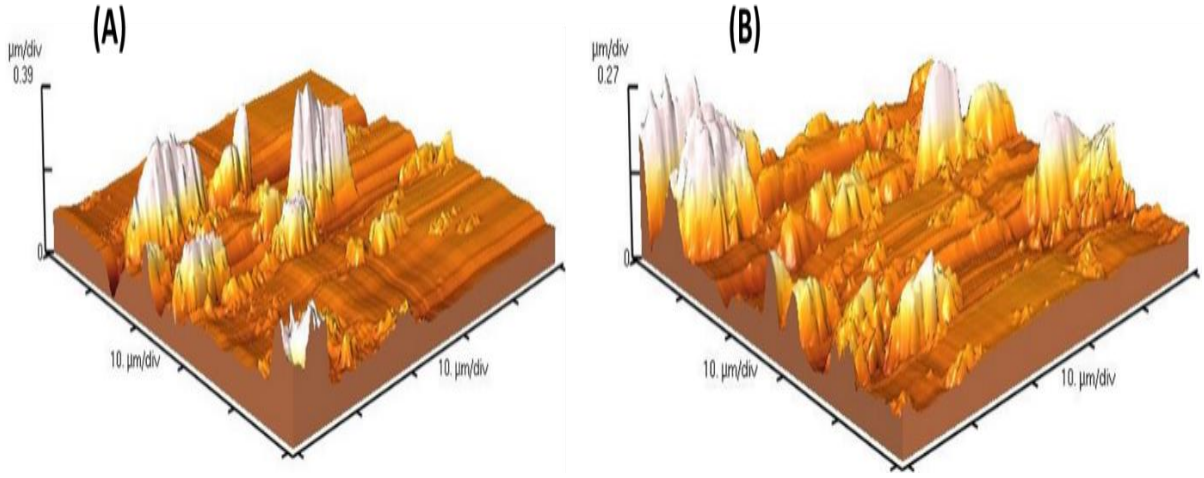

Figures 3.19. 3D AFM images of the silica and organosilica: (A) of silica and (B) of organosilica.

3.2.2. Optimization of experimental condition.

The experimental condition of adsorbent iron from aqueous solution by organosilica including pH, concentration of reagent (salicylaldehyde oxime), amount of sorbent (organosilica), temperature equilibrium and shaking time.

3.2.2.1. pH effect.

It was the most experimental condition to adsorption between Fe (III) –

Salicylaldehyde oxime complex with reduce concentration to ability the organosilica to extract complex with low concentration, the pH effect factor was ranged between (2-1. It was used 0.1 mol/L from HCl and NaOH with using pH glass electrodes to justify pH factor. The results were shown in Figure 3.20, where adsorption with increasing pH factor. The best adsorption of iron at pH 7 that neutral medium was due to the nature of the adsorbent surface and the expected nature of the linkage between adsorbent (organosilica) and adsorbate (Fe (III) – Salicylaldehyde oxime complex). Interaction is iron on the surface of organosilica, while it was decreased for extraction percent of the basic medium with iron (III) due to the formation of complexes between iron and hydroxide ions [125].

Table 3.13 The affect of pH on Fe(III) – salicylaldehyde oxime complex before and after adsorption.

pH	Mean ±SD before adsorption	Mean ±SD before adsorption	D	E%
2	0.066 ± 0.00288	0.038 ± 0.00288	1.765	63.83
3	0.085 ± 0.00115	0.054 ± 0.00264	1.589	61.37
4	0.092 ± 0.00208	0.068 ± 0.00208	1.370	57.80
5	0.095 ± 0.00115	0.047 ± 0.00152	2.020	66.90
6	0..114 ± 0.00208	0.039 ± 0.00200	2.920	74.50
7	0.123 ± 0.00057	0.018 ± 0.00152	6.830	87.20
8	0.091 ± 0.00152	0.038 ± 0.00152	2.470	71.20
9	0.079 ± 0.00100	0.021 ± 0.00115	3.760	79.00
10	0.060 ± 0.00047	0.035 ± 0.00152	1.710	63.10
11	0.050 ± 0.00208	0.013 ± 0.00057	3.850	79.40

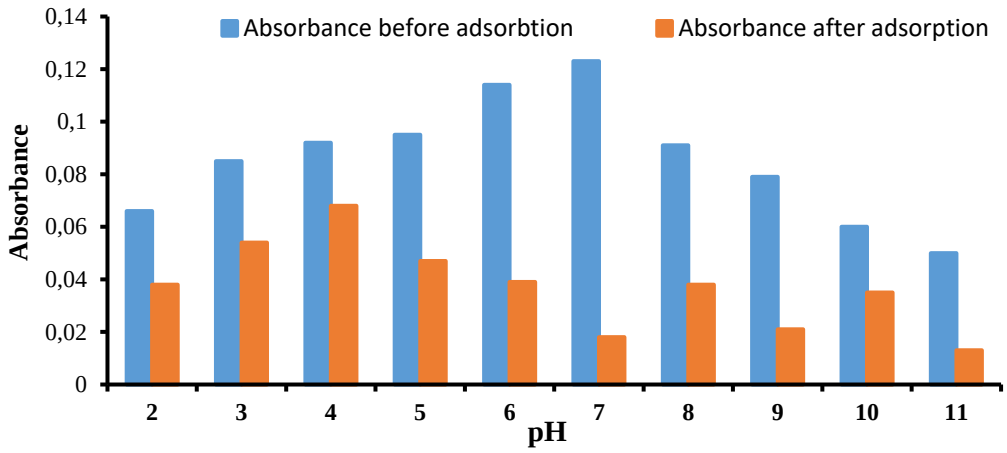

Figure 3.20. Effect of pH solution on Fe(III) – salicylaldehyde oxime complex adsorption on to Organosilica at 520 nm. Condition 2mL of 50 mg/L Fe(III) and 2mL of 0.01 mol/L Slicylaldehyde oxime.

3.2.2.2. Reagent of Concentration effect:

Optimal adsorption at pH 7. The concentration of salicylaldehyde oxime reagent effect was using a series of ranges concentration from 0.01 mol/L to 0.05 mol/L.The interaction of organosilica and salicylaldehyde oxime will increase the overall adsorption capacity for iron (III) by forming stable complex , when increased the absorbance of the iron complex with increasing concentration of reagent [126] , the efficient extraction percent at concentration 0.04mol/L due to have high percent as shown in Table 3.14 and Figure 3.21 the effect concentration.

Table 3.14. The effect of concentration reagent on Fe(III) – salicylaldehyde oxime complex before and after adsorption

Conc.Reagent (mol/L)	Mean ± SD before adsorption	Mean ±SD After adsorption	D	E %
0.01	0.064 ± 0.00100	0.023 ± 0.00115	2.78	73.5
0.02	0.080 ± 0.00100	0.035 ± 0.00305	2.29	69.6
0.03	0.102 ± 0.00057	0.026 ± 0.00152	3.92	79.7
0.04	0.123 ± 0.00057	0.018 ± 0.00100	6.83	87.2
0.05	0.143 ± 0.00100	0.065 ± 0.00152	2.2	68.8

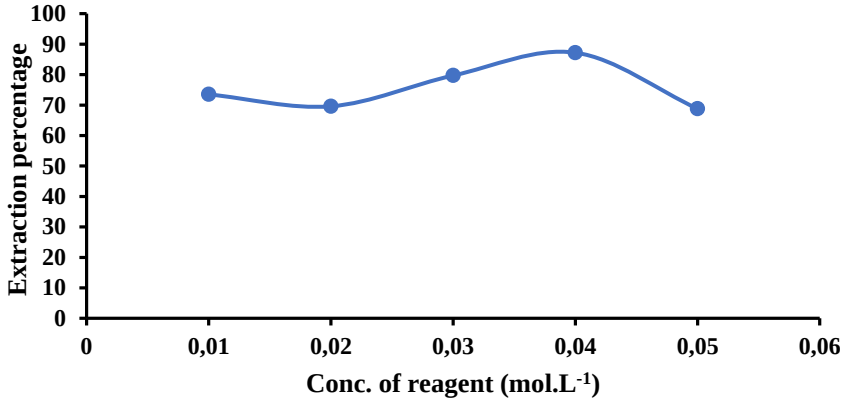

Figure 3.21. Effect of concentration reagent (salicyalaldehyde oxime) on Fe(III) – salicylaldehyde oxime complex adsorbent by Organosilica at 520 nm. at: 2mL of 50 mg. L^{-1} Fe(III), pH (7).

3.2.2.3. Amount of Sorbent Influence

The amount of organosilica affect played a critical role in the adsorption efficiency of iron (III) under optimum conditions natural pH 7 and concentration salicylaldehyde oxime reagent 0.04 mol/L. However, it used different amounts of sorbent of a solid phase (organosilica) at ranged between (0.025 -0.150) g as shown in Figure 3.22. to adsorption iron (III) complex, the most adsorption efficiency to amount of sorbent (organosilica) to adsorbent iron (III) complex at 0.1 g due to depend of the organosilica properties such as specific surface area and the nature of functional groups.

Table 3.15. The affect of amount surface sorbent (organosilica) on Fe(III) – salicylaldehyde oxime complex after adsorption at 520 nm

Amount of sorbent (g)	Mean ±SD After adsorption	E %
0.025	40.71 ± 0.00200	67.5
0.050	26.43 ± 0.00100	76.9
0.075	23.57 ± 0.00115	78.9
0.100	12.86 ± 0.00100	87.2
0.125	12.86 ± 0.00057	87.2
0.150	12.86 ± 0.00100	87.2

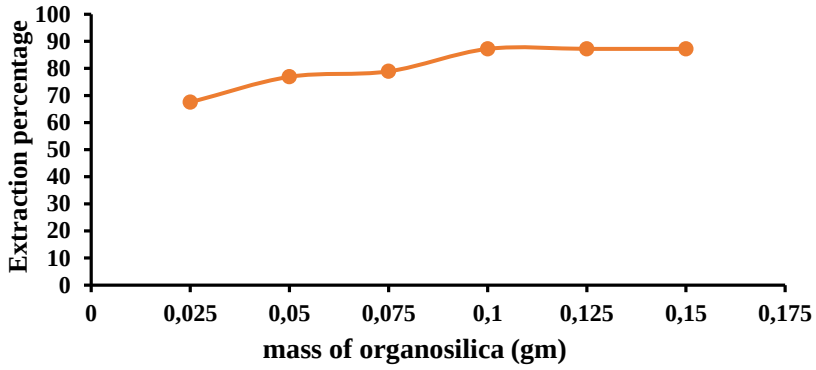

Figure 3.22. Effect of different amounts of sorbent (organosilica) on Fe (III) – salicylaldehyde oxime complex.

3.2.2.4. Temperature affect

The affect of temperature played an important role to the adsorption of Fe(III) – salicylaldehyde oxime complex by organosilica was data investigated are shown in Table 3.16 and Figure 3.23. The temperature ranged from (25 to 50) ^{o}C, while the increase adsorption efficiency with increase with temperature. It was because at higher temperatures at 40 ^{o}C, the adsorbent surface becomes more active, and the adsorbent Fe(III) – salicylaldehyde oxime complex has more energy to interact with the adsorption sites, with the thermodynamic function (ΔHex) were collected these variables at (39.61 KJ/mol), where The adsorption process of iron by using organosilica is an endothermic process and entropy is a positive value that indicating the formation of electrostatic bonding of extracted ionic with organosilica [127].

Table 3.16. The affect of temperature on Fe(III) – salicylaldehyde oxime complex before and after adsorption

Temp (K)	Mean ± SD before adsorption	Mean ± SD after adsorption	$1/T \times 10^{-3}$ (K^{-1})	Log D	ΔG (kJ/mol)	ΔS (kJ/mol. K)
298	0.193 ± 0.00305	0.085 ± 0.00099	3.35	0.360	-2053	7.087
303	0.162 ± 0.00115	0.051 ± 0.00057	3.30	0.510	-2962	9.970
308	0.137 ± 0.00208	0.032 ± 0.00115	3.25	0.646	-3807	12.552
313	0.120 ± 0.00152	0.018 ± 0.00057	3.19	0.853	-5110	16.514
318	0.116 ± 0.00152	0.024 ± 0.00152	3.14	0.705	-4293	13.685
323	0.106 ± 0.00200	0.027 ± 0.00115	3.10	0.611	-3781	11.888

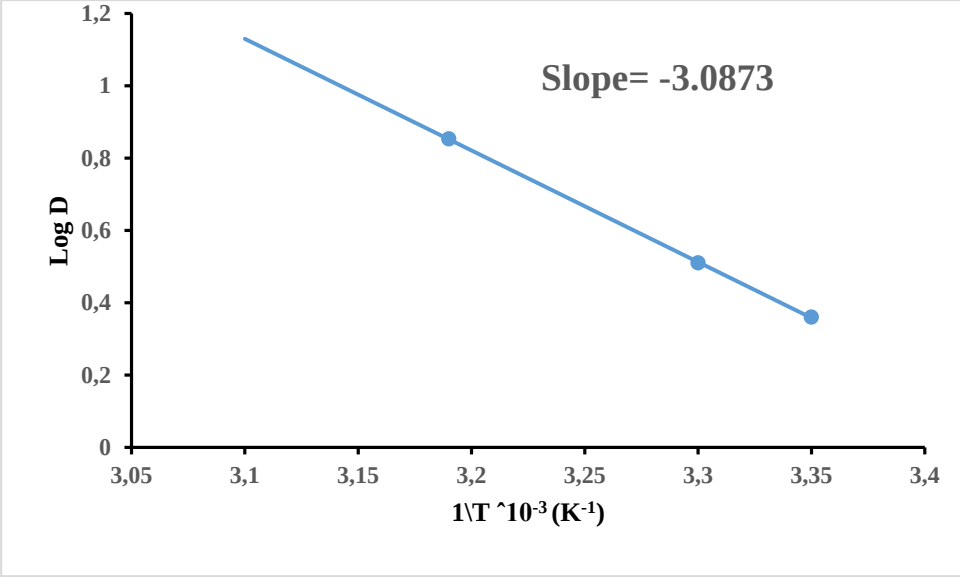

Figure 3.23. The affect of temperature on Fe(III) – salicylaldehyde oxime complex before and after adsorption at pH (7), 2mL of 50 mg/L Fe(III), 2mL of 0.04 mol/L Slicylaldehyde oxime , 0.1 g of organosilica.

3.2.2.5. Time affect

The time affect on the adsorption of Fe(III) – salicylaldehyde oxime complex by organosilica .it was studied kinetic process of shacking time from 5 min to 30 min as shown in Figure 3.24 and Table 3.17 under optimum at pH 7, concentration salicylaldehyde oxime reagent 0.04 mol/L and amount sorbent 0.1 g and temperature 40 ^{o}C. The best time to adsorbed Fe(III) – salicylaldehyde oxime complex by the organosilica at 15 min.

Table 3.17 The Time affect on Fe(III) – salicylaldehyde oxime complex before and after adsorption

Time (min)	Mean ±SD After adsorption	D	E%
5	0.022 ± 0.00100	5.45	84.5
10	0.018 ± 0.00115	6.67	86.7
15	0.014 ± 0.00115	8.6	89.6
20	0.014 ± 0.00100	8.6	89.6
25	0.014± 0.00115	8.6	89.6
30	0.014 ± 0.00100	8.6	89.6

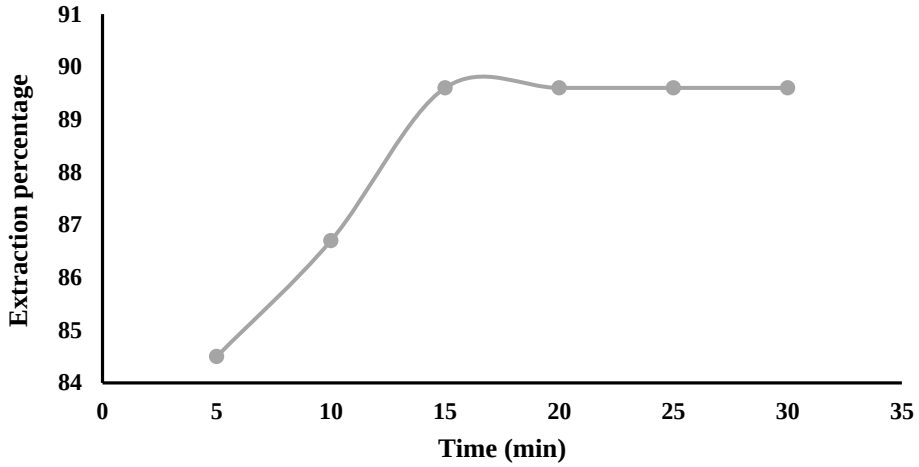

Figure 3.24. The time affect on Fe(III) – salicylaldehyde oxime complex before and after adsorption at pH (7), 2mL of 1000mg.L^{-1} Fe(III), 2mL of 0.04 mol/L Slicylaldehyde oxime , 0.1 g of organosilica, Temp. 40 ^{o}C .

3.2.3. Elution of iron (III) complex from organosilica

Iron (III) was desorbed from a organosilica depending on the interaction between the adsorbed iron ions and different solvents such as distilled water, methanol, and ethanol, as shown in Table 3.18. The solvents have varying abilities to break these interactions, and the determination of iron (III) in the solution was carried out using a spectrometric method. It was found that methanol was the best solvent for desorbing iron (III) from organosilica.

Table 3.18. Desorption of iron (III) from organosilica

Solvents	**Mean Conc.**	**Desorption %** $\% D = \frac{Cads}{Cdes} \times 100$
Distilled water	31.4	35.7
Ethanol	65.7	74.8
Methanol	75.0	85.4

3.2.4. Application of Extracted Iron (III) by organosilica

Organosilica were used of series pharmaceutical samples containing iron (III) ions soluble in aqueous solution, such as (Hemafer, Ferblex, Ferimax, Akourose and Sorbifer Duroles). The pharmaceutical samples were used to adsorb iron (III) ions by organosilica and the concentration of the pharmaceutical samples at 25 mg L^{-1} under the experimental conditions (at 40 °C, pH 7, solid phase amount of 0.1 g and shicking time of 15 min. The adsorption before and after the drugs are shown in Table 3.19. It showed that the organosilica materials have a large surface area, porosity and selective adsorption of iron (III) ions due to the textural characteristics of the organosilica is more selective have functional groups included: naphthalene, nitroso group and hydroxyl groups[128].

Table 3.19. Extraction of iron (III) ions from pharametrical samples by organosilica

Name Of Drug	Dose of drug	Mean ±SD before ads	Mean ±SD after ads	D	E %
Hemafer	100mg/5mL	0.076 ± 0.00100	0.013± 0.00100	5.80	85.3
Ferblex	40mg/15mL	0.084 ±0.00057	0.117 ± 0.00115	0.72	41.9
Ferimax	100mg/2mL	0.076 ±0.00100	0.035 ± 0.00100	2.20	68.8
Akourose	100mg/5mL	0.080± 0.00100	0.045 ± 0.00153	1.80	64.3
Sorbifer Duroles	100mg/60mg	0.158±0.00208	0.046± 0.00152	3.40	77.3

3.3 .Conclusion

Mesoporous silica was successfully synthesized from soil of Karbala city in Iraq by using the sol–gel method. The characterization results from various analytical techniques confirm the formation and quality of the mesoporous structure: EDS analysis confirmed the high purity of the silica, with weight percentage of silicon and oxygen at 31.8 and 50.8 . The XRD analysis is indicative of an amorphous silica structure .SEM images demonstrated morphology a mesoporous structure and particle distribution. The FTIR spectra showed characteristic absorption of Si–O–Si stretching and vibrations. BET texture analyzed a high specific surface area at 252.71 and the pore dimeter at 11.20 that indicate the mesoporous range. Mesoporous silica are highly effective to extract iron (III) complex from Aqueous solution by solid phase extraction method .

The organosilica has been successfully produced from silica extracted from local sandy soil sample and interacted with organic reagent (1-nitroso-2-naphthol). Organosilica was characterization in different techniques to evaluate the organic ligand interaction with silica particles and it was unique pore structure of bundent surface functional sites composite in silica, while the organosilica was considered at candidates preferred for adsorbent metal ion from aqueous solutions due to of their larger specific surface area and high adsorption capacity for target iron(III) ion complex and effectiveness in adsorptive iron (III) ion from pharamictical samples .

3.4. Future works

Through the results were obtained, it can be made future studies on the research plan as follows:

1. Extracted silica would be preparing organosilica by reacting with chelating organic compounds with different functional groups and used them as an adsorbent medium.

2. Using of silica extracted and the organosilica , can be used solid phase extraction methods.

3. Extracting iron complexes is done by the same adsorbent as organosilica by magnetic solid phase extraction

4. Using other heavy metal elements, such as (Cu^{2+},Pb^{2+}, Ni^{2+}) to exract by same method

5. Studying the interfernces of iron (III) complex.

6. Studying and separation organic compounds in soil, such as herbicides and some toxic organic solvents by extracting silica

7. Using of the prepared and extracted materials that separating by solid phase using other techniques, such as Fluorescence and Flame atomic adsorption (FAAS).

References

References

[1] N. Reyes-Garces *et al.*, "Advances in solid phase microextraction and perspective on future directions," *Anal Chem*, vol. 90, no. 1, pp. 302–360, 2017.

[2] M. E. I. Badawy, M. A. M. El-Nouby, P. K. Kimani, L. W. Lim, and E. I. Rabea, "A review of the modern principles and applications of solid-phase extraction techniques in chromatographic analysis," *Analytical Sciences*, vol. 38, no. 12, pp. 1457–1487, 2022.

[3] S. Ötles and C. Kartal, "Solid-Phase Extraction (SPE): Principles and applications in food samples," *Acta Sci Pol Technol Aliment*, vol. 15, no. 1, pp. 5–15, 2016.

[4] S. Tang, H. Zhang, and H. K. Lee, "Advances in sample extraction," *Anal Chem*, vol. 88, no. 1, pp. 228–249, 2016.

[5] Q. Salamat, F. Tatardar, R. Moradi, and M. Soylak, "Recent advancement and prospects of novel nanomaterial-based solid-phase extraction (SPE) techniques," *Anal Lett*, vol. 58, no. 6, pp. 943–983, 2025.

[6] D. Hampel, S. Shahab-Ferdows, J. W. Newman, and L. H. Allen, "Improving LC-MS analysis of human milk B-vitamins by lactose removal," *Journal of Chromatography B*, vol. 1183, p. 122968, 2021.

[7] M. Faraji, Y. Yamini, and M. Gholami, "Recent Advances and Trends in Applications of Solid-Phase Extraction Techniques in Food and Environmental Analysis," Aug. 01, 2019, *Friedr. Vieweg und Sohn Verlags GmbH*. doi: 10.1007/s10337-019-03726-9.

[8] V. I. Isaeva *et al.*, "Modern carbon–based materials for adsorptive removal of organic and inorganic pollutants from water and wastewater," *Molecules*, vol. 26, no. 21, p. 6628, 2021.

References

[9] C. F. Poole, “New trends in solid-phase extraction,” *TrAC Trends in Analytical Chemistry*, vol. 22, no. 6, pp. 362–373, 2003.

[10] A. Żwir-Ferenc and M. Biziuk, “Solid Phase Extraction Technique--Trends, Opportunities and Applications.,” *Pol J Environ Stud*, vol. 15, no. 5, 2006.

[11] M. Kalaboka and V. Sakkas, “Magnetic Solid-Phase Extraction Based on Silica and Graphene Materials for Sensitive Analysis of Emerging Contaminants in Wastewater with the Aid of UHPLC-Orbitrap-MS,” *Molecules*, vol. 28, no. 5, p. 2277, 2023.

[12] B. Buszewski and M. Szultka, “Past, present, and future of solid phase extraction: a review,” *Crit Rev Anal Chem*, vol. 42, no. 3, pp. 198–213, 2012.

[13] H.-L. Jiang, N. Li, L. Cui, X. Wang, and R.-S. Zhao, “Recent application of magnetic solid phase extraction for food safety analysis,” *TrAC Trends in Analytical Chemistry*, vol. 120, p. 115632, 2019.

[14] A. L. Capriotti, C. Cavaliere, G. La Barbera, C. M. Montone, S. Piovesana, and A. Laganà, “Recent applications of magnetic solid-phase extraction for sample preparation,” *Chromatographia*, vol. 82, no. 8, pp. 1251–1274, 2019.

[15] I. E. Uflyand, V. A. Zhinzhilo, V. O. Nikolaevskaya, B. I. Kharisov, C. M. O. González, and O. V Kharissova, “Recent strategies to improve MOF performance in solid phase extraction of organic dyes,” *Microchemical Journal*, vol. 168, p. 106387, 2021.

[16] L. Schipplick, J. Decani, and A. Seubert, “Synthesis of Mixed Acid Stationary Phases with Alkyne Azide Click Chemistry and Atom Transfer Radical Polymerization for the Application in Cation Chromatography,” *Available at SSRN 5217520*.

[17] D. Szynkiewicz, P. Georgiev, S. Ulenberg, T. Bączek, and M. Belka, “Dispersive solid-phase extraction facilitated by newly developed, fully 3D-

References

printed device," *Microchemical Journal*, vol. 187, p. 108367, 2023.

[18] S. Belarbi, M. Vivier, W. Zaghouani, A. De Sloovere, V. Agasse, and P. Cardinael, "Comparison of different d-SPE sorbent performances based on quick, easy, cheap, effective, rugged, and safe (QuEChERS) methodology for multiresidue pesticide analyses in rapeseeds," *Molecules*, vol. 26, no. 21, p. 6727, 2021.

[19] K. Murtada and J. Pawliszyn, "Evolution in understandings of the design, optimization, and application of sorbent-based extraction devices," *TrAC Trends in Analytical Chemistry*, vol. 169, p. 117396, 2023.

[20] K. V Skirdin and O. V Kazmina, "An analysis of oil sorbents: types, characteristics, and effectiveness," *Petroleum Chemistry*, vol. 62, no. 10, pp. 1139–1153, 2022.

[21] N. H. Godage and E. Gionfriddo, "Use of natural sorbents as alternative and green extractive materials: A critical review," *Anal Chim Acta*, vol. 1125, pp. 187–200, 2020.

[22] J. A. Ouimet, J. Xu, C. Flores-Hansen, W. A. Phillip, and B. W. Boudouris, "Design Considerations for Next-Generation Polymer Sorbents: From Polymer Chemistry to Device Configurations," *Macromol Chem Phys*, vol. 223, no. 16, p. 2200032, 2022.

[23] M. Rawa-Adkonis, L. Wolska, and J. Namieśnik, "Modern techniques of extraction of organic analytes from environmental matrices," *Crit Rev Anal Chem*, vol. 33, no. 3, pp. 199–248, 2003.

[24] N. Kumar, R. Gusain, S. Pandey, and S. S. Ray, "Hydrogel nanocomposite adsorbents and photocatalysts for sustainable water purification," *Adv Mater Interfaces*, vol. 10, no. 2, p. 2201375, 2023.

[25] G. Zhou *et al.*, "A highly efficient polyampholyte hydrogel sorbent based

References

fixed-bed process for heavy metal removal in actual industrial effluent," *Water Res*, vol. 89, pp. 151–160, 2016.

[26] M. Wawrzkiewicz, M. Wiśniewska, A. Wołowicz, V. M. Gun'ko, and V. I. Zarko, "Mixed silica-alumina oxide as sorbent for dyes and metal ions removal from aqueous solutions and wastewaters," *Microporous and Mesoporous Materials*, vol. 250, pp. 128–147, 2017.

[27] K. C. Khulbe and T. Matsuura, "Removal of heavy metals and pollutants by membrane adsorption techniques," *Appl Water Sci*, vol. 8, no. 1, p. 19, 2018.

[28] Q. Yu, P. Wang, S. Hu, J. Hui, J. Zhuang, and X. Wang, "Hydrothermal synthesis of hollow silica spheres under acidic conditions," *Langmuir*, vol. 27, no. 11, pp. 7185–7191, 2011.

[29] J. Wang *et al.*, "Recent advances in amine-functionalized silica adsorbents for CO2 capture," *Renewable and Sustainable Energy Reviews*, vol. 203, p. 114724, 2024.

[30] M. Zougagh, J. M. Cano Pavon, and A. Garcia de Torres, "Chelating sorbents based on silica gel and their application in atomic spectrometry," *Anal Bioanal Chem*, vol. 381, no. 6, pp. 1103–1113, 2005.

[31] A. Grisolia *et al.*, "Hybrid polymer-silica nanostructured materials for environmental remediation," *Molecules*, vol. 28, no. 13, p. 5105, 2023.

[32] A. L. M. Gomes *et al.*, "Facile sol–gel synthesis of silica sorbents for the removal of organic pollutants from aqueous media," *Journal of Materials Research and Technology*, vol. 15, pp. 4580–4594, 2021.

[33] K. R. Martin, "The chemistry of silica and its potential health benefits," *J Nutr Health Aging*, vol. 11, no. 2, p. 94, 2007.

[34] B. E. Douglas and S.-M. Ho, "Crystal structures of silica and metal silicates," *Structure and Chemistry of Crystalline Solids*, pp. 233–278, 2006.

References

[35] R. Jin, “Understanding silica from the viewpoint of asymmetry,” *Chemistry–A European Journal*, vol. 25, no. 25, pp. 6270–6283, 2019.

[36] Z. Briceño-Ahumada, J. F. A. Soltero-Martínez, and R. Castillo, “Aqueous foams and emulsions stabilized by mixtures of silica nanoparticles and surfactants: A state-of-the-art review,” *Chemical Engineering Journal Advances*, vol. 7, p. 100116, 2021.

[37] T. T. T. Hien, T. Shirai, and M. Fuji, “Mechanical modification of silica powders,” *Journal of the Ceramic Society of Japan*, vol. 120, no. 1406, pp. 429–435, 2012.

[38] A. Ismail, L. Saputri, A. A. Dwiatmoko, B. H. Susanto, and M. Nasikin, “A facile approach to synthesis of silica nanoparticles from silica sand and their application as superhydrophobic material,” *Journal of Asian Ceramic Societies*, vol. 9, no. 2, pp. 665–672, 2021.

[39] S. D. Karande, S. A. Jadhav, H. B. Garud, V. A. Kalantre, S. H. Burungale, and P. S. Patil, “Green and sustainable synthesis of silica nanoparticles,” *Nanotechnology for environmental engineering*, vol. 6, no. 2, p. 29, 2021.

[40] H.-S. Cho *et al.*, “Recent studies on metal-embedded silica nanoparticles for biological applications,” *Nanomaterials*, vol. 14, no. 3, p. 268, 2024.

[41] K.-S. Chou, H.-L. Liu, L.-H. Kao, C.-M. Yang, and S.-H. Huang, “A quick and simple method to test silica colloids’ ability to resist aggregation,” *Colloids Surf A Physicochem Eng Asp*, vol. 448, pp. 115–118, 2014.

[42] G. Saito and N. Sakaguchi, “Solution plasma synthesis of Si nanoparticles,” *Nanotechnology*, vol. 26, no. 23, p. 235602, 2015.

[43] J. Gao *et al.*, “Pickering emulsion prepared by nano-silica particles–A comparative study for exploring the effect of various mechanical methods,” *Ultrason Sonochem*, vol. 83, p. 105928, 2022.

References

[44] D. Dorairaj, N. Govender, S. Zakaria, and R. Wickneswari, “Green synthesis and characterization of UKMRC-8 rice husk-derived mesoporous silica nanoparticle for agricultural application,” *Sci Rep*, vol. 12, no. 1, p. 20162, 2022.

[45] Y. Zhao, Y. Zheng, H. He, Z. Sun, and A. Li, “Silica extraction from bauxite reaction residue and synthesis water glass,” *Green Processing and Synthesis*, vol. 10, no. 1, pp. 268–283, 2021.

[46] S. Karimkhani, P. Derakhshi, P. Aberoomand Azar, and S. M. Sheikh-Al-Eslamian, “Facile, fast, and green preparation of high-purity and quality silica nanoparticles using a handmade ball mill: comparison with the sol–gel method,” *J Nanostructure Chem*, vol. 14, no. 6, pp. 369–381, 2024.

[47] J. Li *et al.*, “A facile and universal method to purify silica from natural sand,” *Green Processing and Synthesis*, vol. 11, no. 1, pp. 907–914, 2022, doi: 10.1515/gps-2022-0079.

[48] C. Van Hoang *et al.*, “Large-scale synthesis of nanosilica from silica sand for plant stimulant applications,” *ACS Omega*, vol. 7, no. 45, pp. 41687–41695, 2022.

[49] R. P. Bagwe, L. R. Hilliard, and W. Tan, “Surface modification of silica nanoparticles to reduce aggregation and nonspecific binding,” *Langmuir*, vol. 22, no. 9, pp. 4357–4362, 2006.

[50] S. Stopic, F. Wenz, T.-V. Husovic, and B. Friedrich, “Synthesis of silica particles using ultrasonic spray pyrolysis method,” *Metals (Basel)*, vol. 11, no. 3, p. 463, 2021.

[51] X. Chen, J. Jiang, F. Yan, S. Tian, and K. Li, “A novel low temperature vapor phase hydrolysis method for the production of nano-structured silica materials using silicon tetrachloride,” *RSC Adv*, vol. 4, no. 17, pp. 8703–

References

8710, 2014.

[52] K. Kajihara, K. Kanamori, and A. Shimojima, “Current status of sol–gel processing of glasses, ceramics, and organic–inorganic hybrids: a brief review,” *Journal of the Ceramic Society of Japan*, vol. 130, no. 8, pp. 575–583, 2022.

[53] R. M. Almeida and M. C. Gonçalves, “Sol–Gel process and products,” *Encyclopedia of Glass Science, Technology, History, and Culture*, vol. 2, pp. 969–979, 2021.

[54] A.-M. Siouffi, “Silica gel-based monoliths prepared by the sol–gel method: facts and figures,” *J Chromatogr A*, vol. 1000, no. 1–2, pp. 801–818, 2003.

[55] N. Razali and S. A. Othman, “Sol-gel technique in study of titanium dioxide (TiO2) photocatalytic activity-a short review,” *Mater Today Proc*, vol. 66, pp. 4077–4083, 2022.

[56] S. Rovani, J. J. Santos, P. Corio, and D. A. Fungaro, “Highly pure silica nanoparticles with high adsorption capacity obtained from sugarcane waste ash,” *ACS Omega*, vol. 3, no. 3, pp. 2618–2627, 2018.

[57] S. Dervin and S. C. Pillai, “An introduction to sol-gel processing for aerogels,” in *Sol-gel materials for energy, environment and electronic applications*, Springer, 2017, pp. 1–22.

[58] T. Maani, I. Celik, M. J. Heben, R. J. Ellingson, and D. Apul, “Environmental impacts of recycling crystalline silicon (c-SI) and cadmium telluride (CDTE) solar panels,” *Science of The Total Environment*, vol. 735, p. 138827, 2020.

[59] K. Deshmukh, T. Kovářík, T. Křenek, D. Docheva, T. Stich, and J. Pola, “Recent advances and future perspectives of sol–gel derived porous bioactive glasses: a review,” *RSC Adv*, vol. 10, no. 56, pp. 33782–33835, 2020.

References

[60] H. Pérez *et al.*, “Green and facile sol–gel synthesis of the mesoporous SiO 2–TiO 2 catalyst by four different activation modes,” *RSC Adv*, vol. 10, no. 65, pp. 39580–39588, 2020.

[61] J. A. S. Costa, R. A. de Jesus, D. O. Santos, J. B. Neris, R. T. Figueiredo, and C. M. Paranhos, “Synthesis, functionalization, and environmental application of silica-based mesoporous materials of the M41S and SBA-n families: A review,” *J Environ Chem Eng*, vol. 9, no. 3, p. 105259, 2021.

[62] M. Greger, T. Landberg, and M. Vaculík, “Silicon influences soil availability and accumulation of mineral nutrients in various plant species,” *Plants*, vol. 7, no. 2, p. 41, 2018.

[63] S. Kim *et al.*, “Eco-friendly and facile synthesis of size-controlled spherical silica particles from rice husk,” *Nanoscale Adv*, vol. 3, no. 24, pp. 6965–6973, 2021.

[64] J. Kuhla, J. Pausch, and J. Schaller, “Effect on soil water availability, rather than silicon uptake by plants, explains the beneficial effect of silicon on rice during drought,” *Plant Cell Environ*, vol. 44, no. 10, pp. 3336–3346, 2021.

[65] B. S. Tubaña and J. R. Heckman, “Silicon in soils and plants,” in *Silicon and plant diseases*, Springer, 2015, pp. 7–51.

[66] A. Javed, E. Ali, K. B. Afzal, A. Osman, and S. Riaz, “Soil fertility: Factors affecting soil fertility, and biodiversity responsible for soil fertility,” *International Journal of Plant, Animal and Environmental Sciences*, vol. 12, no. 1, pp. 21–33, 2022.

[67] C. A. Heinrich and P. A. Candela, “Fluids and ore formation in the Earth’s crust,” in *Treatise on Geochemistry (Second Edition)*, vol. 13, Elsevier, 2014, pp. 1–28.

[68] N. LePan and B. Venditti, “Visualizing the Abundance of Elements in the

References

Earth’s Crust,” in *World Econ. Forum*, 2021.

[69] M. H. Roozitalab, N. Toomanian, V. R. Ghasemi Dehkordi, and F. Khormali, “Major soils, properties, and classification,” in *The soils of Iran*, Springer, 2018, pp. 93–147.

[70] M. Rashid, S. Kanwal, S. Ghafar, K. Nawwal, S. Ajmal, and S. Rasib, “Assessment of soil texture on Triticum aestivum growth,” *Engineering Proceedings*, vol. 12, no. 1, p. 14, 2021.

[71] L. Lin *et al.*, “Soil surface properties and infiltration response to crust forming of a sandy loam and silt loam,” *Soil Tillage Res*, vol. 248, p. 106440, 2025.

[72] F. J. Matus, “Fine silt and clay content is the main factor defining maximal C and N accumulations in soils: a meta-analysis,” *Sci Rep*, vol. 11, no. 1, p. 6438, 2021.

[73] H. Afrin, “A review on different types soil stabilization techniques,” *International Journal of Transportation Engineering and Technology*, vol. 3, no. 2, pp. 19–24, 2017.

[74] B. McLean and I. Yarovsky, “Structure, properties, and applications of silica nanoparticles: Recent theoretical modeling advances, challenges, and future directions,” *Small*, vol. 20, no. 51, p. 2405299, 2024.

[75] T. D. Martins, T. Ribeiro, and J. P. S. Farinha, “Overview of silica-polymer nanostructures for waterborne high-performance coatings,” *Polymers (Basel)*, vol. 13, no. 7, p. 1003, 2021.

[76] A. Nair, C. M. Day, S. Garg, Y. Nayak, P. A. Shenoy, and U. Y. Nayak, “Polymeric functionalization of mesoporous silica nanoparticles: Biomedical insights,” *Int J Pharm*, vol. 660, p. 124314, 2024.

[77] D. Macina, Z. Piwowarska, K. Tarach, K. Góra-Marek, J. Ryczkowski, and

References

L. Chmielarz, “Mesoporous silica materials modified with alumina polycations as catalysts for the synthesis of dimethyl ether from methanol,” *Mater Res Bull*, vol. 74, pp. 425–435, 2016.

[78] U. DE Montpellier and M. M. Richa Eric B MmeCo M Ahma M Karim, “THÈSE POUR OBTENIR LE GRADE DE DOCTEUR 3 :Matériaux Poreux et Hybrides Sous la direction d’Ahmad MEHDI et Karim BOUCHMELLA Devant le jury composé de Hydrolytic vs. nonhydrolytic sol-gel routs to prepare mixed oxide catalysts for ethylene oligomerization.”

[79] E. J. M. Hensen, D. G. Poduval, P. Magusin, A. E. Coumans, and J. A. R. Van Veen, “Formation of acid sites in amorphous silica-alumina,” *J Catal*, vol. 269, no. 1, pp. 201–218, 2010.

[80] R. J. Davis and Z. Liu, “Titania− Silica: a model binary oxide catalyst system,” *Chemistry of materials*, vol. 9, no. 11, pp. 2311–2324, 1997.

[81] H. Li, X. Chen, D. Shen, F. Wu, R. Pleixats, and J. Pan, “Functionalized silica nanoparticles: classification, synthetic approaches and recent advances in adsorption applications,” *Nanoscale*, vol. 13, no. 38, pp. 15998–16016, 2021.

[82] R. K. Kankala *et al.*, “Nanoarchitectured structure and surface biofunctionality of mesoporous silica nanoparticles,” *Advanced materials*, vol. 32, no. 23, p. 1907035, 2020.

[83] M. V. Rivas, M. J. A. Muñetón, A. V Bordoni, M. V. Lombardo, C. C. Spagnuolo, and A. Wolosiuk, “Revisiting carboxylic group functionalization of silica sol–gel materials,” *J Mater Chem B*, vol. 11, no. 8, pp. 1628–1653, 2023.

[84] S. M. Alahmadi and S. S. Aljuhani, “Synthesis of Silica Gel Chelated with Alizarin and 1-Nitroso-2-Naphthol for Solid Phase Extraction of Lead in

Ground Water Samples," *Separations*, vol. 10, no. 10, p. 544, 2023.

[85] N. Meftah, A. Hani, and A. Merdas, "Extraction and Physicochemical Characterization of Highly-pure Amorphous Silica Nanoparticles from Locally Available Dunes Sand," *Chemistry Africa*, vol. 6, no. 6, pp. 3039–3048, 2023, doi: 10.1007/s42250-023-00688-2.

[86] N. Setyawan and S. Yuliani, "Synthesis of silica from rice husk by sol-gel method," in *Iop Conference Series: Earth and Environmental Science*, IOP Publishing, 2021, p. 012149.

[87] A. F. Khudhair and M. K. Hassan, "Cloud point extraction and determination trace iron (III) in urine samples by spectrophotometry and flame atomic absorption spectrometry," *Asian J. Chem*, vol. 29, no. 12, pp. 2725–2733, 2017.

[88] S. Sumari, M. R. Asrori, Y. F. Prakasa, and D. R. Baharintasari, "Silica extract from Malang beach sand via leaching and sol-gel methods," vol. 12, no. 1, pp. 74–81, 2023, doi: 10.11591/ijaas.v12.i1.pp74-81.

[89] H. A. Al-Saad, F. W. Al-Halfi, and Y. I. Khalaf, "Suitability evaluation of selected sand geological formations for synthesis high purity crystalline silica, Iraq," in *IOP Conference Series: Earth and Environmental Science*, IOP Publishing, 2024, p. 012015.

[90] N. Elizondo-Villarreal *et al.*, "Synthesis and characterization of SiO2 nanoparticles for application as nanoadsorbent to clean wastewater," *Coatings*, vol. 14, no. 7, p. 919, 2024.

[91] R. Ellerbrock, M. Stein, and J. Schaller, "Comparing amorphous silica, short-range-ordered silicates and silicic acid species by FTIR," *Sci Rep*, vol. 12, no. 1, p. 11708, 2022.

[92] D.-P. Sui, H.-X. Chen, and D.-W. Li, "Sol–gel-derived thiocyanato-

functionalized silica gel sorbents for adsorption of Fe (III) ions from aqueous solution: Kinetics, isotherms and thermodynamics," *J Solgel Sci Technol*, vol. 80, no. 2, pp. 504–513, 2016.

[93] D. R. Eddy, S. N. Ishmah, M. D. Permana, and M. L. Firdaus, "Synthesis of titanium dioxide/silicon dioxide from beach sand as photocatalyst for Cr and Pb remediation," *Catalysts*, vol. 10, no. 11, p. 1248, 2020.

[94] J. B. Condon, *Surface area and porosity determinations by physisorption: measurement, classical theories and quantum theory*. Elsevier, 2019.

[95] M. M. Rahman, M. Muttakin, A. Pal, A. Z. Shafiullah, and B. B. Saha, "A statistical approach to determine optimal models for IUPAC-classified adsorption isotherms," *Energies (Basel)*, vol. 12, no. 23, p. 4565, 2019.

[96] M. Thommes *et al.*, "Physisorption of gases, with special reference to the evaluation of surface area and pore size distribution (IUPAC Technical Report)," *Pure and applied chemistry*, vol. 87, no. 9–10, pp. 1051–1069, 2015.

[97] K. Lazaar, R. Pullar, W. Hajjaji, S. Mefteh, M. Medhioub, and F. Jamoussi, "Preparation of silica gel obtained from early cretaceous Sidi Aich Sands (Central Tunisia) and its potential to remove Pollutant Dye Anionic from Wastwaters," *Silicon*, vol. 14, no. 5, pp. 2351–2362, 2022.

[98] A. Boualem, L. Leontie, S. A. G. Lopera, and S. Hamzaoui, "Synthesis and characterization of mesoporous silica from Algerian river sand for solar grade silicon: Effect of alkaline concentration on the porosity and purity of silica powder," *Silicon*, vol. 14, no. 10, pp. 5231–5240, 2022.

[99] G. Mladin *et al.*, "Silica-iron oxide nanocomposite enhanced with porogen agent used for arsenic removal," *Materials*, vol. 15, no. 15, p. 5366, 2022.

[100] A. Al Khudhair, K. Bouchmella, P. H. Mutin, V. Hulea, O. Gimello, and A.

References

Mehdi, “Hydrolytic vs. nonhydrolytic sol-gel in preparation of mixed oxide silica–alumina catalysts for esterification,” *Molecules*, vol. 27, no. 8, p. 2534, 2022.

[101] R. Sharafudeen, J. M. Al-Hashim, M. O. Al-Harbi, A. I. Al-Ajwad, and A. A. Al-Waheed, “Preparation and characterization of precipitated silica using sodium silicate prepared from Saudi Arabian desert sand,” *Silicon*, vol. 9, no. 6, pp. 917–922, 2017.

[102] N. Meftah, A. Hani, and A. Merdas, “Extraction and physicochemical characterization of highly-pure amorphous silica nanoparticles from locally available dunes sand,” *Chemistry Africa*, vol. 6, no. 6, pp. 3039–3048, 2023.

[103] M. Wei, Y. Zhang, Y. Wang, X. Liu, X. Li, and X. Zheng, “Employing atomic force microscopy (AFM) for microscale investigation of interfaces and interactions in membrane fouling processes: new perspectives and prospects,” *Membranes (Basel)*, vol. 14, no. 2, p. 35, 2024.

[104] D. Sinkhonde, “Employing spatial, hybrid and amplitude roughness parameters for unveiling the surface roughness features of mineral and organic admixtures,” *Heliyon*, vol. 9, no. 10, 2023.

[105] J. Y. Chun, B. G. Kim, W. Jang, and D. H. Wang, “Loosening effect of perovskite intermolecular exchanger with strong steric hindrance for highly sensitive photodetector,” *Appl Surf Sci*, vol. 591, p. 153207, 2022.

[106] K. Garg, C. Majumder, S. K. Gupta, D. K. Aswal, S. K. Nayak, and S. Chattopadhyay, “Stable negative differential resistance in porphyrin based σ–π–σ monolayers grafted on silicon,” *RSC Adv*, vol. 5, no. 62, pp. 50234–50244, 2015.

[107] R. P. Renz, “Design and synthesis of benign, N-and O-containing, organic ligands for surface engineering,” 2007.

References

[108] F. I. Nwabue and F. S. Nworie, "Chemometric Extractive Synthesis, Characterization and Antimicrobial Studies of Fe (II) and Fe (III) Complexes of N2O2 Chelating Ligand, Bis (Salicylidene) Ethylenediamine," *Chemistry Africa*, vol. 6, no. 2, pp. 867–880, 2023.

[109] M. E. Mahmoud and M. S. M. Al Saadi, "Selective solid phase extraction and preconcentration of iron (III) based on silica gel-chemically immobilized purpurogallin," *Anal Chim Acta*, vol. 450, no. 1–2, pp. 239–246, 2001.

[110] T. X. Bui and H. Choi, "Adsorptive removal of selected pharmaceuticals by mesoporous silica SBA-15," *J Hazard Mater*, vol. 168, no. 2–3, pp. 602–608, 2009.

[111] T. Shen, M. Gao, W. Zang, F. Ding, and J. Wang, "Architecting organo silica nanosheets for regenerable cost-effective organics adsorbents," *Chemical Engineering Journal*, vol. 331, pp. 211–220, 2018.

[112] B. Samiey, C.-H. Cheng, and J. Wu, "Organic-inorganic hybrid polymers as adsorbents for removal of heavy metal ions from solutions: a review," *Materials*, vol. 7, no. 2, pp. 673–726, 2014.

[113] S. Bashir and J. Liu, "Overviews of synthesis of nanomaterials," *Advanced Nanomaterials and their Applications in Renewable Energy*, vol. 51, 2015.

[114] H. Liu, H. Kaya, Y. Lin, A. Ogrinc, and S. H. Kim, "Vibrational spectroscopy analysis of silica and silicate glass networks," *Journal of the American Ceramic Society*, vol. 105, no. 4, pp. 2355–2384, 2022.

[115] M. Sambuu *et al.*, "Solubility property of Baganuur coal: Performance assessment by FTIR spectroscopic analysis," in *Solid State Phenomena*, Trans Tech Publ, 2021, pp. 28–41.

[116] M. Addy, B. Losey, R. Mohseni, E. Zlotnikov, and A. Vasiliev, "Adsorption of heavy metal ions on mesoporous silica-modified montmorillonite

References

containing a grafted chelate ligand," *Appl Clay Sci*, vol. 59, pp. 115–120, 2012.

[117] N. Alvisi *et al.*, "Self-assembly of elastin-like polypeptide brushes on silica surfaces and nanoparticles," *Biomacromolecules*, vol. 22, no. 5, pp. 1966–1979, 2021.

[118] E. S. A. Al-Sammarraie, T. M. Sabirova, H. Meskher, R. A. Al-Juboori, G. V Zyryanov, and Q. F. Alsalhy, "Nanocomposite UF membrane of PVC/nano-silica modified with SDS for carwash wastewater treatment," *Environmental Science: Advances*, vol. 4, no. 3, pp. 469–488, 2025.

[119] M. Schöbinger and B. Stöger, "1-Nitronaphthalene, a non-OD, non-MDO polytype," *Zeitschrift für Kristallographie-Crystalline Materials*, vol. 239, no. 9–10, pp. 331–338, 2024.

[120] D. R. Mujiyanti, D. Ariyani, and M. Lisa, "Silica Content Analysis of Rice Husks Siam Unus from South Kalimantan," *Indonesian Journal of Chemical Research*, vol. 9, no. 2, pp. 81–87, 2021.

[121] S. H. Ahn, S. H. Kim, and S. G. Lee, "Surface-modified silica nanoparticle–reinforced poly (ethylene 2, 6-naphthalate)," *J Appl Polym Sci*, vol. 94, no. 2, pp. 812–818, 2004.

[122] H. Du, P. D. Hamilton, M. A. Reilly, A. d'Avignon, P. Biswas, and N. Ravi, "A facile synthesis of highly water-soluble, core–shell organo-silica nanoparticles with controllable size via sol–gel process," *J Colloid Interface Sci*, vol. 340, no. 2, pp. 202–208, 2009.

[123] H. REZALA, J. L. VALVERDE, A. ROMERO, A. MOLINARI, and A. MALDOTTI, "Synthesis of carbonylic derivatives from alkylaromatics by a photocatalytic oxidation using Fe/Ti-pillared clays.," *Moroccan Journal of Chemistry*, vol. 3, no. 2, p. J-Chem, 2015.

References

[124] O. Tevfik, I. TELCI, G. U. L. Fatih, and I. DEMIRTAS, “A Comprehensive Study on Phytochemical Contents, Isolation and Antioxidant Capacities in wild mind, Mentha longifolia subsp. typhoides var. typhoides PH. Davis,” *Moroccan Journal of Chemistry*, vol. 6, no. 4, p. J-Chem, 2018.

[125] F. Fu and Q. Wang, “Removal of heavy metal ions from wastewaters: a review,” *J Environ Manage*, vol. 92, no. 3, pp. 407–418, 2011.

[126] A.-A. Abd-Elshafi, A. A. Amer, A. El-Shater, E. F. Newair, and M. Elrouby, “Organo-modified Montmorillonite-based adsorbents for selective removal of Iron (II) from aqueous solutions,” *J Mol Liq*, vol. 383, p. 122092, 2023.

[127] P. L. Edmiston, C. Osborne, K. P. Reinbold, D. C. Pickett, and L. A. Underwood, “Pilot scale testing composite swellable organosilica nanoscale zero-valent iron—Iron-Osorb®—for in situ remediation of trichloroethylene,” *Remediation Journal*, vol. 22, no. 1, pp. 105–123, 2011.

[128] C. A. Howell, S. V Mikhalovsky, E. N. Markaryan, and A. V Khovanov, “Investigation of the adsorption capacity of the enterosorbent Enterosgel for a range of bacterial toxins, bile acids and pharmaceutical drugs,” *Sci Rep*, vol. 9, no. 1, p. 5629, 2019.

Appendix

Table S1. EDS of ZA_1, ZA_2 and ZA_3 before and after extraction

Before extraction					After extraction			
Elements ZA_1	**Atomic %**	**Atomic % Error**	**Weight %**	**Weight % Error**	**Atomic %**	**Atomic % Error**	**Weight %**	**Weight % Error**
C	11.0	0.3	7.0	0.2	13.4	0.6	8.5	0.4
O	63.3	0.4	53.9	0.3	59.8	0.6	50.8	0.6
Mg	0.8	0.0	1.0	0.0	0.0	0.0	0.0	0.0
Al	1.2	0.0	1.8	0.0	1.2	0.0	1.7	0.0
Si	23.0	0.1	34.4	0.1	21.3	0.1	31.8	0.1
Ca	0.5	0.0	1.0	0.0	0.0	0.0	0.0	0.0
Fe	0.3	0.0	0.9	0.1	0.3	0.0	0.8	0.1
Na	0.0	0.0	0.0	0.0	2.2	0.1	2.7	0.1
Cl	0.0	0.0	0.0	0.0	1.7	0.0	3.3	0.1
Elements ZA_2	**Atomic %**	**Atomic % Error**	**Weight %**	**Weight % Error**	**Atomic %**	**Atomic % Error**	**Weight %**	**Weight % Error**
C	17.9	0.4	11.1	0.2	36.9	0.5	27.4	0.4
O	58.3	0.7	48.3	0.5	49.9	0.5	49.4	0.5
Na	0.6	0.0	0.7	0.1	2.3	0.0	3.3	0.1
Mg	2.8	0.0	3.5	0.1	0.4	0.0	0.5	0.0
Al	2.7	0.0	3.7	0.1	1.4	0.0	2.3	0.0
Si	8.9	0.0	13.0	0.1	7.7	0.0	12.4	0.1
S	0.4	0.0	0.7	0.0	0.0	0.0	0.0	0.0
K	0.4	0.0	0.8	0.0	0.0	0.0	0.0	0.0
Ca	6.2	0.0	12.8	0.1	0.0	0.0	0.0	0.0
Ti	0.1	0.0	0.3	0.0	0.1	0.0	0.2	0.0
Fe	1.7	0.0	5.0	0.1	0.4	0.0	1.3	0.0
F	0.0	0.0	0.0	0.0	0.1	0.1	0.1	0.1
Cl	0.0	0.0	0.0	0.0	0.9	0.0	1.9	0.0
Elements ZA_3	**Atomic %**	**Atomic % Error**	**Weight %**	**Weight % Error**	**Atomic %**	**Atomic % Error**	**Weight %**	**Weight % Error**
C	18.8	0.3	12.1	0.2	16.4	0.4	10.6	0.2
O	58.7	0.5	58.2	0.5	50.2	0.4	50.1	0.4
Na	0.6	0.0	0.8	0.0	2.2	0.0	2.8	0.0
Mg	2.5	0.0	3.2	0.0	0.0	0.0	0.0	0.0
Al	3.4	0.0	4.9	0.1	0.1	0.0	0.2	0.0
Si	10.1	0.0	15.2	0.1	11.4	0.1	12.5	0.1
Cl	0.0	0.0	0.0	0.0	1.5	0.0	2.9	0.0
Ca	3.7	0.0	8.0	0.1	0.0	0.0	0.0	0.0
Ti	0.2	0.0	0.4	0.0	0.1	0.0	0.2	0.0
Fe	1.4	0.0	4.3	0.1	0.1	0.0	0.2	0.0
Cu	0.0	0.0	0.0	0.0	0.1	0.0	0.3	0.0
Cl	0.0	0.0	0.0	0.0	1.5	0.0	2.9	0.0

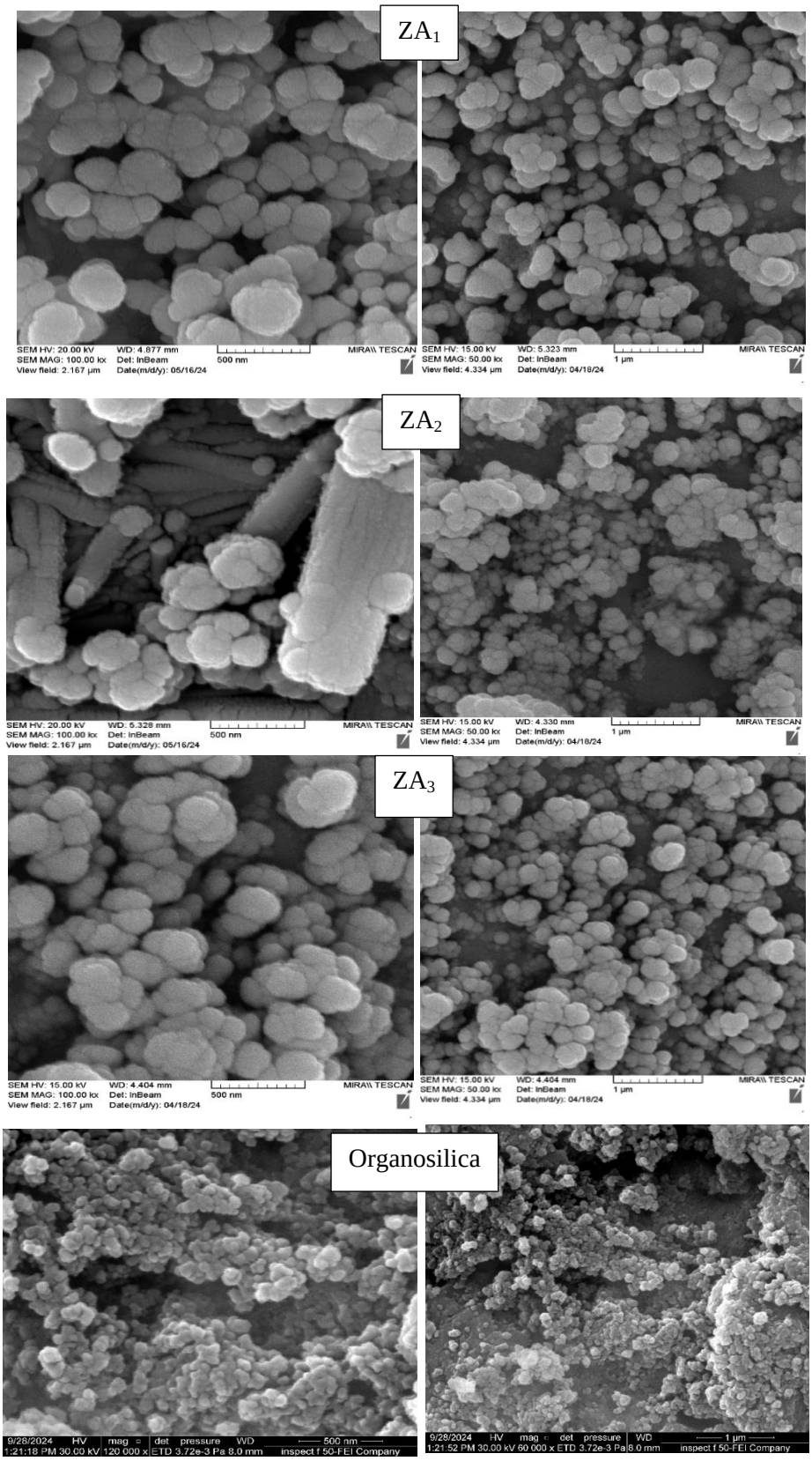

Figure S1. SEM of Silica in samples ZA_1,ZA_2,ZA_3 and Organosilica

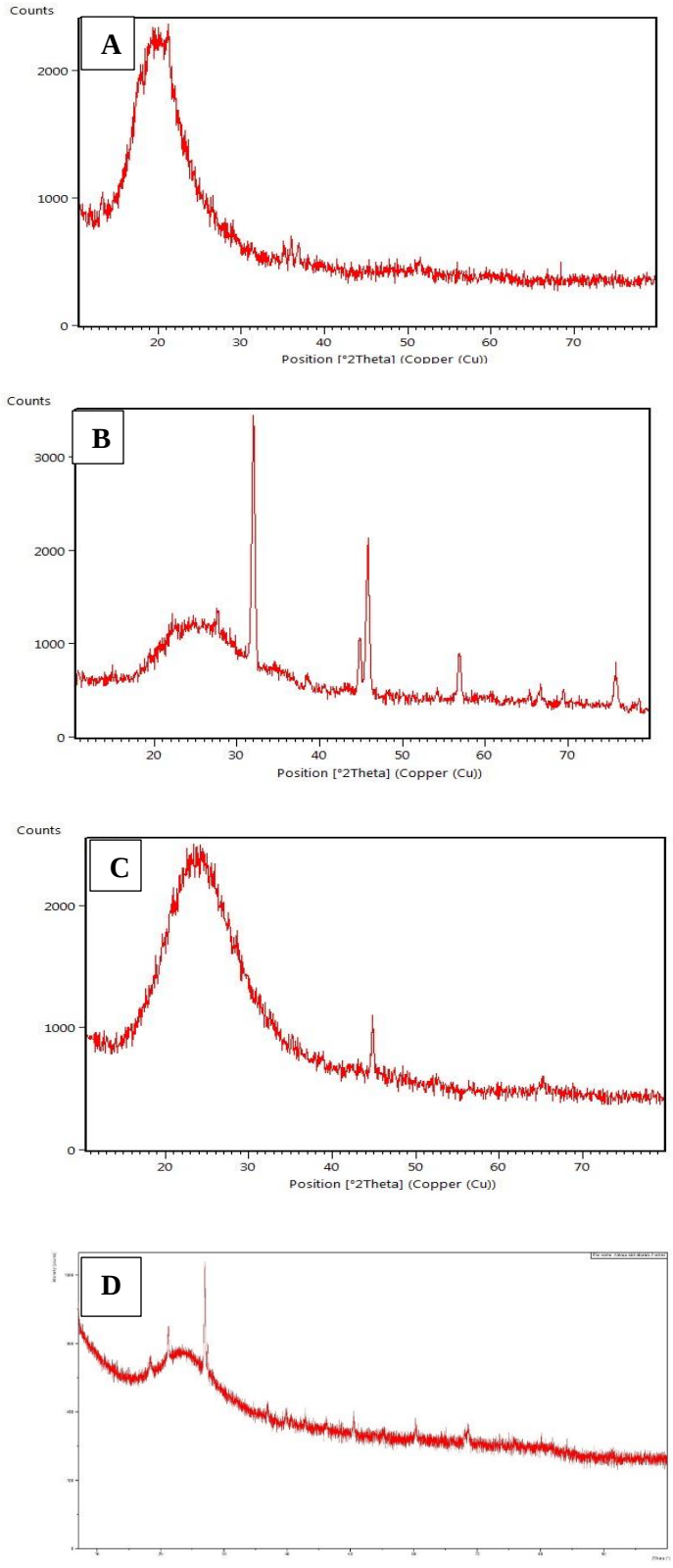

Figure S2. XRD Silica in samples (A- ZA_1, B- ZA_2,C-ZA_3 and D- Organosilica).

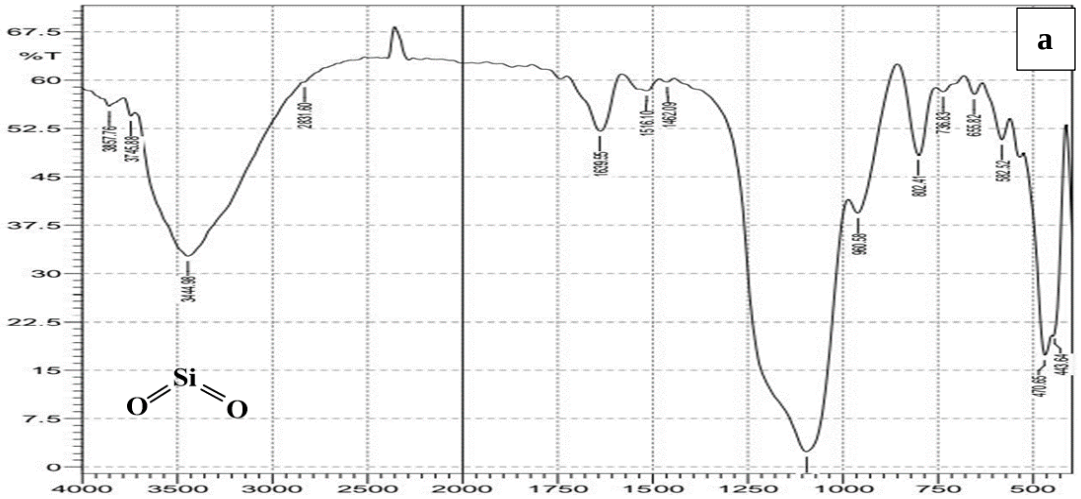
a
%T
3444.88
2331.60
1629.55
1516.10
1462.09
980.08
800.41
726.83
655.82
592.42
470.85
440.64
O=Si=O

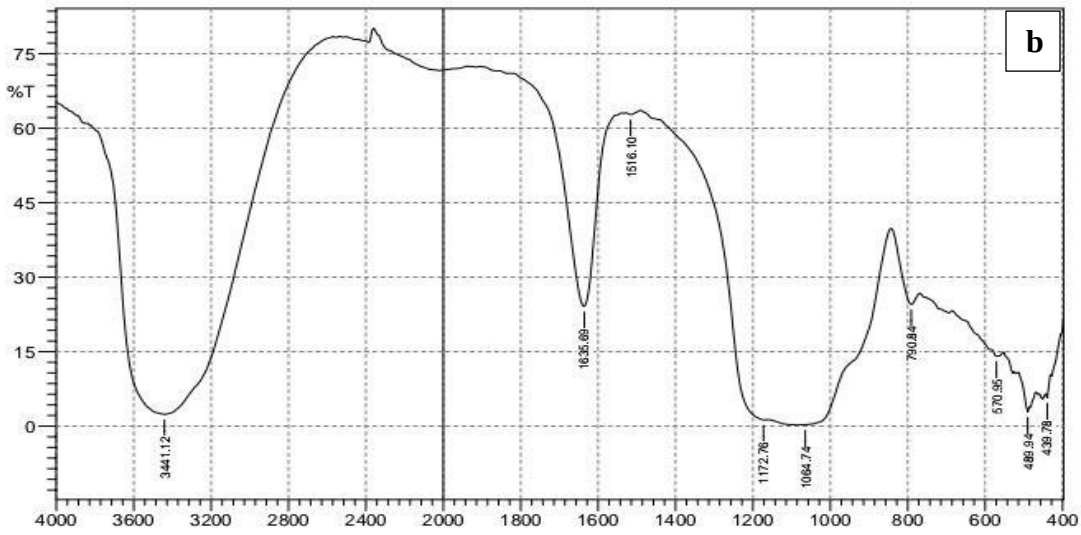
b
%T
3441.12
1635.69
1516.10
1172.76
1064.74
790.84
570.95
489.94
439.78

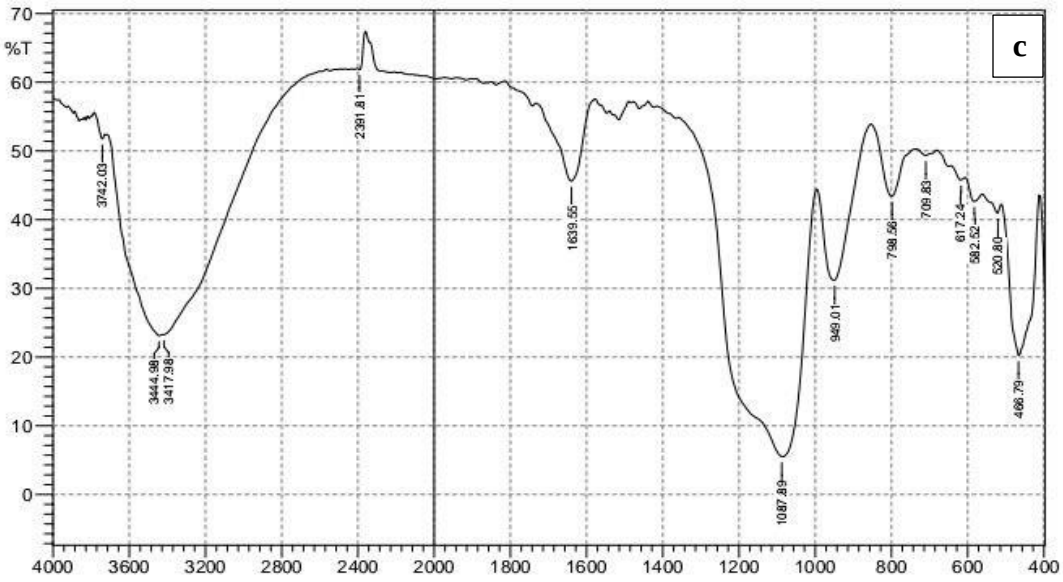
c
%T
3742.03
3444.98
3417.98
2391.81
1639.55
1087.89
949.01
798.56
709.83
617.24
582.62
520.80
466.79

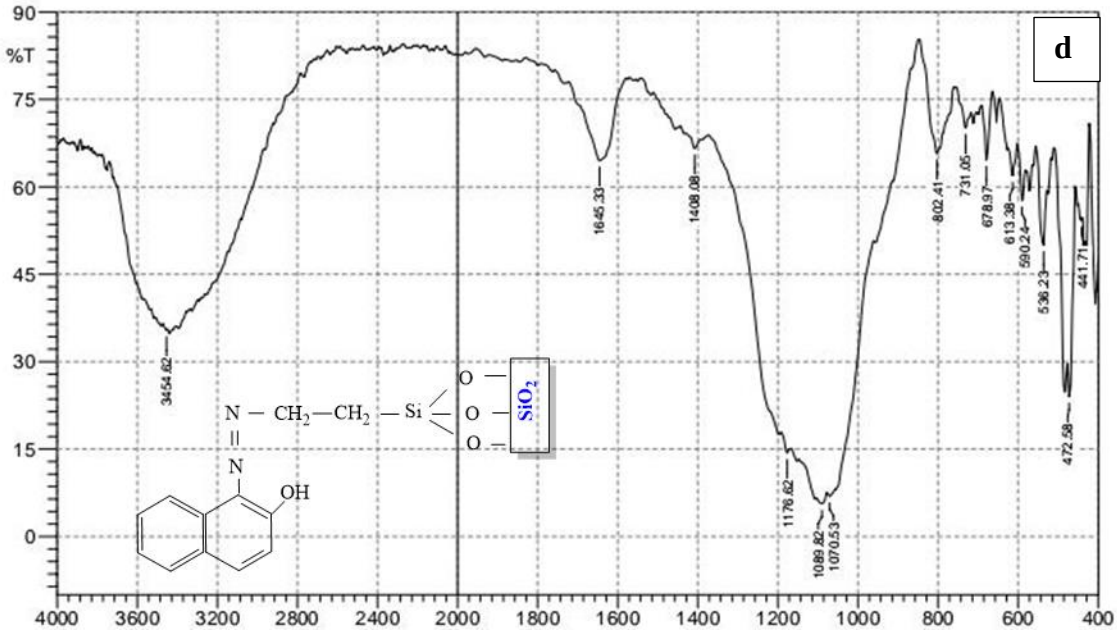

Figure S3. FTIR of Silica in samples (a- ZA_1, b- ZA_2, c -ZA_3 and d-Organosilica).

Table S2. BET of Silica in samples (ZA_1, ZA_2 and ZA_3) , and Organosilica

Samples name	$V_m$cm^3(STP) g^{-1}]	$a_{s,BET}$ [m^2 g^{-1}]	C	Total pore volume(p/p_0) [cm^3 g^{-1}]	Mean pore diameter [nm]
Silica in sample ZA_1	58.062	252.71	8.0667	0.7081	11.207
Silica in sample ZA_2	2.9333	12.767	6.7649	0.043444	13.611
Silica in sample ZA_3	4.5442	19.778	3.2485	0.064395	13.023
Organosilica	20.024	87.154	117.64	0.3088	14.173

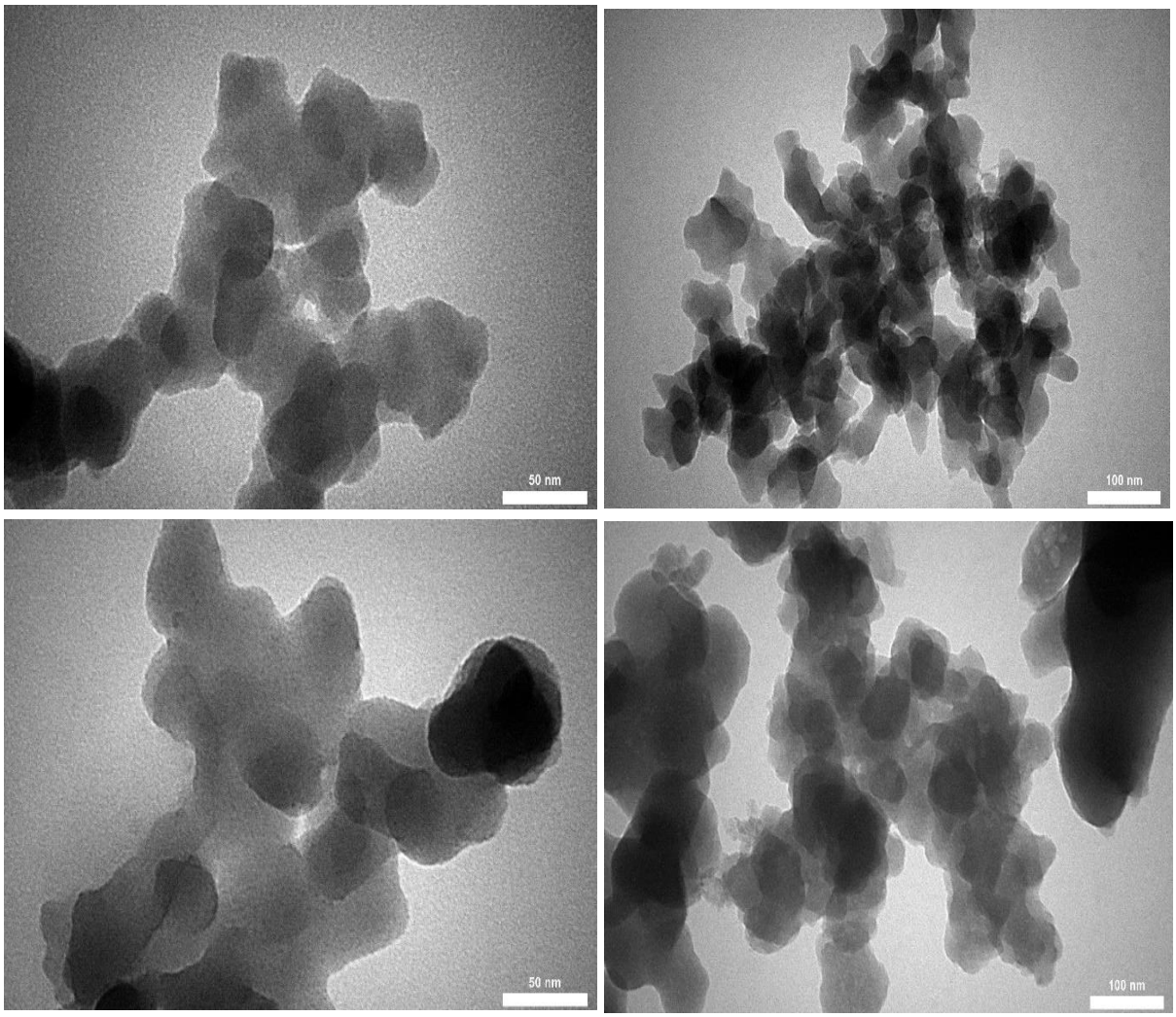

Figure S4. TEM amages of silica Organosilica

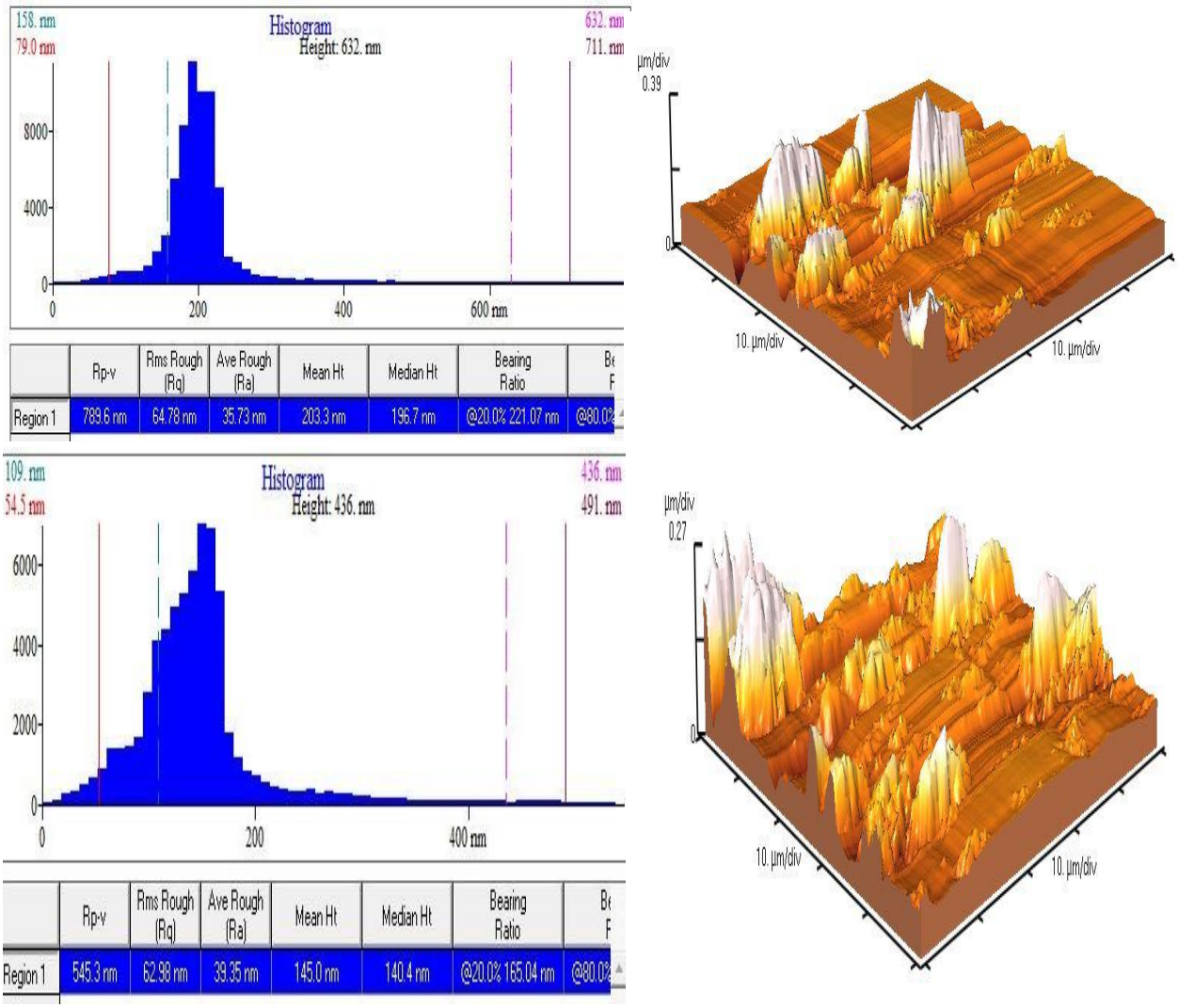

Figure S5. The surface roughness parameters and AFM images of Silica and Organosilica

law used in the study.

Name	**Symbol**	**The law**
Distribution ratio	D	$\frac{\text{Abs. of metal before Ads.}}{\text{Abs. of metal after Ads.}}$
Enthalpy	ΔH	$-\text{Slope} \times 2.303\text{R}$
Entropy extraction	Δsex	$\frac{(\Delta\text{Hex} - \Delta\text{Gex})}{\text{T}}$
Extraction contestant	Kex	$\frac{\text{D}}{(\text{Con. rich phase} \times \text{Con. aq})}$
Extraction Percentage	E%	$(\frac{\text{D}}{1+\text{D}}) \times 100$
Free energy extraction	Δgex	$-\text{RT} \times \ln \text{Kex}$
Standard Deviation	SD	$\sqrt{\frac{\sum(\text{xi} - \bar{\text{x}})^2}{\text{n} - 1}}$
Desorbtion percent	D%	$\frac{\text{Cads}}{Cdes} \times 100$

الخلاصة:

تم استخلاص السيليكا بنجاح من عينات تربة محلية مختارة من مناطق مختلفة من مدينة كربلاء باستخدام طريقة Sol-Gel حيث كانت طريقة الاستخلاص بسيطة وصديقة للبيئة. بعد ذلك تم تخليق السيلكا العضوية (1-نيتروزو-2-نفثال السيليكا) من تفاعل السيليكا المستخلصة من العينة الرملية مع كاشف مخلبي عضوي (1-نيتروزو-2-نفثال).ثم تم تشخيص السيليكا ومركب السيليكا العضوية بتقنيات مختلفة مثل (EDX , FTIR, XRD , AFM , BET ,SEM و.TEM).وتبين من خلال قياس EDX أن التربة الرملية تحتوي على نسبة عالية من السيليكا . تم استخدام تقنية SEM لدراسة مورفولوجيا السيليكا والسيليكا العضوية. أظهرت تقنية XRD أن السيلكا والسيلكا العضوية ذات قمم عريضة تدل على انها ذات طبيعة غير بلورية ووجود بعض القمم الحادة في السيليكا العضوية تدل على وجود الكاشف العضوي. تحليل FTIR أظهر المجاميع الوظيفية في السيليكا السيليكا العضوية هي السيلوكسان السيلانول في السيليكا. وأكدت مساحة سطح وحجم مسام السيليكا والسيليكا العضوية باستخدام تقنية BET أن كليهما يتميز ببنية مسامية متوسطة. علاوة على ذلك، اظهرت كل من قياس (AFM,TEM) البنية الداخلية وخشونة سطح للسيليكا والسيليكا العضوية. تم استخدام السيليكا والسيليكا العضوية بنجاح كطور صلب لطريقة الاستخلاص بالطور الصلب المتشتت وتم تطبيقها بنجاح لاستخلاص معقدات الحديد من محاليلها المائية وتم دراسة الظروف الفيزيائية والكيميائية للاستخلاص حيث تم فصل معقد الحديد باستخدام السيلكا والسيلكا العضوية عند الظروف المثلى للقياس (وسط متعادل، وتركيز الكاشف 0.04 مول/لتر، ، ودرجة حرارة ٤٠ - ٣٥ درجة مئوية، وزمن التحريك 15 دقيقة) حيث تم الحصول على نسبة استخلاص معقد الحديد باستخدام السيلكا 99.5 % بينما نسبة الاستخلاص باستخدام السيلكا العضوية 87 %. كما تم تطبيق الطريقة بنجاح على عينات صيدلانية تحتوي على أيونات الحديد وهذا يوكد انها طريقة دقيقة وذات انتقائية وتحسسية عالية ،سهلة وسريعة.

جامعة كربلاء

كلية العلوم

قسم الكيمياء

استخلاص و تقييم لمركبات السيلكون من تربة محلية، استخلاص ايون الحديد الثلاثي من محاليله المائية وتطبيقاته المختلفة

رسالة مقدمة الى مجلس كلية العلوم / جامعة كربلاء

وهي جزء من متطلبات نيل درجة

الماجستير في علوم الكيمياء

من قبل

زهراء عبد الصاحب قاسم الساعدي

بكالوريوس علوم كيمياء / جامعة كربلاء (٢٠٢١)

بأشراف

أ. د. أحمد فاضل خضير

أ.م. د. اثير حسن ياس

٢٠٢٥ م ايار ذو القعدة ١٤٤٦ هـ